MECHANISMS OF ECOSYSTEM CARBON STORAGE AND STABILITY IN TEMPERATE BIOENERGY CROPPING SYSTEMS

by

Adam Charles von Haden

A dissertation submitted in partial fulfillment of

the requirements for the degree of

Doctor of Philosophy

(Environment & Resources)

at the

UNIVERSITY OF WISCONSIN-MADISON

2017

Date of final oral examination: 11/17/2017

The dissertation is approved by the following members of the Final Oral Committee:

Christopher J. Kucharik, Professor, Agronomy
Erika Marín-Spiotta, Associate Professor, Geography
Randall D. Jackson, Professor, Agronomy
Matthew D. Ruark, Associate Professor, Soil Science
Mark G. Rickenbach, Professor, Forest and Wildlife Ecology

Abstract

MECHANISMS OF ECOSYSTEM CARBON STORAGE AND STABILITY
IN TEMPERATE BIOENERGY CROPPING SYSTEMS

Adam C. von Haden

Under the supervision of Professor Christopher J. Kucharik,
Associate Professor Erika Marín-Spiotta,
and Professor Randall D. Jackson
at the University of Wisconsin-Madison

Consumption of fossil fuels and conversion of native landscapes into agricultural systems has significantly increased atmospheric CO_2 and caused a shift in the global climate, which threatens to harm humans and the ecosystems on which they rely. Current U.S. legislation requiring the production of biofuels from agricultural systems seeks to reduce net CO_2 emissions by providing a carbon neutral fuel feedstock and by sequestering additional carbon (C) belowground in soils and plant biomass. Owing primarily to greater belowground C allocation, perennial, cellulosic-based bioenergy cropping systems are generally expected to provide greater C sequestration than annual, grain-based systems, but few direct comparisons exist. Moreover, C sequestration among cropping system types is likely to be context-dependent, and thus a deeper understanding of the mechanisms underlying major ecosystem C processes is necessary to make predictions of C storage potential across a wider range of conditions. Accurate predictions are needed to help inform land management and environmental policy decisions.

The broad objective of this work was to gain a better understanding of the mechanisms that drive key ecosystem C process and therefore control ecosystem C storage and stability. In a comparison between no-till maize (annual) and switchgrass (perennial), maize had a slightly more favorable net ecosystem carbon balance (NECB) during the two study years. Autotrophic

respiration from roots (R_A), heterotrophic respiration from soil and litter decomposition (R_H), and residue retention rates all differed between the two cropping systems. R_A was much greater in switchgrass than maize, owing both to greater respiratory growth demand and to more extensive root biomass stocks, which require continual maintenance respiration. Seasonal differences in soil temperature and soil moisture (soil microclimate) existed among cropping systems, and the differences were hypothetically large enough to moderately affect annual R_H, but the soil microclimates could not explain the observed R_H differences between the cropping systems. Changes in the aggregate and mineral-associated soil organic C fractions five years after cropping system establishment were more favorable on fine-textured soils, under high above- and belowground litter input rates, and with high quality (low C:N) litter.

These results illustrate that greater belowground C allocation in perennial biofuel cropping systems may not translate into greater ecosystem C storage since the conversion of belowground C allocation into biomass is less efficient than in annual cropping systems. Site-specific properties such as soil texture will most likely influence the short-term C storage potential of bioenergy cropping systems and thus must be explicitly considered when making predictions. In line with established views regarding the importance of residue return in traditional row crop systems, the quantity of aboveground biomass that is harvested from bioenergy cropping systems will likely have a strong influence on the NECB, and thus the benefits of high biomass harvest must be weighed against the potential costs of C loss from soils. Site- and crop-specific management practices will therefore have a considerable influence on the overall potential for belowground C storage in annual and perennial bioenergy cropping systems across the landscape.

Acknowledgements

This work would not have been possible without the dedication of many individuals who have contributed directly or indirectly throughout the years. I would first like to thank my co-advisors, Chris Kucharik, Erika Marín-Spiotta, and Randy Jackson, who have all helped me become a better scientist and citizen. I am greatly indebted to them for giving me the opportunity to be a part of their research programs, and I look forward to continued collaborations. I also want to thank my other committee members, Matt Ruark and Mark Rickenbach, for challenging me to think less about carbon and more about the bigger picture (and sometimes nitrogen).

Gary Oates coordinated many of the field measurements and ran many of the plant and soil samples for carbon and nitrogen. Gregg Sanford was always there to answer my never-ending supply of questions was very accommodating of my field needs. Jimmy Sustachek was a dependable conduit between myself and the unpredictable world of Area 4.1. Thanks to the field crews for all their hard work and dedication: Casey Menick, James Tesmer, Alex Butz, Mark Walsh, Haley Melampey, Becca Fahney, Dylan Gawne, Alex Henkel, Alice D'orlando, and Bleuenn LeSauze. In addition, Cadan Cummings, Chris Cavadini, Brett Dvorak, Coleton King, and Claire Rebman provided tremendous assistance with field and lab measurements.

Thanks to everyone past and present in the Kucharik, Marín-Spiotta, and Jackson lab groups for providing a constructive environment. I especially want to thank Mike Cruse, Laura Szymanski, and Emily Atkinson for their help with getting me started with various methods early on. Conversations with Anna Cates, David Duncan, and Laura Smith were always enjoyable.

Finally, I want to thank my family for everything they have done for me. My parents, Chuck and Diane, and my sister, Mallory, have always been there for me. Erin has been very understanding and supportive of my needs during graduate school, and for that I am thankful.

Table of Contents

Chapter 1

Introduction

1.1 Motivation

Humans have significantly altered the Earth's climate, causing shifts in temperature and precipitation regimes that threaten societies and the ecosystems on which they depend (IPCC 2015; Lewis & Maslin 2015; Scheffers et al. 2016). Since the industrial revolution, global surface temperatures have risen 0.78 °C, polar ice sheets have melted at faster rates, and mean sea level has risen 0.19 m (IPCC 2015). Climate change has directly and indirectly increased human health risks, threatened food and water security, and exacerbated losses of crucial ecosystem services (IPCC 2015; Pecl et al. 2017; Tilman et al. 2017). Although the ramifications of climate change are felt globally, developing countries and disadvantaged people are disproportionally affected (Mora et al. 2013; Dennig et al. 2015; IPCC 2015). Without significant and timely intervention, global climate change will continue to accelerate, and the effects will become effectively irreversible (Solomon et al. 2009; Mora et al. 2013; Bahn et al. 2014; IPCC 2015).

The majority of climate change forcing is attributed to human alterations to the global carbon (C) cycle in the form of a 40% increase in atmospheric CO_2 concentration since 1850 (Keeling 1997; IPCC 2015). Approximately two-thirds of the historic increase in atmospheric CO_2 stems from fossil fuel combustion, while the remaining one-third is a consequence of land use and land cover change (IPCC 2015). Most of the CO_2 emissions associated with land use and land cover change have come from the expansion of agricultural lands, with losses from soils comprising a significant portion of those CO_2 emissions (Houghton & Nassikas 2017;

Sanderman et al. 2017). A positive feedback between climate warming and soil organic carbon (SOC) loss threatens to exacerbate climate change (Crowther et al. 2016; Hicks Pries et al. 2017; Melillo et al. 2017). Thus, the response of soils to climate change and concurrent heightened agricultural demands will play a central part in future human well-being (Amundson et al. 2015; Smith et al. 2015).

Biological sequestration of atmospheric CO_2 in soils has been proposed as one part of the overall strategy to mitigate global climate change (Pacala & Socolow 2004; IPCC 2015; Minasny et al. 2017). Globally, soils store approximately three times as much C as the atmosphere (Schlesinger & Bernhardt 2013), and thus it is generally thought that soils can provide a substantial sink for atmospheric CO_2 (Lal 2004). In addition, the economic cost of C sequestration in soils is low and the technological requirement is relatively small compared to other means (Smith 2012; IPCC 2015). For example, implementing no-till agricultural practices or converting degraded agricultural lands to perennial vegetation have generally been shown to build SOC stocks (Post & Kwon 2000; Angers & Eriksen-Hamel 2008; Kopittke et al. 2017). As an added benefit, when SOC sequestration occurs on agricultural soils, increased agricultural productivity, nutrient retention, and water holding capacity may also be realized (Lal 2004).

Considering that the current annual fossil fuel C emission rate is three times larger than the annual rate of C uptake in terrestrial ecosystems (Le Quéré et al. 2016), reducing fossil fuel C emissions is a top priority for mitigating global climate change (IPCC 2015; Boysen et al. 2017; Walsh et al. 2017). In 2007, the United States Congress passed the Energy Independence and Security Act (EISA), which was aimed in part at reducing net fossil fuel emissions (Pub. L. No. 110-140). The Renewable Fuel Standard created by EISA mandates the production of 136 billion liters per year of biofuel by 2022, of which 61 billion liters must be derived from cellulosic

feedstocks (Pub. L. No. 110-140). Compared to fossil fuels, biofuels can reduce net CO_2 emissions by providing a renewable energy source that effectively recycles atmospheric CO_2 in lieu of adding fossil-derived CO_2 to the atmosphere (Robertson et al. 2011).

To fully assess the net C impact of bioenergy cropping systems on atmospheric CO_2, it is necessary to consider the full biofuel life cycle including the effects on ecosystem C storage (Davis et al. 2009; Robertson et al. 2011). Perennial, cellulose-based biofuel systems are generally considered to provide greater C storage potential than annual, grain-based biofuel systems largely due to less soil disturbance and greater plant-derived belowground C allocation (Holland et al. 2015; Robertson et al. 2017). However, there is a high amount of uncertainty regarding the rate and even the direction of C change under different biofuel cropping systems (Qin et al. 2016). For example, the current SOC stock, previous land use, and rates of residue removal are important determinants of SOC change (Bellamy et al. 2005, Qin et al. 2016), and SOC storage potential varies as a function of climate and edaphic properties (Doetterl et al. 2015; Luo et al. 2017). Thus, generalizations regarding the efficacy of C storage for a given bioenergy cropping system are difficult (Robertson et al. 2017).

To properly inform biofuel policy and land management decisions, ecosystem models must be used to make predictions of C storage under different scenarios and contexts (Campbell & Paustian 2015). Considering that many potential bioenergy crops have not been widely studied, many of the mechanisms required to adequately model ecosystem C dynamics have not been well quantified (Nair et al. 2012; Qin et al. 2015). Furthermore, belowground ecosystem C processes in general are much less understood than their aboveground counterparts (Norby & Jackson 2000), and thus belowground processes are more coarsely represented in many ecosystem models (Smithwick et al. 2014). Thus, improvements to belowground components of

ecosystem models are necessary to better predict C cycling in biofuel cropping systems and in other land use change scenarios (Nair et al. 2012; Campbell & Paustian 2015).

1.2 Objectives

The overarching objective of my research was to better understand the mechanisms contributing to belowground C storage in bioenergy cropping systems so that improved predictions of ecosystem C storage under land use change scenarios could be made. While all major ecosystem C processes were considered, my research largely focused on belowground processes including autotrophic soil respiration from roots (R_A), heterotrophic soil respiration from decomposers (R_H), and SOC stabilization (Fig. 1.1).

In Chapter 2, I evaluated the annual ecosystem C balance in long-term no-till maize and post-establishment phase switchgrass bioenergy systems, and I determined the processes that were most important for ecosystem C storage. Since maize and switchgrass are annual and perennial biofuel systems, respectively, I expected that switchgrass would have a more favorable C balance due to increased belowground inputs. I used multiple *in situ* approaches to estimate annual C fluxes of net photosynthesis, aboveground net primary production, belowground net primary production, R_A, and R_H.

In Chapter 3, I sought to better understand the physiological basis for differences in R_A between maize and switchgrass to improve the representation of root respiration in ecosystem models. Considering that maize is a fast-growing annual plant and that switchgrass is a slower-growing perennial, I hypothesized that maize and switchgrass would have differences in the quantity of C allocated to growth and maintenance root respiration. I used *in situ* diel and

seasonal soil respiration measurements to parametrize and validate a mechanistic root respiration model and subsequently elucidate physiological differences between species.

In Chapter 4, I investigated whether differences in soil microclimate (i.e. soil temperature and soil moisture) among bioenergy cropping systems were sufficient to drive differences in annual ecosystem C losses from R_H. I expected that less extreme soil temperature and moisture regimes would be found under perennial systems, and that the contrasting soil microclimates could cause seasonal differences in R_H. I used six years of high-frequency soil temperature and moisture data to illustrate temporal differences in soil microclimate, and I parametrized a simple model to evaluate the direct effects of soil temperature and soil moisture on R_H.

In Chapter 5, I examined changes in SOC fractions five years after bioenergy cropping system establishment to better understand the mechanisms underpinning bulk SOC change. I expected that changes in SOC fractions would be related to crop- and site-specific differences in plant litter input quantity, litter quality (i.e. C:N), and soil texture (i.e. clay content). This study encompassed four bioenergy cropping systems and was performed at two sites with contrasting soil textures. I used a density-based fractionation method to isolate three SOC fractions from archived soil samples taken in 2008 and 2013, and I used measurements of above- and belowground litter inputs to better understand the changes within each fraction.

In Chapter 6, I outlined the root regression method for separating R_A and R_H *in situ*. While the method has been suggested as an effective approach for separating the two sources of respiration, the assumptions, limitations, and logistical considerations have not been thoroughly elucidated. I used a literature survey and field-based measurements to evaluate the potential use of the root regression method under different circumstances.

1.3 References

Amundson, R., Berhe, A. A., Hopmans, J. W., Olson, C., Sztein, A. E., Sparks, D. L. 2015. Soil and human security in the 21st century. Science 348: 1261071.

Angers, D. A., Eriksen-Hamel, N. S. 2008. Full-inversion tillage and organic carbon distribution in soil profiles: A meta-analysis. Soil Science Society of America Journal 72:1370–1374.

Bahn, M., Reichstein, M., Dukes, J. S., Smith, M. D., McDowell, N. G. 2014. Climate-biosphere interactions in a more extreme world. New Phytologist 202:356–359.

Bellamy, P. H., Loveland, P. J., Bradley, R. I., Lark, R. M., Kirk, G. J. D. 2005. Carbon losses from all soils across England and Wales 1978-2003. Nature 437:245–248.

Boysen, L. R., Lucht, W., Gerten, D., Heck, V., Lenton, T. M., Schellnhuber, H. J. 2017. The limits to global-warming mitigation by terrestrial carbon removal. Earth's Future 5:463–474.

Campbell, E. E., Paustian, K. 2015. Current developments in soil organic matter modeling and the expansion of model applications: a review. Environmental Research Letters 10:123004.

Crowther, T. W., Todd-Brown, K. E. O., Rowe, C. W., Wieder, W. R., Carey, J. C., Machmuller, M. B., Snoek, B. L., Fang, S., Zhou, G. et al. 2016. Quantifying global soil carbon losses in response to warming. Nature 540:104–108.

Davis, S. C., Anderson-Teixeira, K. J., DeLucia, E. H. 2009. Life-cycle analysis and the ecology of biofuels. Trends in Plant Science 14:140–146.

Dennig, F., Budolfson, M. B., Fleurbaey, M., Siebert, A., Socolow, R. H. 2015. Inequality, climate impacts on the future poor, and carbon prices. Proceedings of the National Academy of Sciences of the United States of America 112:15827–15832.

Doetterl, S., Stevens, A., Six, J., Merckx, R., Van Oost, K., Casanova Pinto, M., Casanova-Katny, A., Munoz, C., Boudin, M. et al. 2015. Soil carbon storage controlled by interactions between geochemistry and climate. Nature Geoscience 8:780–783.

Hicks Pries, C. E., Castanha, C., Porras, R. C., Torn, M. S. 2017. The whole-soil carbon flux in response to warming. Science 355:1420–1422.

Holland, R. A., Eigenbrod, F., Muggeridge, A., Brown, G., Clarke, D., Taylor, G. 2015. A synthesis of the ecosystem services impact of second generation bioenergy crop production. Renewable and Sustainable Energy Reviews 46:30–40.

Houghton, R. A., Nassikas, A. A. 2017. Global and regional fluxes of carbon from land use and land cover change 1850-2015. Global Biogeochemical Cycles 31:456–472.

Intergovernmental Panel on Climate Change (IPCC). 2015. Climate Change 2014: Synthesis

Report. Contribution of Working Groups I, II and III to the Fifth Assessment Report of the Intergovernmental Panel on Climate Change. Core Writing Team, Pachauri, R.K., Meyer, L.A. (eds.). IPCC, Geneva, Switzerland.

Keeling, C. D. 1997. Climate change and carbon dioxide: An introduction. Proceedings of the National Academy of Sciences 94:8273–8274.

Kopittke, P. M., Dalal, R. C., Finn, D., Menzies, N. W. 2017. Global changes in soil stocks of carbon, nitrogen, phosphorus, and sulphur as influenced by long-term agricultural production. Global Change Biology 23:2509–2519.

Lal, R. 2004. Soil carbon sequestration impacts on global climate change and food security. Science 304:1623-1627.

Le Quéré, C., Andrew, R. M., Canadell, J. G., Sitch, S., Korsbakken, J. I., Peters, G. P., Manning, A. C., Boden, T. A., Tans, P. P. et al. 2016. Global carbon budget 2016. Earth System Science Data 8:605–649.

Lewis, S. L., Maslin, M. A. 2015. Defining the Anthropocene. Nature 519:171–180.

Luo, Z. K., Feng, W. T., Luo, Y. Q., Baldock, J., Wang, E. L. 2017. Soil organic carbon dynamics jointly controlled by climate, carbon inputs, soil properties and soil carbon fractions. Global Change Biology 23:4430–4439.

Melillo, J. M., Frey, S. D., DeAngelis, K. M., Werner, W. J., Bernard, M. J., Bowles, F. P., Pold, G., Knorr, M. A., Grandy, A. S. 2017. Long-term pattern and magnitude of soil carbon feedback to the climate system in a warming world. Science 358:101–104.

Minasny, B., Malone, B. P., McBratney, A. B., Angers, D. A., Arrouays, D., Chambers, A., Chaplot, V., Chen, Z.-S., Cheng, K. et al. 2017. Soil carbon 4 per mille. Geoderma 292:59–86.

Mora, C., Frazier, A. G., Longman, R. J., Dacks, R. S., Walton, M. M., Tong, E. J., Sanchez, J. J., Kaiser, L. R., Stender, Y. O. et al. 2013. The projected timing of climate departure from recent variability. Nature 502:183–187.

Nair, S. S., Kang, S. J., Zhang, X. S., Miguez, F. E., Izaurralde, R. C., Post, W. M., Dietze, M. C., Lynd, L. R., Wullschleger, S. D. 2012. Bioenergy crop models: descriptions, data requirements, and future challenges. Global Change Biology Bioenergy 4:620–633.

Norby, R. J., Jackson, R. B. 2000. Root dynamics and global change: seeking an ecosystem perspective. New Phytologist 147:3–12.

Pacala, S., Socolow, R. 2004. Stabilization wedges: Solving the climate problem for the next 50 years with current technologies. Science 305:968–972.

Pecl, G. T., Araujo, M. B., Bell, J. D., Blanchard, J., Bonebrake, T. C., Chen, I. C., Clark, T. D., Colwell, R. K., Danielsen, F. et al. 2017. Biodiversity redistribution under climate

change: Impacts on ecosystems and human well-being. Science 355:eaai9214.

Post, W. M., Kwon, K. C. 2000. Soil carbon sequestration and land-use change: processes and potential. Global Change Biology 6:317–327.

Public Law Number (Pub. L. No.) 110-140 § 202 112S1492. Energy Independence and Security Act of 2007.

Qin, Z., Dunn, J. B., Kwon, H., Mueller, S., Wander, M. M. 2016. Soil carbon sequestration and land use change associated with biofuel production: empirical evidence. Global Change Biology Bioenergy 8:66–80.

Qin, Z. C., Zhuang, Q. L., Cai, X. M. 2015. Bioenergy crop productivity and potential climate change mitigation from marginal lands in the United States: An ecosystem modeling perspective. Global Change Biology Bioenergy 7:1211–1221.

Robertson, G. P., Hamilton, S. K., Barham, B. L., Dale, B. E., Izaurralde, R. C., Jackson, R. D., Landis, D. A., Swinton, S. M., Thelen, K. D., Tiedje, J. M. 2017. Cellulosic biofuel contributions to a sustainable energy future: Choices and outcomes. Science 356:eaal2324.

Robertson, G. P., Hamilton, S. K., Del Grosso, S. J., Parton, W. J. 2011. The biogeochemistry of bioenergy landscapes: carbon, nitrogen, and water considerations. Ecological Applications 21:1055–1067.

Sanderman, J., Hengl, T., Fiske, G. J. 2017. Soil carbon debt of 12,000 years of human land use. Proceedings of the National Academy of Sciences 114:9575–9580.

Scheffers, B. R., De Meester, L., Bridge, T. C. L., Hoffmann, A. A., Pandolfi, J. M., Corlett, R. T., Butchart, S. H. M., Pearce-Kelly, P., Kovacs, K. M. et al. 2016. The broad footprint of climate change from genes to biomes to people. Science 354:aaf7671.

Schlesinger W.H., Bernhardt, E.H. 2013. Biogeochemistry: An analysis of global change. Academic Press, Oxford, UK.

Smith, P. 2012. Soils and climate change. Current Opinion in Environmental Sustainability 4:539–544.

Smith, P., House, J. I., Bustamante, M., Sobocká, J., Harper, R., Pan, G., West, P. C., Clark, J. M., Adhya, T. et al. 2015. Global change pressures on soils from land use and management. Global Change Biology 22:1008–1028.

Smithwick, E. A. H., Lucash, M. S., McCormack, M. L., Sivandran, G. 2014. Improving the representation of roots in terrestrial models. Ecological Modelling 291:193–204.

Solomon, S., Plattner, G.-K., Knutti, R., Friedlingstein, P. 2009. Irreversible climate change due to carbon dioxide emissions. Proceedings of the National Academy of Sciences 106:1704–1709.

Tilman, D., Clark, M., Williams, D. R., Kimmel, K., Polasky, S., Packer, C. 2017. Future threats to biodiversity and pathways to their prevention. Nature 546:73–81.

Walsh, B., Ciais, P., Janssens, I. A., Penuelas, J., Riahi, K., Rydzak, F., van Vuuren, D. P., Obersteiner, M. 2017. Pathways for balancing CO_2 emissions and sinks. Nature Communications 8:14856.

1.4 Figures

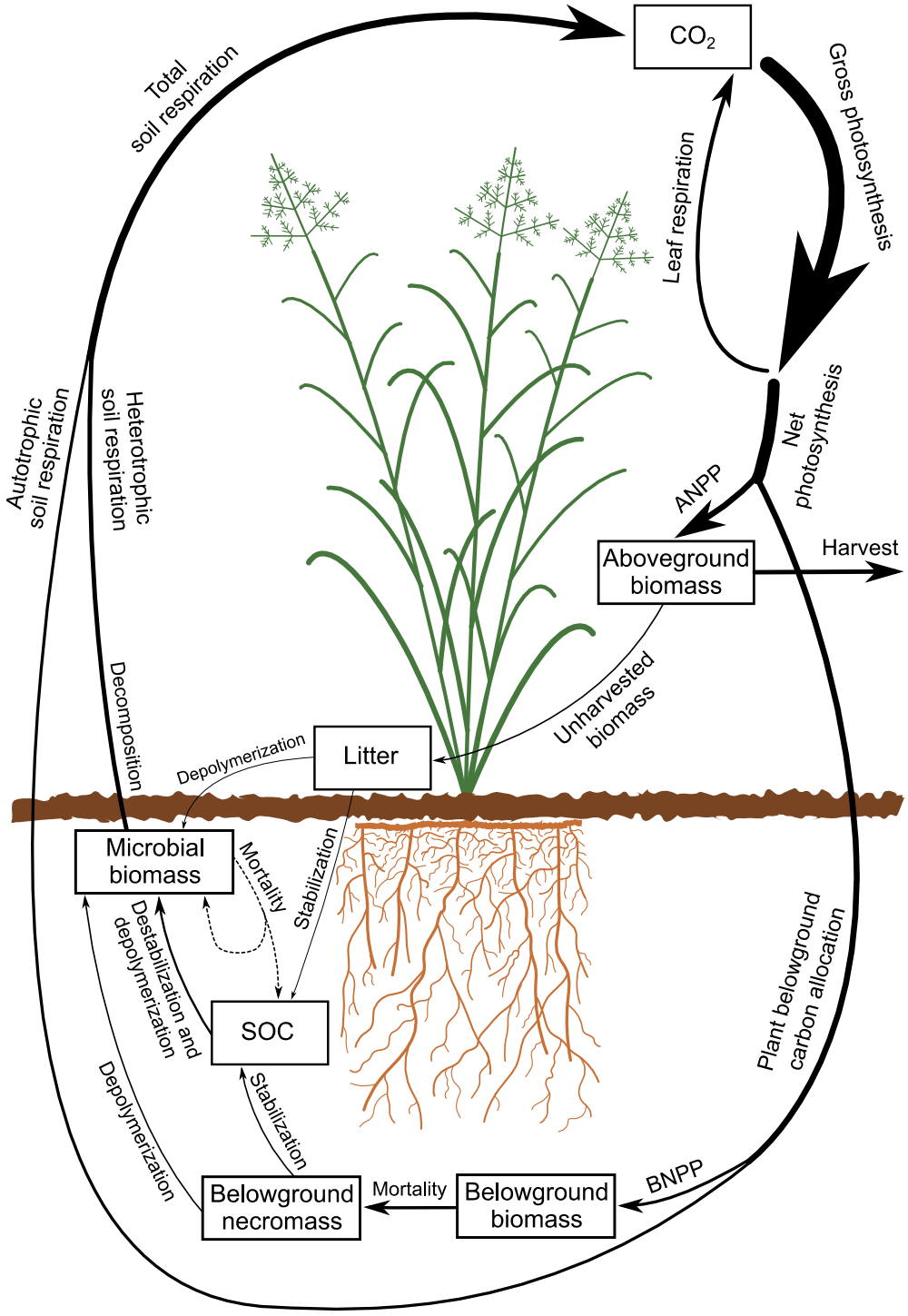

Figure 1.1 – Major ecosystem carbon fluxes within a hypothetical temperate bioenergy cropping system. The arrow widths are proportional to the flux sizes.

Chapter 2

Annual ecosystem carbon balances in long-term no-till maize and mature switchgrass bioenergy cropping systems: evaluating methods and processes

von Haden, A.C., Marín-Spiotta, E., Jackson, R.D., Kucharik, C.J.

Target journal: Agriculture, Ecosystems & Environment

Abstract

As biofuel production continues to rise, feedstock selection decisions will have larger consequences for ecosystem carbon (C) storage. Although perennial cropping systems such as switchgrass are generally thought to sequester more C relative to annual systems such as maize, few direct comparisons have been made, particularly in long-term no-till maize and post-establishment phase perennial systems. We used two methods based on net photosynthesis and biometric measurements, respectively, to estimate net ecosystem production (NEP) in 8- and 9-year-old no-till maize and switchgrass bioenergy cropping systems on highly productive soils in south central Wisconsin. Both methods indicated that annual NEP was considerably greater in maize than switchgrass for both study years, but the methods showed better agreement for switchgrass. Differences in canopy net photosynthesis, autotrophic soil respiration, and heterotrophic soil respiration all contributed to divergent NEP estimates between crops. After accounting for harvested C, the average net ecosystem carbon balances (NECB) were -100 ± 22 and 145 ± 74 for maize and -241 ± 85 and -267 ± 56 for switchgrass using the photosynthesis and biometric methods, respectively. The relatively favorable NECB of maize could stem from low residue harvest, no-till management, and low-stress growing conditions during the years of study, while the relatively unfavorable NECB of switchgrass could be a result of the older stand

age or switchgrass cultivar. Although there are many other important ecological and economic considerations with biofuel feedstock selection, mature switchgrass does not appear to enhance ecosystem C sequestration relative to no-till maize at our highly productive site.

2.1 Introduction

Between 2007 and 2016, U.S. consumption of biomass-based ethanol fuels more than doubled, with most of the ethanol being produced from maize (*Zea mays* L.) grain (U.S. EIA 2017). As the U.S. transportation sector continues to rely more heavily on biofuels, feedstock selection and other land management decisions will have increasingly greater impacts on net carbon (C) emissions and ecosystem C storage (Robertson et al. 2011). Biofuel cropping systems have the potential to reduce net C emissions by providing a non-fossil renewable fuel source and through removal of atmospheric CO_2 via enhanced C sequestration in soils (Adler et al. 2007; Follett et al. 2012). Annual biofuel cropping systems such as maize may only offer marginal net C reductions over conventional fuels (Hill et al. 2006), although improved management practices such as conservation tillage and cover cropping often improve C storage potential (Post et al. 2004). Perennial, cellulosic biofuel feedstocks such as switchgrass (*Panicum virgatum* L.) are expected to offer greater net C reductions due to reduced external inputs and improved ecosystem C sequestration (Robertson et al. 2011). Yet, few empirical studies have directly compared ecosystem C changes between annual and perennial bioenergy cropping systems.

Temporal changes in ecosystem C storage can be calculated as the change in soil organic carbon (SOC) stocks plus the change in above-and belowground plant biomass C stocks. However, due to high SOC spatial variability, short-term changes in SOC are notoriously difficult to detect, and more than a decade is required to detect typical management-induced

SOC changes with most soil sampling schemes (Necpálová et al. 2014). Eddy covariance systems can provide high-frequency estimates of net ecosystem C exchange, but they require large fetch areas in the range of 150 to 200 m for biofuel cropping systems (Bhardwaj et al. 2011) and therefore are not practical for most replicated field trials. Importantly, neither method provides comprehensive estimates of detailed ecosystem C processes such as net canopy photosynthesis, autotrophic soil respiration, and heterotrophic soil respiration. Thus, while C stock and eddy covariance methods can provide estimates of ecosystem C change among different agronomic systems, the ecosystem-level processes underlying C change remain unresolved with these approaches.

Two other approaches, the photosynthesis method (Arkebauer et al. 2009) and the biometric method (Cahill et al. 2009), can be used independently to estimate net ecosystem production (NEP), and when combined they may provide more detailed insight into ecosystem C processes. Each method uses an independent approach to estimate NEP. Net ecosystem production is equal to the difference between gross photosynthetic C uptake and ecosystem respiratory C loss (Woodwell and Whittaker 1968; Chapin et al. 2006):

$$NEP = \text{Gross photosynthesis} - (\text{leaf respiration} + \text{total soil respiration}) \quad (2.1)$$

Typically, gross photosynthesis and respiration are not measured separately but instead are integrated into net photosynthesis (i.e. gross photosynthesis minus leaf respiration). Thus, the photosynthesis (PS) method quantifies NEP as the difference between net photosynthesis and total soil respiration (Arkebauer et al. 2009):

$$NEP_{PS} = \text{Net photosynthesis} - \text{total soil respiration} \quad (2.2)$$

However, scaling leaf-level photosynthesis to the canopy-level can be challenging, due in part to the complex interactions between the plant canopy structure and light attenuation. Alternatively, the biometric (BM) approach estimates NEP as the difference between net primary production and heterotrophic soil respiration (Cahill et al. 2009):

$$NEP_{BM} = \text{Net primary production} - \text{heterotrophic respiration} \quad (2.3)$$

Heterotrophic respiration is particularly difficult to measure, because it requires partitioning total soil respiration into root-derived (autotrophic) and microbial-derived (heterotrophic) respiration. While several approaches for partitioning total soil respiration into the source components exist, all approaches have inherent limitations (Subke et al. 2006).

The net ecosystem carbon balance (NECB) represents the difference between NEP and other C fluxes such as methane, dissolved C leaching, and erosion (Chapin et al. 2006). In agronomic systems, the primary C flux is biomass harvest. Therefore, for the two methods:

$$NECB_{PS} = \text{Net photosynthesis} - \text{total soil respiration} - \text{harvest} \quad (2.4)$$

$$NECB_{BM} = \text{Net primary production} - \text{heterotrophic respiration} - \text{harvest} \quad (2.5)$$

While both photosynthesis and biometric methods have inherent challenges, using both methods simultaneously generates two separate estimates of NEP and NECB, allowing an additional assessment of uncertainty. Our overall objective was to assess NEP and NECB in maize and switchgrass bioenergy cropping systems using both the PS and BM methods. In doing so, we explored the ecosystem C processes most responsible for divergences in NEP and NECB between cropping systems.

2.2 Methods

2.2.1 Study site

This study was undertaken within the DOE-Great Lakes Bioenergy Research Center's Biofuel Cropping Systems Experiment (BCSE) at the Arlington Agricultural Research Station in southcentral Wisconsin, USA (43.296° N, 89.380° W). Soils at the site are dominated by Plano silt loam, which is classified as a Fine-silty, mixed, superactive, mesic Typic Argiudoll (Soil Survey Staff 2017). Thirty-year (1981-2010) site mean annual temperature and precipitation are 6.9 °C and 869 mm, respectively (NOAA 2017). The BCSE was established in 2008 and consisted of a randomized complete block design with five replicates (Sanford et al. 2016). Each plot was 27.4 x 42.7 m wide with at least 12 m between any two plots. We conducted our experiments in continuous no-till maize (*Zea mays* L.) and "Cave-In-Rock" switchgrass (*Panicum virgatum* L.) bioenergy cropping systems within three of the five replicated blocks. Maize and alfalfa crops were grown for many years prior to the establishment of the BCSE experiment in 2008 (Sanford et al. 2016). Switchgrass was planted in June 2008 and maize was planted annually each spring beginning in 2008. In line with local best management practices, maize received an average of 167 kg N ha^{-1} yr^{-1} and P and K as necessary, whereas switchgrass received 56 kg N ha yr^{-1} (Sanford et al. 2016). Herbicides were applied to maintain near-monoculture systems. Additional agronomic details were provided in Sanford et al. (2016). All measurements reported in our study were taken within the center 18.3 x 42.7 m section of each plot.

2.2.2 Canopy net photosynthesis

Canopy net photosynthesis was estimated by integrating a two-layer (sunlit and shaded) light attenuation model with sunlit and shaded leaf-level net photosynthetic light responses (de Pury & Farquhar 1997; Arkebauer et al. 2009). Complete details of this procedure are provided in the supplemental methods (2.9.1). In summary, photosynthetic light response measurements were made throughout three growing seasons, and the light responses for each crop were fit to a saturating exponential function that also accounted for leaf temperature (T_{leaf}) and leaf vapor pressure deficit (VPD_{leaf}). Model performance was assessed using a Monte Carlo cross-validation procedure. Above-canopy direct and diffuse photosynthetically active radiation (PAR) were measured throughout 2015 and 2016 using a shadowband apparatus as described in Cruse et al. (2015). Seasonal patterns of leaf area index (L_t), leaf zenith angle distribution (LAD), and apparent vegetation clumping (Ω) were estimated using an LAI-2000 plant canopy analyzer (LI-COR Inc., Lincoln, Nebraska, USA) with 40 below-canopy measurements per plot per measurement date. Hourly weather dynamics were measured at a nearby weather station (AWON 2017). A canopy light attenuation model following Campbell & Norman (1998) was used to estimate hourly PAR in the sunlit and shaded fractions of the canopy. The light attenuation model was integrated with the photosynthetic light response model, and hourly air temperature, vapor pressure deficit, PAR, and canopy parameters were used to drive the model from the date of plant emergence through the date of complete plant senescence (hereafter defined as the growing season).

Since it was not possible to directly validate the canopy-level net photosynthesis model at our site, we performed a series of sensitivity analyses to evaluate which model inputs and assumptions would cause the largest deviation in annual canopy net photosynthesis. First, we

compared our estimated LAD with six theoretical LADs that spanned from planophile to erectophile (de Wit 1965). Since maize may display non-uniform leaf azimuth distribution (Girardin & Tollenaar 1994), we also evaluated the maize model sensitivity to our assumption of uniform leaf azimuth distribution by assigning a bimodal leaf azimuth distribution (Teh et al. 2000). We independently varied L_t, above canopy total PAR (Q_t), and diffuse PAR (Q_{od}) between -20% and +20% of measured values. Finally, we separately varied daytime and nighttime leaf temperatures ($T_{leaf,day}$ and $T_{leaf,night}$) from -5 °C to +5 °C of measured temperatures. The changes in $T_{leaf,day}$ and $T_{leaf,night}$ also accounted for subsequent changes to VPD_{leaf}. We converted the absolute deviation in annual net photosynthesis to percent change to standardize the sensitivity analyses among cropping systems and years. A complete description of the sensitivity analysis is given in the supplemental methods (2.9.2).

2.2.3 Soil respiration

Total soil respiration (R_T) and heterotrophic-derived soil respiration (R_H) were measured throughout 2015 and 2016 using an LI-6400XT portable photosynthesis system with an LI-6400-09 soil CO_2 flux chamber (LI-COR Inc., Lincoln, NE, USA). In each plot, six 5 cm tall, 10.2 cm inner-diameter polyvinyl chloride (PVC) collars were inserted approximately 2 cm into the soil for R_T measurements. We attempted to capture R_T spatial heterogeneity by stratifying the collar placement across zones likely to vary in root biomass and thus R_T (Prolingheuer et al. 2014). For maize, two collars were placed within the rows, two were place in the interrow, and two were placed halfway between the row and interrow. For switchgrass, two collars were placed on a plant crown, two were placed in the center of the interstitial space, and two were places halfway between the crown and center interstitial space. To further reduce spatial autocorrelation, we

located half of the collars in the south end of the plot, and half of the collars in the north side of the plot such that the north and south collar locations were separated by approximately 33 m. Live aboveground plant biomass growing within the collars was clipped near the soil surface and removed prior to measuring R_T, but all dead plant litter was left within the collars. Soil temperature measurements at were taken near each collar at 2 cm deep using a thermistor probe (Hanna Instruments, Woonsocket, RI, USA). The R_T measurements were made approximately semi-weekly during the summer, weekly to semi-monthly during the spring and fall, and monthly during the winter.

We estimated R_H using the root exclusion approach, where the CO_2 respiration of root-free soil was assumed to represent R_H (Vogel & Valentine 2005; Subke et al. 2006). In spring 2014, 2015, and 2016, we used a 12.7 cm diameter bucket auger to make holes for two root exclusion collars per plot. The root exclusion collars were located near each set of R_T collars so that the two root exclusion collars within each plot were separated by about 33 m. The soil was removed in 10 cm intervals and kept separate so that it could be backfilled into the root exclusion collars in the correct order. Each layer of soil was sieved *in situ* with a 5 mm mesh to remove living roots, but dead roots were left in the soil. The holes for the root exclusion collars were augured down to the C horizon, which typically occurred at 100 cm. A 10.2 cm inner diameter PVC tube was cut to extend from the bottom of the hole to 3 cm above the soil surface. The PVC tube was then placed into the hole and each soil layer was backfilled and packed to the original bulk density. After the final layer was added and packed, a 5 mm diameter hole was drilled in the PVC collar at the soil surface to allow water to drain from inside the collar. One Decagon 5TM soil moisture sensor (Decagon Devices Inc., Pullman, WA, USA) was inserted vertically into the soil in the center of each root exclusion collar ($M_{soil,in}$) and another sensor inserted vertically

approximately 10 cm from the outside of each R_H collar ($M_{soil,out}$). When soils were not frozen, the soil moisture sensors were monitored concurrent with R_H measurements using a Decagon ProCheck (Decagon Devices Inc., Pullman, WA, USA). Measurement timing and frequency for R_H was the same as for R_T except for one date in November 2015 when only R_H was measured. The R_H measurements were taken on the root exclusion collars that had most recently been installed (i.e. within the last year) to minimize the effect of substrate depletion on R_H (Vogel & Valentine 2005).

Measured R_H values were corrected for differences in soil moisture between the inside and outside of the root exclusion collars based on data-fitted soil temperature and moisture models (Prolingheuer et al. 2014). Full details are given in the supplemental methods (2.9.3). Measured R_T and moisture-corrected R_H values were converted to g C m^{-2} day^{-1}, linearly interpolated to daily intervals, and summed to estimate annual soil respiration fluxes (Gomez-Casanovas et al. 2013).

2.2.4 Biometric measurements

Aboveground net primary productivity was estimated using the peak standing biomass method (Scurlock et al. 2002). For maize, aboveground biomass was clipped at the soil surface at crop physiological maturity in late September 2015 and 2016 using three 1.5 x 0.65 m quadrats per plot. This quadrat size was selected to accommodate the maize row spacing. For switchgrass, aboveground biomass was clipped at the soil surface in late August 2015 and 2016 using three 1 x 1 m quadrats per plot. All aboveground biomass was bagged and placed into a 65 °C oven until dried to a constant weight.

Belowground net primary productivity was estimated with the root ingrowth method (Persson et al. 1979) using an approach similar to von Haden & Dornbush (2017b). Root ingrowth cores consisted of 50 cm long, 6.9 cm inner diameter, 7.4 cm outer diameter plastic mesh tubes (Industrial Netting Inc., Minneapolis, MN, USA) with a fiberglass mesh screen affixed to the bottom. Root ingrowth was measured in approximately monthly increments during the growing season of each crop. At the beginning of each ingrowth period, six 7.6 cm diameter holes per plot were bucket augured to 40 cm deep. The soil was removed in 10 cm layers, and each layer was kept separate so that the soil could be backfilled in the correct order. Each layer was sieved to 5 mm to remove root biomass, and the root biomass was washed with water over an 800 μm sieve and dried at 65 °C to a constant weight. Soil from each layer was dried overnight at 65 °C and weighed. Root ingrowth cores were inserted into the augured holes, the soil layers were serially backfilled into the cores, and each layer was packed to the original bulk density. After each layer was added and packed, 300 mL of water was added so that the soil structure and water content would return to near-field conditions. Following each ingrowth period, a machete was used to severe the roots around the outside the ingrowth cores, and the cores were then extracted. Soil from the ingrowth cores was serially sieved through a 5 mm mesh screen to remove roots, and the sieved soil was hand-picked free of any visible remaining root fragments. Ingrowth roots were washed with water over an 800 μm sieve until all visible soil was removed, and the clean roots were placed in a 65 °C oven until weight was constant. Corrections for belowground growth below 40 cm and rhizodeposition were made following von Haden & Dornbush (2017b). First, root biomass depth profiles were modelled as:

$$R_B(D_C) = j[1 - \exp(-kD_C)] \quad (2.6)$$

where R_B is measured root biomass, D_C is the measured cumulative depth below the soil surface, and *j* and *k* are fitted coefficients. A correction factor for biomass below 40 cm was calculated as $R_B(100\ cm)/R_B(40\ cm)$ and multiplied by measured root ingrowth values to estimate root ingrowth to 100 cm. We chose a cutoff depth of 100 cm because this is the typical depth of the coarse-textured, gravelly C horizon at which root growth is likely to be limited. A correction factor of 1.06 was also applied to the switchgrass root growth to adjust for the deeper distribution of root growth compared to root biomass in perennial grasslands (von Haden & Dornbush 2017a). A median rhizodeposition estimate of 163 ug C mg^{-1} belowground biomass production (Nguyen 2003) was applied to the depth-corrected root ingrowth values for maize and switchgrass. For each plot, corrected root ingrowth plus rhizodeposition was summed over all ingrowth periods to estimate annual BNPP to 100 cm.

Aboveground biomass was harvested from the entire plots at the end of the growing season using large-scale farm equipment (Sanford et al. 2016). Maize grain was harvested using a six-row grain combine with grain wagon, while maize stover was harvested at approximately 5 to 10 cm above the soil surface using a flail-chopper with forage wagon. Switchgrass was harvested after the first killing frost using a self-propelled forage harvester with dump wagon, leaving approximately 15 cm of stubble. All harvested biomass was weighed using load-cells within the wagons. Maize grain moisture was determined with a GAC 2100 AGRI grain moisture meter (Dickey-John Corp., Auburn, IL, USA) while subsamples of maize stover and switchgrass were dried at 65 °C to determine moisture content. All wet harvest values were then corrected to dry matter.

Subsamples of above- and belowground plant samples were pulverized prior to determination of carbon and nitrogen on a Flash EA 1112 elemental analyzer (Thermo Electron Corp., Milan, Italy).

2.2.5 Model fitting and computations

All non-linear models were fit using the 'nlsLM' non-linear least squares function (Elzhov et al. 2016) in R version 3.4.1 (R Core Team 2017). Integrals were numerically approximated by dividing the interval into 10° subintervals (i.e. 9 subintervals per 90°), calculating the area of a rectangle under each subinterval, and summing the areas. Light attenuation and photosynthesis models were coded and executed in R. NEP and NECB were calculated using equations 2.2 through 2.5.

2.3 Results

2.3.1 Leaf-level net photosynthesis models

Leaf-level photosynthesis models explained 80% to 94% of the variability in measured leaf-level net photosynthesis ($A_{net,leaf}$) (Fig. 2.1). Maize models fit marginally better than switchgrass models, and upper canopy models fit slightly better than lower canopy models. The differences in model fit were likely due in part to the intrinsically greater range of $A_{net,leaf}$ in maize than switchgrass and in the upper leaves compared to lower canopy leaves. Median absolute error ranged from 1.06 to 1.29 μmol CO_2 m^{-2} s^{-1} and was somewhat greater in maize than switchgrass and greater in the upper canopy than in the lower canopy (Table 2.S.3).

2.3.2 Growing season conditions and plant canopy dynamics

Both 2015 and 2016 were warmer and wetter than normal, with the growing season in 2016 being slightly warmer and wetter than in 2015 (Table 2.1). The switchgrass growing season was 22 and 42 days longer than the maize growing season in 2015 and 2016, respectively, owing both to an earlier start and a later end in switchgrass (Table 2.2). Mean T_{leaf} and VPD_{leaf} were slightly greater in maize than in switchgrass and were greater in 2016 than 2015 (Table 2.2).

Maize leaf area index (L_t) peaked at approximately 6.2 m^2 m^{-2} in 2015 and 4.9 m^2 m^{-2} in 2016, whereas switchgrass peaked near 6.6 and 7.0 m^2 m^{-2} in 2015 and 2016, respectively (Fig. 2.2). Switchgrass L_t also tended to be more variable among plots than maize, likely reflecting true differences among the three switchgrass replicates. Canopy measurements from the LAI-2000 indicated that maize and switchgrass approximated uniform leaf angle distributions with extremophile tendencies (Fig. 2.S.2b). Subsequently, seasonal mean tip angle was between 43.2° and 44.4° except for switchgrass in 2016 when seasonal mean tip angle was 35.1° (Table 2.2). Mean apparent vegetation clumping index was 0.96 for maize and 0.90 in switchgrass, thus indicating more non-randomness in switchgrass. Partitioning of Q_{od} and Q_{ob} varied between years, with a greater proportion of Q_{od} in 2015 than 2016 (Table 2.2). Mean total above canopy PAR (Q_{ob} + Q_{od}) was also slightly greater in 2015 compared to 2016. In maize, mean Q_{sh} and mean Q_{sl} were nearly identical between years, but in switchgrass mean Q_{sh} and mean Q_{sl} both decreased from 2015 to 2016 (Table 2.2).

2.3.3 Ecosystem C fluxes and C balance

Seasonal patterns of $A_{net,canopy}$ largely reflected the combination of green L_t and leaf-level photosynthetic potential, with a longer but less intensive period of C uptake in switchgrass compared to maize (Fig 2.3). Despite a shorter growing season, annual $A_{net,canopy}$ was 7% and 5% greater in maize compared to switchgrass in 2015 and 2016, respectively (Table 2.3). During the growing season, patterns of R_T mostly mirrored those of $A_{net,canopy}$ (Fig. 2.3). However, R_T was nearly always higher in switchgrass than maize, particularly during the growing season (Fig. 2.3). Consequently, annual R_T was 74% and 65% greater in switchgrass compared to maize in 2015 and 2016, respectively (Table 2.3). Similarly, R_H was 43% and 55% greater in switchgrass than maize in 2015 and 2016, respectively.

On average, maize ANPP was more than double that of switchgrass, and the differences between 2015 and 2016 were minor (Table 2.3). Conversely, BNPP was 30% greater in switchgrass than maize. Harvested C was 153% and 100% greater in maize than switchgrass in 2015 and 2016, respectively. Harvested maize C was relatively consistent between years, but harvested C in switchgrass was 31% greater in 2016 than 2015.

On average, NEP was 748 and 71 g C m^{-2} y^{-1} in maize and switchgrass, respectively (Table 2.3). The NEP_{BM} method had greater NEP values than the NEP_{PS} method for both crops and years except for switchgrass in 2015. The largest difference between NEP_{BM} and NEP_{PS} occurred in 2016 maize when NEP_{BM} was 863 g C m^{-2} y^{-1} and NEP_{PS} was 537 g C m^{-2} y^{-1}. Average NECB was 22.5 g C m^{-2} y^{-1} and -254 g C m^{-2} y^{-1} in switchgrass and maize, respectively. However, the two methods showed much better agreement for switchgrass than maize, with two-year NECB differences of 26 g C m^{-2} y^{-1} and 245 g C m^{-2} y^{-1}, respectively.

2.3.4 Sensitivity analyses

Leaf area index (L_t) had a relatively small effect on annual $A_{net,canopy}$, with a maximum response range of -2.6% to +1.3% over the -20% to +20% L_t range (Table 2.4; Fig. 2.S.4). Daytime Q_{od} and Q_{ot} elicited a positive $A_{net,canopy}$ response, while T_{leaf} day and T_{leaf} night induced negative $A_{net,canopy}$ responses. Daytime Q_{ot} evoked the largest response of all tested environmental variables, with a nearly 1:1 response across the -20% to 20% range. On average, the bimodal leaf azimuth angle distribution reduced annual $A_{net,canopy}$ by less than 1%. However, alternative leaf zenith angle distributions (LAD) had a significant effect on annual $A_{net,canopy}$, ranging from a -6% average difference for the planophile distribution to a +16% average difference for the erectophile distribution (Fig 2.4). The spherical distribution, which is a commonly used distribution when canopy architectural data is absent (Campbell 1986), evoked an average response of +12%. Extremophile, uniform, and plagiophile distributions elicited relatively small changes, but all distributions except for planophile caused positive changes relative to our remotely sensed distributions. The effect of differing LADs on $A_{net,canopy}$ appeared to result largely from changes to the shaded canopy PAR (Q_{sh}) (Fig. 2.4).

2.4 Discussion

2.4.1 NEP and NECB

Estimated NEP was substantially greater in maize than switchgrass for both study years regardless of the method used. While average annual $A_{net,canopy}$ was 6% greater in maize than switchgrass, average annual R_T was 69% greater in maize, and therefore the majority of the estimated difference in NEP_{PS} between maize and switchgrass was due to higher R_T in

switchgrass. Root-derived soil respiration ($R_A = R_T - R_H$) in switchgrass was more than double that of maize, and thus the conversion efficiency of $A_{net,canopy}$ to NPP (ANPP + BNPP) was much lower in switchgrass, resulting in average NPP that was 46% lower in switchgrass relative to maize. Significantly greater NPP in maize, combined with lower R_H in maize, led to dramatically higher NEP_{BM} in maize compared to switchgrass. Although the absolute quantity of harvested biomass was greater in maize, a greater quantity of biomass was also left unharvested in maize. Thus, differences in $A_{net,canopy}$, R_A, R_H, and residue return all contributed significantly to the observed differences in NEP between maize and switchgrass in our study.

Our maize NEP estimates were on the high end of those reported for other maize systems, which have been reported to peak around 800 g C m^{-2} yr^{-1} (West et al. 2010; Hernandez-Ramirez et al. 2011; Sulaiman et al. 2017). These relatively high maize NEP values could be due in part to the highly productive soils at our site, no-till management, or the ideal growing season conditions during our study. Relatively few switchgrass NEP estimates are available, and most estimates have been made in their 2-to 3-year establishment phase. For switchgrass stands between two and six years old, NEP has been reported in the range of -14 to 531 g C m^{-2} yr^{-1} (Skinner & Adler 2010; Zeri et al. 2011; Zenone et al. 2013; Joo et al. 2016). Our switchgrass NEP estimates were on the lower end of this range, which could be due to differences in management practices, switchgrass cultivar, or older stand age (e,g, Parrish & Fike 2005; Fike et al. 2006; Kucharik 2007; Jungers et al. 2015).

The absolute differences in NECB between systems were more nuanced than the differences in NEP. Nonetheless, maize NECB was more favorable than switchgrass in both years regardless of the method employed. While both methods placed switchgrass mean NECB near -250 g C m^{-2} yr^{-1}, the $NECB_{PS}$ and $NECB_{BM}$ methods were less consistent, placing maize

NECB at -100 and 145 g C m^{-2} yr^{-1}, respectively. Considering that the SOC stocks at a proximal agricultural site are on the order of 13 kg C m^{-2} to 90 cm (Sanford et al. 2012), the magnitude of the annual NECB estimates is significant. The variability between methods in maize may be due to an underestimation of $A_{net,canopy}$ with the $NECB_{PS}$ method, as evidenced by the fact that NPP alone exceeded $A_{net,canopy}$ during both years in maize. Of course this is not possible, and it indicates that either NPP was overestimated or $A_{net,canopy}$ was underestimated. Since the methods we used to estimate ANPP and BNPP are generally regarded as conservative (Scurlock et al. 2002; Milchunas 2009), it is more likely that $A_{net,canopy}$ was underestimated than that NPP was overestimated in maize.

The NECB of other maize systems has been reported to vary widely between positive and negative, with the proportion of harvested biomass having a considerable influence (Sulaiman et al. 2017). This finding is echoed by SOC studies that typically show SOC gains in maize bioenergy systems when less than 70% of residue is harvested (Qin et al. 2016). In our maize system, approximately 50% of residue was harvested (Sanford et al. 2016), which may have contributed to the relatively favorable NECB. To our knowledge, no studies have directly evaluated NECB in tilled versus no-till systems (e.g. Bernacchi et al. 2005), but SOC studies show on average a slight SOC increase under no-till (Angers & Eriksen-Hamel 2008). Therefore, it is plausible that the lack of tillage in our maize system may have positively affected NECB.

Direct comparisons of NECB in maize and switchgrass systems are rare, but in contrast to our findings, several studies have reported switchgrass to generally have a more favorable C balance than maize (Zeri et al. 2011; Anderson-Teixeira et al. 2013; Joo et al. 2016). However, consistent with our findings, several other NECB studies have independently found maize to be C neutral or a slight C sink (Bernacchi et al. 2005; Verma et al. 2005) and switchgrass systems to

be a C source (Skinner & Adler 2010). In agreement, a meta-analysis of previous croplands that had been converted to bioenergy systems showed that the average percent SOC increase was slightly greater in maize than switchgrass (Qin et al. 2016). Some of the discrepancy between our study and other maize-to-switchgrass NECB comparisons could be due to the differences in management practices, soil type, site legacy, weather, stand age, and plant varieties. In addition, most NECB studies use the eddy covariance method, while our study combined models and measurements of individual C fluxes. Although the eddy covariance method provides high frequency C balance estimates, typically 30 to 40% of the data must be gap-filled, (Baldocchi 2008), and measurements often are not spatially replicated (e.g. Zenone et al. 2013; Joo et al. 2016). Thus, combining our NECB approaches with eddy covariance may further constrain ecosystem C balances while also offering insight into ecosystem C processes.

2.4.2 Ecosystem C fluxes

Our finding that annual $A_{net,canopy}$ was always greater in maize than switchgrass is perhaps not surprising considering the long history of maize productivity breeding (Troyer 2004). Intrinsically greater leaf-level light use efficiency in maize was apparent from the light response curves and subsequent upper range of $A_{net,leaf}$. Lower L_t in maize also favored $A_{net,canopy}$, as maize L_t was at or only slightly below optimal L_t, whereas switchgrass was above optimal L_t. Canopy structure also played a role, as more vertically-oriented leaves in maize favored greater $A_{net,canopy.}$ We also cannot rule out the possibility that differences in fertilization regime played a role in $A_{net,canopy}$, as maize received N, P, and K, but switchgrass only received N and it was at a lower rate than maize (Sanford et al. 2016). However, N, P and K have generally shown

inconsistent effects on switchgrass net primary productivity (Parrish & Fike 2005; Jach-Smith & Jackson 2015).

Although soil respiration (R_T) is often regarded as an ecosystem flux, it is really comprised of two independent fluxes, R_H and R_A. Fundamentally, R_A is the product of the root quantity and the relative root respiration rate (i.e. respiration per unit of root). The respiration rate per unit root biomass tends to be greater in maize, but switchgrass has a much larger root system to maintain (von Haden 2017). In addition, maize R_A is limited to the growing season whereas switchgrass R_A must be continuous to maintain a perennial root system. Specific root respiration is also a function of soil temperature and photosynthate supply (Savage et al. 2013), which also may differ between maize and switchgrass systems. Thus, while it is difficult to assess the exact reason for higher annual R_A in switchgrass, greater root biomass and continuous maintenance R_A are the most likely causes.

R_H is the CO_2 flux resulting from the microbial decomposition of organic matter, and therefore R_H is controlled in part by organic matter availability and heterotrophic microbial activity (Moyano et al. 2013). More aboveground litter is left unharvested in maize, there are greater root litter inputs in switchgrass, but the overall quantity of litter inputs was much greater in maize. While we did not quantify differences in soil organic matter quality and protection within aggregates, differences between these parameters could also cause differences in R_H (Mueller et al. 2012). Microbial biomass and microbial community structure are known to differ between maize and switchgrass in our study area (Liang et al. 2012; Herzberger et al. 2014), but it is not clear how these differences would alter R_H. Considering the important effects of soil temperature and soil moisture on heterotrophic microbial activity (Moyano et al. 2013),

differences in the soil microclimate between maize and switchgrass could also lead to differences in R_H.

2.4.3 Methods considerations

Overall, our two NECB approaches provided reasonable agreement with each other, particularly in switchgrass. Our study combined two commonly used NECB approaches, but integrating several methods within each approach creates compound error in the final C balance estimate. For the photosynthesis approach, the primary challenge is scaling leaf-level photosynthetic responses to the canopy-level. This requires a complex light attenuation model that relies upon knowledge or assumptions of the plant canopy structure and leaf-level conditions. Our analysis revelated that annual canopy photosynthesis was particularly sensitive to changes in the LAD. More sophisticated remote sensing instrumentation may provide more reliable LAD estimates (e.g. Bailey & Mahaffee 2017). Not surprisingly, alterations in daytime Q_{od} and Q_{ot} also caused substantial changes in the annual net photosynthesis, thus illustrating the importance of accurately measuring and partitioning PAR. Finally, our analysis showed moderate sensitivity of net canopy photosynthesis to T_{leaf}. Using an energy balance approach would help to improve T_{leaf} predictions, although it would also add a substantial amount of model complexity (Campbell & Norman 1998).

Estimating R_H and BNPP are the primary methodological challenges associated with the biometric method. While there are several known limitations to the root exclusion method for R_H, other approaches also have drawbacks (Subke et al. 2006). For example, lack of C inputs from living roots likely reduces substrate for heterotrophs and completely removes root-induced rhizosphere priming, both of which are likely to cause an underestimation of R_H (Kuzyakov

2006). Similarly, all BNPP methods have biases, and the root ingrowth method used in our study is typically considered to be conservative (Milchunas 2009). While it is difficult to assess the overall uncertainty associated with these methods in our study, the fact that the photosynthesis and biometric approaches were reasonably consistent suggests that our R_H and BNPP values were realistic. Using several methods for both R_H and BNPP may help to further constrain the estimates, but the additional time and monetary requirements would probably preclude the use of multiple methods for most studies.

Neither of our approaches accounted for other potentially important NECB fluxes including DOC leaching, methane fluxes, and erosion (Chapin et al. 2006). Prior to this study, DOC leaching had been measured at rates < 2.0 g C m^{-2} yr^{-1} (Anita Thompson, pers. comm.) and thus is not considered a significant NECB component. Trivial methane consumption rates in the range of 0.05 to 0.6 g C m^{-2} yr^{-1} have been measured in grain and forage-based cropping systems within 5 km of our study site (Osterholz et al. 2014). However, topsoil erosion has been reported to have occurred at a rate of 6 cm over 53 years at a maize cropping trial adjacent to our study site (Collier et al. 2017). Assuming erosion occurs consistently among years, and using mean bulk density (1.23 g cm^{-3}) and SOC (2.28%) values for the 0-10 cm horizon for maize at our site, erosion would remove 32 g C m^{-2} yr^{-1}. Presumably, erosion rates would be about an order of magnitude lower in switchgrass than maize (e.g. Helmers et al. 2012). However, it is important to note that SOC removal via erosion does not necessarily translate into C loss to the atmosphere, as C may be simply reallocated on the landscape or become buried sediment (Doetterl et al. 2016).

2.4.4 Implications for bioenergy crop production

Our study was undertaken at a highly productive site with high SOC Mollisols, and thus our results may not be representative of candidate bioenergy production sites which are marginal for row crop agriculture (Gelfand et al. 2013). In addition, our study took place during two years when growing conditions were near ideal for maize. Considering that switchgrass is generally more resistant to stressful growing conditions than maize (e.g. Joo et al. 2016; Sanford et al. 2016), it is plausible that NECB would have been less favorable for maize under more stressful conditions. Nonetheless, at a site 5 km from ours on similar soils, direct measurements of SOC in grain and forage systems have indicated general trends toward SOC loss over 20 years (Sanford et al. 2012). In northeast Wisconsin, NEP in series of restored prairies was not different from zero (von Haden & Dornbush 2017b), and thus harvesting aboveground biomass would have likely caused a negative NECB in those systems. Therefore, it is perhaps not surprising that NECB was negative to near-neutral at our study site. In the Midwest U.S., changes in SOC have been observed to occur in proportion to baseline SOC levels such that soils with the highest initial SOC content lose the most C (or gain the least C), even in conservation tillage and perennial grassland systems (Senthilkumar et al. 2009). Thus, more favorable C balances are likely to be realized on marginal, low SOC soils (Gelfand et al. 2013), but more empirical work is necessary to validate this hypothesis within the context of bioenergy production.

Fundamentally, a favorable C balance is achieved when $A_{net,canopy}$ is relatively large while R_A, R_H, and harvest are relatively small. However, these components are not equally manageable nor independent, which makes agricultural C management challenging. $A_{net,canopy}$ is largely determined by plant type, soil productivity, and weather, but for many crops is manageable to a certain extent by fertilization, pesticide application, and other practices. Plant R_A is largely a

function of plant type and environmental conditions and therefore management options may be limited for a given plant type. Harvest is the most easily manageable parameter, but it is always constrained to less than NPP and in most cases to less than ANPP. Harvest may be linked to R_H, as unharvested biomass is a primary substrate for R_H. However, the relationship between unharvested biomass and an R_H is not straightforward, as the quantity and quality of unharvested biomass may affect a suite of parameters including the microbial community structure, carbon use efficiency, soil aggregation, and priming of native SOC, which in turn may be site-dependent (Cotrufo et al. 2013). In addition, feedbacks between the amount of unharvested biomass and NPP are likely (Blanco-Canqui & Lal 2009). Thus, general recommendations for optimum harvest and residue return rates to produce a favorable C balance cannot be given, and instead must be evaluated with agroecosystem models that adequately capture complex plant and SOC dynamics.

NECB is only one component of the overall ecological footprint of biofuel cropping systems (Robertson et al. 2017). For example, over three years, nitrous oxide (N_2O) fluxes from maize were double that of switchgrass during the establishment phase at our study site (Oates et al. 2016), which thus dramatically influences the overall greenhouse gas balance (e.g. Gelfand et al. 2013). Moreover, other ecosystem services such as pest suppression and pollinator richness are enhanced in switchgrass relative to maize (Werling et al. 2014). Fossil fuel offset credits, which quantify the net amount of fossil fuel emissions replaced by the biofuel system, must also be considered (Gelfand et al. 2013). The economic favorability of bioenergy cropping systems is also likely to vary geographically (Jain et al. 2010). Thus, while it was beyond the scope of this study to provide a comprehensive analysis of the overall viability of our maize and switchgrass

systems, there are clearly many considerations in addition to ecosystem C balance that must be made when selecting a bioenergy cropping system (Robertson et al. 2017).

2.5 Conclusions

We used two methods to estimate NEP in maize and switchgrass. Both methods consistently showed greater NEP in maize than switchgrass, but there was better agreement between methods for switchgrass than for maize. While all components of the NEP estimates are subject to measurement error, the remotely-sensed leaf zenith angle distributions are the most likely source for the disagreement among NEP methods in maize. Refining and combining these two NEP methods with eddy covariance measurements would help to better constrain NECB and would provide additional insight into the underlying ecosystem C processes.

At our site, no-till maize had a slightly more favorable NECB than switchgrass in 2015 and 2016. When considering both of our methods averaged over both years, maize was near C-neutral, while switchgrass was a C source in the range of 250 g C m^{-2} yr^{-1}. However, we have lower confidence in our maize NECB estimate due to the relatively high variability between methods. The more favorable NECB in maize was a function of greater annual $A_{net,canopy}$ and lower annual R_A and R_H in maize relative to switchgrass. Thus, a better understanding of the controls on these ecosystem C processes will improve our ability to predict ecosystem C storage in biofuel cropping systems.

2.6 Acknowledgements

Funding was provided by the Great Lakes Bioenergy Research Center (DOE BER Office of Science DE-FC02-07ER64494 and DOE OBP Office of Energy Efficiency and Renewable Energy DE-AC05-76RL01830), the USDA National Institute of Food and Agriculture (Hatch project 0225417-WIS01586), and the National Science Foundation (grant DEB-1038759). L.G. Oates and G. Sanford provided logistical support and technical expertise. C. Cummings, M. Cruse, J. Sustachek, A. D'orlando, C. Menick, B. Fahney, B. Le Sauz, H. Melampy, A. Henkel, D. Gawne, A. Butz, M. Walsh, C. King, B. Dvorak, and C. Cavadini provided field and lab assistance. Additional thanks to E. Wagner and B. Spaier for help with leaf spectroscopy.

2.7 References

Adler, P. R., Del Grosso, S. J., Parton, W. J. 2007. Life-cycle assessment of net greenhouse-gas flux for bioenergy cropping systems. Ecological Applications 17:675–691.

Anderson-Teixeira, K. J., Masters, M. D., Black, C. K., Zeri, M., Hussain, M., Bernacchi, C. J., DeLucia, E. H. 2013. Altered belowground carbon cycling following land-use change to perennial bioenergy crops. Ecosystems 16:508–520.

Angers, D. A., Eriksen-Hamel, N. S. 2008. Full-inversion tillage and organic carbon distribution in soil profiles: A meta-analysis. Soil Science Society of America Journal 72:1370–1374.

Arkebauer, T. J., Walter-Shea, E. A., Mesarch, M. A., Suyker, A. E., Verma, S. B. 2009. Scaling up of CO_2 fluxes from leaf to canopy in maize-based agroecosystems. Agricultural and Forest Meteorology 149:2110–2119.

Automated Weather Observation Network (AWON). 2017. University of Wisconsin-Extension. http://agwx.soils.wisc.edu.

Bailey, B. N., Mahaffee, W. F. 2017. Rapid measurement of the three-dimensional distribution of leaf orientation and the leaf angle probability density function using terrestrial LiDAR scanning. Remote Sensing of Environment 194:63–76.

Baldocchi, D. 2008. Breathing of the terrestrial biosphere: lessons learned from a global network of carbon dioxide flux measurement systems. Australian Journal of Botany 56:1–26.

Bernacchi, C. J., Hollinger, S. E., Meyers, T. 2005. The conversion of the corn/soybean ecosystem to no-till agriculture may result in a carbon sink. Global Change Biology 11:1867–1872.

Bhardwaj, A. K., Zenone, T., Jasrotia, P., Robertson, G. P., Chen, J., Hamilton, S. K. 2011. Water and energy footprints of bioenergy crop production on marginal lands. Global Change Biology Bioenergy 3:208–222.

Blanco-Canqui, H., Lal, R. 2009. Crop residue removal impacts on soil productivity and environmental quality. Critical Reviews in Plant Sciences 28:139–163.

Cahill, K. N., Kucharik, C. J., Foley, J. A. 2009. Prairie restoration and carbon sequestration: difficulties quantifying C sources and sinks using a biometric approach. Ecological Applications 19:2185–2201.

Campbell, G. 1986. Extinction coefficients for radiation in plant canopies calculated using an ellipsoidal inclination angle distribution. Agricultural and Forest Meteorology 36:317–321.

Campbell, G. S., Norman, J. M. 1998. An Introduction to Environmental Biophysics, 2nd ed. Springer, New York, USA.

Chapin III, F. S., Woodwell, G. M., Randerson, J. T., Rastetter, E. B., Lovett, G. M., Baldocchi, D. D., Clark, D. A., Harmon, M. E., Schimel, D. S. et al. 2006. Reconciling carbon-cycle concepts, terminology, and methods. Ecosystems 9:1041–1050.

Collier, S. M., Ruark, M. D., Naber, M. R., Andraski, T. W., Casler, M. D. 2017. Apparent stability and subtle change in surface and subsurface soil carbon and nitrogen under a long-term fertilizer gradient. Soil Science Society of America Journal 81:310–321.

Cotrufo, M. F., Wallenstein, M. D., Boot, C. M., Denef, K., Paul, E. 2013. The Microbial Efficiency-Matrix Stabilization (MEMS) framework integrates plant litter decomposition with soil organic matter stabilization: do labile plant inputs form stable soil organic matter? Global Change Biology 19:988–995.

Cruse, M. J., Kucharik, C. J., Norman, J. M. 2015. Using a simple apparatus to measure direct and diffuse photosynthetically active radiation at remote locations. PLoS ONE 10:e0115633.

de Pury, D. G. G., Farquhar, G. D. 1997. Simple scaling of photosynthesis from leaves to canopies without the errors of big-leaf models. Plant, Cell & Environment 20:537–557.

de Wit, C. T. 1965. Photosynthesis of leaf canopies. Agricultural Research Report No. 663. Center for Agricultural Publications and Documentation, Wageningen, The Netherlands.

Doetterl, S., Berhe, A. A., Nadeu, E., Wang, Z., Sommer, M., Fiener, P. 2016. Erosion, deposition and soil carbon: A review of process-level controls, experimental tools and models to address C cycling in dynamic landscapes. Earth-Science Reviews 154:102–

122.

Elzhov, V. T., Mullen, K. M., Spiess, A.-N., Bolker, B. 2016. minpack.lm: R Interface to the Levenberg-Marquardt Nonlinear Least-Squares Algorithm Found in MINPACK, Plus Support for Bounds.

Fike, J. H., Parrish, D. J., Wolf, D. D., Balasko, J. A., Green, J. T., Rasnake, M., Reynolds, J. H. 2006. Switchgrass production for the upper southeastern USA: Influence of cultivar and cutting frequency on biomass yields. Biomass & Bioenergy 30:207–213.

Follett, R. F., Vogel, K. P., Varvel, G. E., Mitchell, R. B., Kimble, J. 2012. Soil carbon sequestration by switchgrass and no-till maize grown for bioenergy. Bioenergy Research 5:866–875.

Gelfand, I., Sahajpal, R., Zhang, X., Izaurralde, R. C., Gross, K. L., Robertson, G. P. 2013. Sustainable bioenergy production from marginal lands in the US Midwest. Nature 493:514–519.

Girardin, P., Tollenaar, M. 1994. Effects of intraspecific interference on maize leaf azimuth. Crop Science 34:151–155.

Gomez-Casanovas, N., Anderson-Teixeira, K., Zeri, M., Bernacchi, C. J., DeLucia, E. H. 2013. Gap filling strategies and error in estimating annual soil respiration. Global Change Biology 19:1941–1952.

Helmers, M. J., Zhou, X. B., Asbjornsen, H., Kolka, R., Tomer, M. D., Cruse, R. M. 2012. Sediment removal by prairie filter strips in row-cropped ephemeral watersheds. Journal of Environmental Quality 41:1531–1539.

Helmers, M. J., Zhou, X. B., Asbjornsen, H., Kolka, R., Tomer, M. D., Cruse, R. M. 2012. Sediment removal by prairie filter strips in row-cropped ephemeral watersheds. Journal of Environmental Quality 41:1531–1539.

Hernandez-Ramirez, G., Hatfield, J. L., Parkin, T. B., Sauer, T. J., Prueger, J. H. 2011. Carbon dioxide fluxes in corn-soybean rotation in the midwestern US: Inter- and intra-annual variations, and biophysical controls. Agricultural and Forest Meteorology 151:1831–1842.

Herzberger, A. J., Duncan, D. S., Jackson, R. D. 2014. Bouncing back: Plant-associated soil microbes respond rapidly to prairie establishment. PLoS ONE 9:e115775.

Hill, J., Nelson, E., Tilman, D., Polasky, S., Tiffany, D. 2006. Environmental, economic, and energetic costs and benefits of biodiesel and ethanol biofuels. Proceedings of the National Academy of Sciences of the United States of America 103:11206–11210.

Jach-Smith, L. C., Jackson, R. D. 2015. Nitrogen conservation decreases with fertilizer addition in two perennial grass cropping systems for bioenergy. Agriculture, Ecosystems & Environment 204:62–71.

Jain, A. K., Khanna, M., Erickson, M., Huang, H. 2010. An integrated biogeochemical and economic analysis of bioenergy crops in the Midwestern United States. Global Change Biology Bioenergy 2:217–234.

Joo, E., Hussain, M. Z., Zeri, M., Masters, M. D., Miller, J. N., Gomez-Casanovas, N., DeLucia, E. H., Bernacchi, C. J. 2016. The influence of drought and heat stress on long-term carbon fluxes of bioenergy crops grown in the Midwestern USA. Plant Cell and Environment 39:1928–1940.

Jungers, J. M., Clark, A. T., Betts, K., Mangan, M. E., Sheaffer, C. C., Wyse, D. L. 2015. Long-term biomass yield and species composition in native perennial bioenergy cropping systems. Agronomy Journal 107:1627–1640.

Kucharik, C. J. 2007. Impact of prairie age and soil order on carbon and nitrogen sequestration. Soil Science Society of America Journal 71:430–441.

Kuzyakov, Y. 2006. Sources of CO_2 efflux from soil and review of partitioning methods. Soil Biology & Biochemistry 38:425–448.

Liang, C., Jesus, E. D., Duncan, D. S., Jackson, R. D., Tiedje, J. M., Balser, T. C. 2012. Soil microbial communities under model biofuel cropping systems in southern Wisconsin, USA: Impact of crop species and soil properties. Applied Soil Ecology 54:24–31.

Milchunas, D. G. 2009. Estimating root production: Comparison of 11 methods in shortgrass steppe and review of biases. Ecosystems 12:1381–1402.

Moyano, F. E., Manzoni, S., Chenu, C. 2013. Responses of soil heterotrophic respiration to moisture availability: An exploration of processes and models. Soil Biology & Biochemistry 59:72–85.

Mueller, C. W., Schlund, S., Prietzel, J., Kogel-Knabner, I., Gutsch, M. 2012. Soil aggregate destruction by ultrasonication increases soil organic matter mineralization and mobility. Soil Science Society of America Journal 76:1634–1643.

National Oceanic and Atmospheric Administration (NOAA). 2017. National Centers for Environmental Information: Climate Data Online. www.ncdc.noaa.gov.

Necpálová, M., Anex, R. P., Kravchenko, A. N., Abendroth, L. J., Del Grosso, S. J., Dick, W. A., Helmers, M. J., Herzmann, D., Lauer, J. G. et al. 2014. What does it take to detect a change in soil carbon stock? A regional comparison of minimum detectable difference and experiment duration in the north central United States. Journal of Soil and Water Conservation 69:517–531.

Nguyen, C. 2003. Rhizodeposition of organic C by plants: mechanisms and controls. Agronomie 23:375–396.

Oates, L. G., Duncan, D. S., Gelfand, I., Millar, N., Robertson, G. P., Jackson, R. D. 2016. Nitrous oxide emissions during establishment of eight alternative cellulosic bioenergy

cropping systems in the North Central United States. Global Change Biology Bioenergy 8:539–549.

Osterholz, W. R., Kucharik, C. J., Hedtcke, J. L., Posner, J. L. 2014. Seasonal nitrous oxide and methane fluxes from grain- and forage-based production systems in Wisconsin, USA. Journal of Environmental Quality 43:1833–1843.

Parrish, D. J., Fike, J. H. 2005. The biology and agronomy of switchgrass for biofuels. Critical Reviews in Plant Sciences 24:423-459.

Persson, H. 1979. Fine root production, mortality and decomposition in forest ecosystems. Vegetatio 41:101–109.

Post, W. M., Izaurralde, R. C., Jastrow, J. D., McCarl, B. A., Amonette, J. E., Bailey, V. L., Jardine, P. M., West, T. O., Zhou, J. Z. 2004. Enhancement of carbon sequestration in US soils. BioScience 54:895–908.

Prolingheuer, N., Scharnagl, B., Graf, A., Vereecken, H., Herbst, M. 2014. On the spatial variation of soil rhizospheric and heterotrophic respiration in a winter wheat stand. Agricultural and Forest Meteorology 195-196:24–31.

Qin, Z., Dunn, J. B., Kwon, H., Mueller, S., Wander, M. M. 2016. Soil carbon sequestration and land use change associated with biofuel production: empirical evidence. Global Change Biology Bioenergy 8:66–80.

R Core Team. 2017. R: A language and environment for statistical computing. R Foundation for Statistical Computing, Vienna, Austria. R-project.org

Robertson, G. P., Hamilton, S. K., Barham, B. L., Dale, B. E., Izaurralde, R. C., Jackson, R. D., Landis, D. A., Swinton, S. M., Thelen, K. D., Tiedje, J. M. 2017. Cellulosic biofuel contributions to a sustainable energy future: Choices and outcomes. Science 356:eaal2324.

Robertson, G. P., Hamilton, S. K., Del Grosso, S. J., Parton, W. J. 2011. The biogeochemistry of bioenergy landscapes: carbon, nitrogen, and water considerations. Ecological Applications 21:1055–1067.

Sanford, G. R., Oates, L. G., Jasrotia, P., Thelen, K. D., Robertson, G. P., Jackson, R. D. 2016. Comparative productivity of alternative cellulosic bioenergy cropping systems in the North Central USA. Agriculture, Ecosystems & Environment 216:344–355.

Sanford, G. R., Posner, J. L., Jackson, R. D., Kucharik, C. J., Hedtcke, J. L., Lin, T.-L. 2012. Soil carbon lost from Mollisols of the North Central U.S.A. with 20 years of agricultural best management practices. Agriculture, Ecosystems & Environment 162:68–76.

Savage, K., Davidson, E. A., Tang, J. 2013. Diel patterns of autotrophic and heterotrophic respiration among phenological stages. Global Change Biology 19:1151–1159.

Scurlock, J. M. O., Johnson, K., Olson, R. J. 2002. Estimating net primary productivity from grassland biomass dynamics measurements. Global Change Biology 8:736–753.

Senthilkumar, S., Basso, B., Kravchenko, A. N., Robertson, G. P. 2009. Contemporary evidence of soil carbon loss in the US corn belt. Soil Science Society of America Journal 73:2078–2086.

Skinner, R. H., Adler, P. R. 2010. Carbon dioxide and water fluxes from switchgrass managed for bioenergy production. Agriculture, Ecosystems & Environment 138:257–264.

Soil Survey Staff. 2017. Natural Resources Conservation Service, U.S. Department of Agriculture. Official Soil Series Descriptions. www.nrcs.usda.gov.

Subke, J. A., Inglima, I., Cotrufo, M. F. 2006. Trends and methodological impacts in soil CO_2 efflux partitioning: A metaanalytical review. Global Change Biology 12:921–943.

Sulaiman, M. F., Wagner-Riddle, C., Brown, S. E., Warland, J., Voroney, P., Rochette, P. 2017. Greenhouse gas mitigation potential of annual and perennial dairy feed crop systems. Agriculture Ecosystems & Environment 245:52–62.

Teh, C. B. S., Simmonds, L. P., Wheeler, T. R. 2000. An equation for irregular distributions of leaf azimuth density. Agricultural and Forest Meteorology 102:223–234.

Troyer, A. F. 2004. Background of US hybrid corn II: Breeding, climate, and food. Crop Science 44:370–380.

U.S. Energy Information Administration (EIA). 2017. Monthly Energy Review July 2017. www.eai.gov.

Verma, S. B., Dobermann, A., Cassman, K. G., Walters, D. T., Knops, J. M., Arkebauer, T. J., Suyker, A. E., Burba, G. G., Amos, B. et al. 2005. Annual carbon dioxide exchange in irrigated and rainfed maize-based agroecosystems. Agricultural and Forest Meteorology 131:77–96.

Vogel, J. G., Valentine, D. W. 2005. Small root exclusion collars provide reasonable estimates of root respiration when measured during the growing season of installation. Canadian Journal of Forest Research 35:2112–2117.

von Haden, A.C. 2017. Autotrophic soil respiration in maize and switchgrass bioenergy cropping systems: an assessment of the growth-maintenance respiration framework at the ecosystem level. *In:* Mechanisms of ecosystem carbon storage and stability in temperature bioenergy cropping systems. Doctoral Dissertation. University of Wisconsin-Madison, Madison, WI, USA.

von Haden, A. C., Dornbush, M. E. 2017a. Depth-distributions of belowground production, biomass, and decomposition in restored tallgrass prairie. Pedosphere. In press. DOI: 10.1016/S1002-0160(17)60455-7.

von Haden, A. C., Dornbush, M. E. 2017b. Ecosystem carbon pools, fluxes, and balances within mature tallgrass prairie restorations. Restoration Ecology 25:549–558.

Werling, B. P., Dickson, T. L., Isaacs, R., Gaines, H., Gratton, C., Gross, K. L., Liere, H., Malmstrom, C. M., Meehan, T. D. et al. 2014. Perennial grasslands enhance biodiversity and multiple ecosystem services in bioenergy landscapes. Proceedings of the National Academy of Sciences of the United States of America 111:1652–1657.

West, T. O., Brandt, C. C., Baskaran, L. M., Hellwinckel, C. M., Mueller, R., Bernacchi, C. J., Bandaru, V., Yang, B., Wilson, B. S. et al. 2010. Cropland carbon fluxes in the United States: increasing geospatial resolution of inventory-based carbon accounting. Ecological Applications 20:1074–1086.

Woodwell, G. M., Whittaker, R. H. 1968. Primary production in terrestrial ecosystems. American Zoologist 8:19–30.

Zenone, T., Gelfand, I., Chen, J., Hamilton, S. K., Robertson, G. P. 2013. From set-aside grassland to annual and perennial cellulosic biofuel crops: Effects of land use change on carbon balance. Agricultural and Forest Meteorology 182–183:1–12.

Zeri, M., Anderson-Teixeira, K., Hickman, G., Masters, M., DeLucia, E., Bernacchi, C. J. 2011. Carbon exchange by establishing biofuel crops in Central Illinois. Agriculture, Ecosystems & Environment 144:319–329.

2.8 Tables and figures

Table 2.1 – Monthly mean temperature and total precipitation for the two study years and the 1981-2010 normal. Deviations from the normal are given in parentheses. Data is from the Arlington University Farm weather station (NOAA 2017).

	2015		**2016**		**30-year mean**	
	Temp (°C)	*Precip. (mm)*	*Temp (°C)*	*Precip. (mm)*	*Temp (°C)*	*Precip. (mm)*
Jan	-8.1 (+0.9)	9.4 (-19.6)	-7.9 (+1.1)	20.1 (-8.9)	-9.0	29.0
Feb	-12.6 (-6.1)	25.9 (-7.4)	-3.8 (+2.7)	9.9 (-23.4)	-6.5	33.3
Mar	0.4 (+0.8)	9.9 (-37.8)	3.6 (+3.9)	108.7 (+61.0)	-0.3	47.8
Apr	8.3 (+1.3)	162.3 (+73.4)	7.1 (0.0)	37.3 (-51.6)	7.1	88.9
May	14.8 (+1.7)	112.0 (+18.3)	14.3 (+1.2)	87.6 (-6.1)	13.2	93.7
Jun	18.6 (-0.1)	79.8 (-39.1)	20.3 (+1.7)	104.1 (-14.7)	18.7	118.9
Jul	20.3 (-0.4)	80.3 (-25.4)	21.8 (+1.1)	164.8 (+59.2)	20.8	105.7
Aug	19.8 (+0.2)	110 (+10.9)	21.4 (+1.8)	138.7 (+39.6)	19.6	99.1
Sep	18.9 (+3.8)	144.8 (+54.9)	17.9 (+2.8)	156.7 (+66.8)	15.2	89.9
Oct	10.4 (+1.8)	49.8 (-15.0)	11.3 (+2.7)	85.6 (+20.8)	8.6	64.8
Nov	4.9 (+3.9)	123.2 (+62.2)	6.3 (+5.3)	41.4 (-19.6)	0.9	61.0
Dec	1.2 (+7.7)	86.4 (+49.0)	-6.1 (+0.3)	33.0 (-4.3)	-6.4	37.3
Total	8.1 (+1.3)	993.6 (+124.5)	8.8 (+2.0)	988.1 (+118.9)	6.8	869.2

Table 2.2 – Growing season properties for maize and switchgrass in 2015 and 2016 (plant emergence through complete senescence). Above- and within-canopy PAR (Q_{od}, Q_{ob}, Q_{sh}, and Q_{sl}) are reported for daylight hours only. Values are mean with standard error, where applicable.

Year		Maize	Switchgrass
2015			
	Start Date	5/13/2015	4/28/2015
	End Date	10/26/2015	11/2/2015
	Length (days)	166	188
	T_{leaf} (°C)	17.2	16.5
	VPD_{leaf} (kPa)	0.486	0.473
	Green leaf area (m^2 m^{-2})	2.70 (0.06)	3.50 (0.17)
	Mean Tip Angle (°)	44.4 (0.5)	43.2 (1.2)
	Apparent clumping (Ω)	0.96 (0.0019)	0.92 (0.0072)
	Q_{od} (µmol quanta m^{-2} s^{-1})	218	218
	Q_{ob} (µmol quanta m^{-2} s^{-1})	429	420
	Q_{sh} (µmol quanta m^{-2} s^{-1})	137 (1.1)	114 (3.7)
	Q_{sl} (µmol quanta m^{-2} s^{-1})	524 (1.7)	486 (2.0)
2016			
	Start Date	5/18/2016	4/25/2016
	End Date	10/19/2016	11/7/2016
	Length (days)	154	196
	T_{leaf} (°C)	18.9	16.9
	VPD_{leaf} (kPa)	0.568	0.525
	Green leaf area (m^2 m^{-2})	2.31 (0.03)	3.51 (0.17)
	Mean Tip Angle (°)	43.5 (0.6)	35.1 (2.1)
	Apparent clumping (Ω)	0.96 (0.0007)	0.88 (0.0008)
	Q_{od} (µmol quanta m^{-2} s^{-1})	188	190
	Q_{ob} (µmol quanta m^{-2} s^{-1})	444	418
	Q_{sh} (µmol quanta m^{-2} s^{-1})	136 (1.4)	103 (4.3)
	Q_{sl} (µmol quanta m^{-2} s^{-1})	525 (1.2)	477 (2.1)

Table 2.3 – Annual ecosystem C fluxes, net ecosystem production (NEP), and net ecosystem carbon balance (NECB) for maize and switchgrass using the net photosynthesis (PS) and biometric (BM) approaches. All units are g C m^{-2} y^{-1}.

Year		Maize	Switchgrass
2015			
	$A_{net,canopy}$	1348 (5)	1256 (8)
	R_T	636 (38)	1105 (107)
	NEP_{PS}	712 (33)	152 (100)
	ANPP	1273 (14)	553 (45)
	BNPP	90 (7)	112 (10)
	R_H	486 (28)	695 (55)
	NEP_{BM}	877 (43)	-30 (50)
	Harvest	715 (7)	282 (3)
	$NECB_{PS}$	-3 (40)	-130 (99)
	$NECB_{BM}$	162 (44)	-311 (53)
2016			
	$A_{net,canopy}$	1240 (14)	1177 (23)
	R_T	703 (32)	1162 (55)
	NEP_{PS}	537 (23)	16 (78)
	ANPP	1146 (103)	602 (20)
	BNPP	100 (10)	135 (20)
	R_H	383 (6)	593 (45)
	NEP_{BM}	863 (117)	144 (63)
	Harvest	735 (16)	368 (14)
	$NECB_{PS}$	-197 (39)	-352 (89)
	$NECB_{BM}$	128 (131)	-223 (68)
Mean			
	NEP_{PS}	625 (17)	84 (82)
	NEP_{BM}	870 (68)	57 (50)
	$NECB_{PS}$	-100 (22)	-241 (85)
	$NECB_{BM}$	145 (74)	-267 (56)

Table 2.4 – Sensitivity analysis of mean annual net canopy photosynthesis ($A_{n,canopy}$) across a range of canopy and environmental conditions. Daytime Q_{od} was varied without changing Q_{ot} and therefore represents differences in partitioning between Q_{od} and Q_{ob}. $T_{leaf} \rightarrow VPD_{leaf}$ indicates that VPD_{leaf} was adjusted to the saturation vapor pressure at T_{leaf}.

		Maize	**Switchgrass**
Variable	*Sensitivity range*	*Annual $A_{n,canopy}$ response range*	
L_t (Leaf area index)	-20% to + 20%	-2.6% to +0.2%	+1.3% to -4.0%
Daytime Q_{od}	-20% to + 20%	-4.1% to +3.7%	-6.2% to +5.7%
Daytime Q_{ot}	-20% to + 20%	-21.8% to +19.7%	-24.7% to +22.1%
Daytime $T_{leaf} \rightarrow VPD_{leaf}$	-5 °C to +5 °C	+4.0% to -8.2%	+5.4% to -11.1%
Nighttime $T_{leaf} \rightarrow VPD_{leaf}$	-5 °C to +5 °C	+3.8% to -3.8%	+6.6% to -6.7%
Leaf azimuth (bimodal)	N/A	-0.8% to -0.6%	N/A

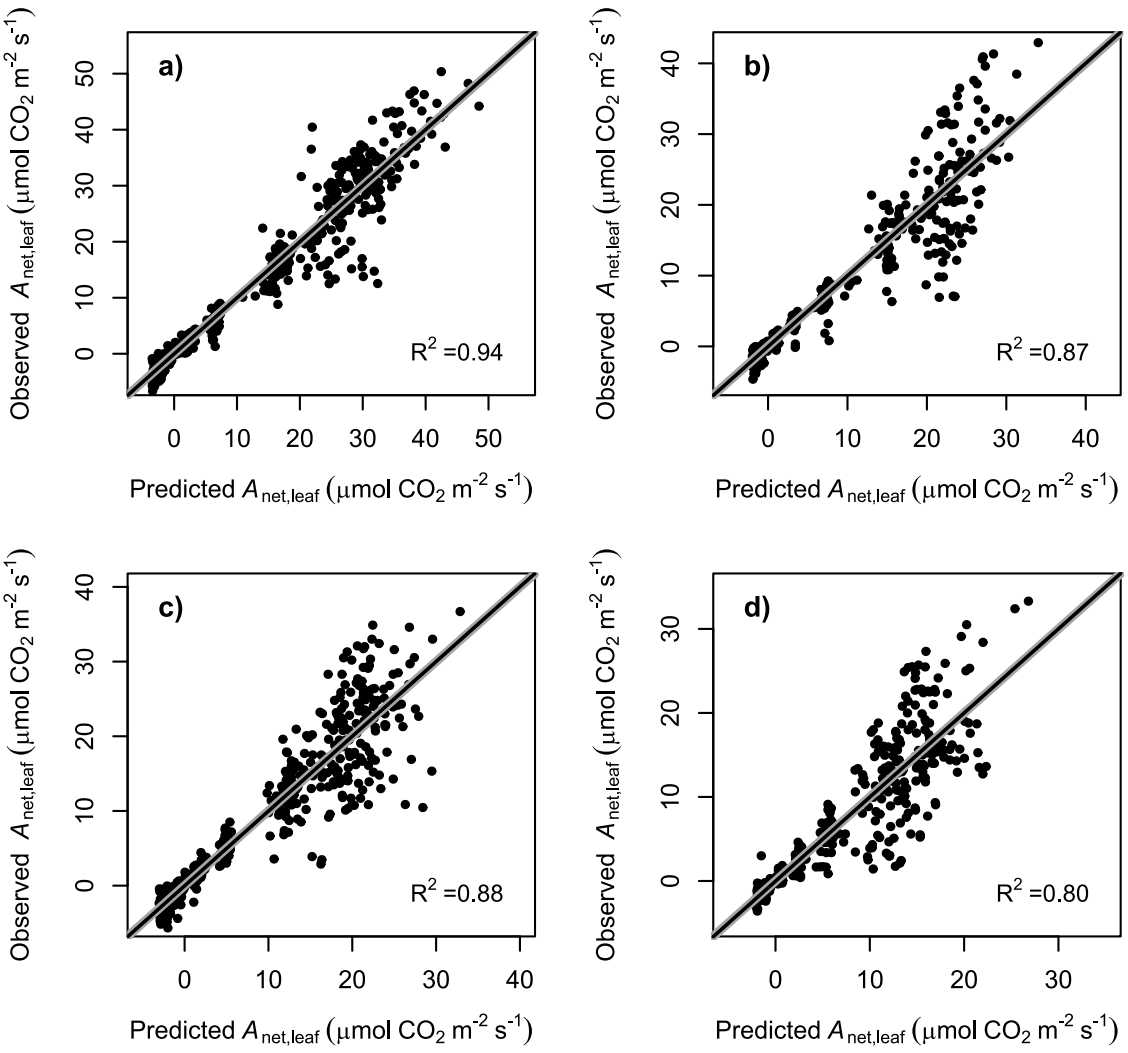

Figure 2.1 – Model predicted versus observed leaf-level net photosynthesis ($A_{net,leaf}$) for (a) maize upper canopy leaves, (b) maize lower canopy leaves, (c) switchgrass upper canopy leaves, and (d) switchgrass lower canopy leaves. The black line shows the linear regression between predicted and observed values, and the gray line is 1:1.

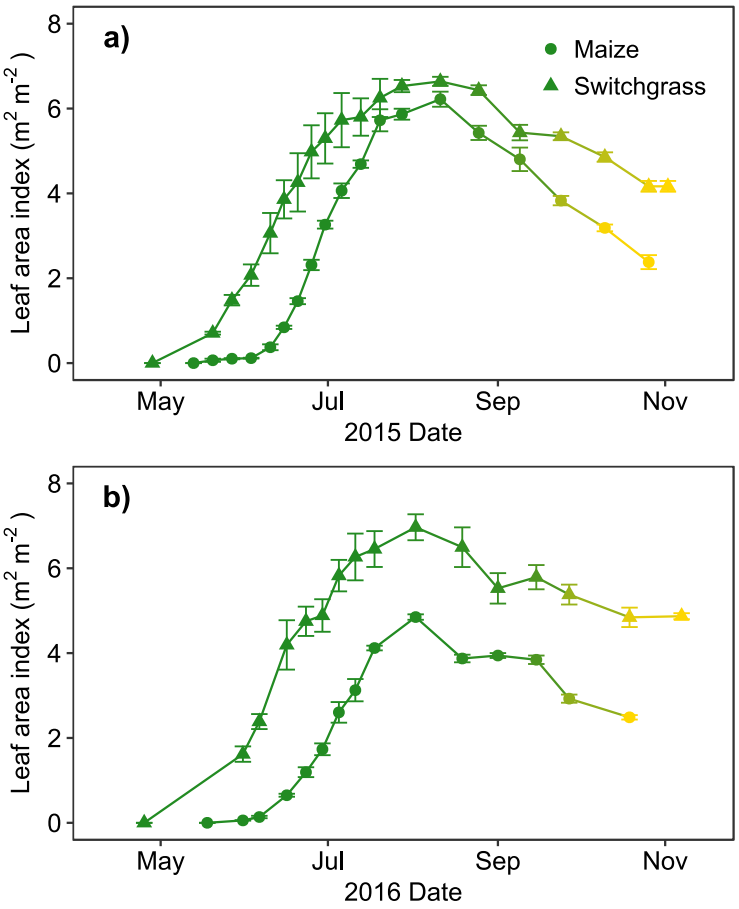

Figure 2.2 – Leaf area index (mean with standard error) for maize and switchgrass during the (a) 2015 and (b) 2016 growing seasons. The color gradient reflects the estimated vegetation status ranging from fully photosynthetic (green) to fully non-photosynthetic (yellow).

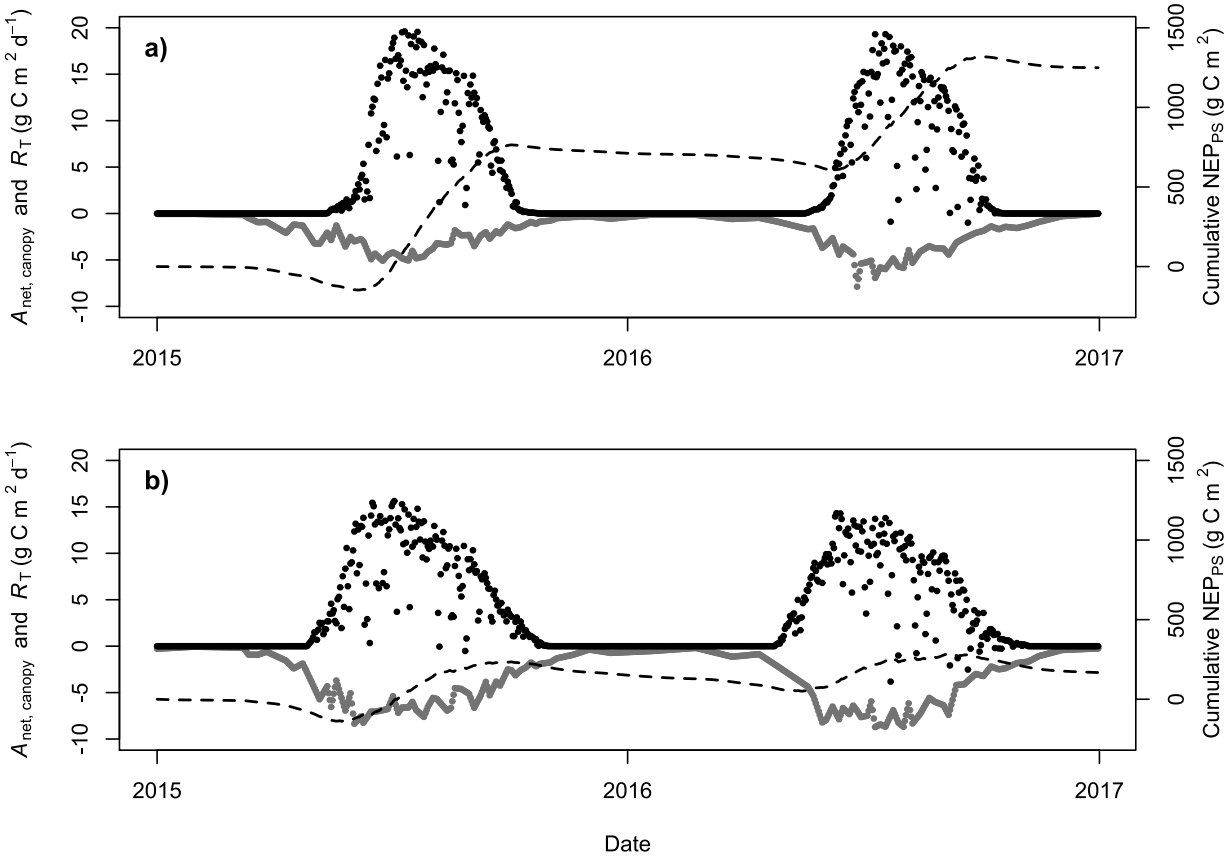

Figure 2.3 – Seasonal patterns of canopy net photosynthesis (black dots), total soil respiration (grey dots), and cumulative NEP_{PS} (dashed line) for (a) maize and (b) switchgrass.

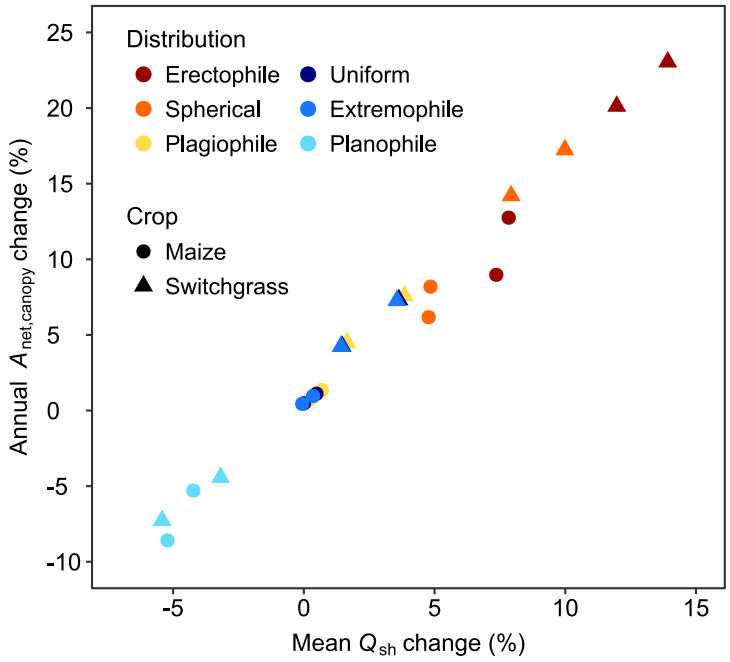

Figure 2.4 – Relative changes in mean shaded canopy PAR (Q_{sh}) and annual canopy net photosynthesis ($A_{net,canopy}$) for various theoretical leaf angle distributions. Replicates reflect the two study years (2015 and 2016).

2.9 Supplemental methods

2.9.1 Canopy net photosynthesis

Leaf photosynthesis, plant canopy, and environmental measurements

Sunlit and shaded leaf light response curves were measured approximately weekly in both cropping systems throughout the 2010, 2011, and 2012 growing seasons, providing a minimum of 43 light response curves per crop and leaf type. Light response curves were measured using a LI-COR LI-6400XT portable photosynthesis system with a LI-6400-02B red/blue LED light source (LI-COR Inc., Lincoln, Nebraska, USA). For each light response curve, the CO_2 concentration was set near ambient and net photosynthesis was measured at 2000, 1500, 1000, 500, 200, 100, 50, 20 and 0 μmol photons m^{-2} s^{-1} photosynthetically active radiation (PAR). In 2010 the measurements were made near ambient leaf temperature, whereas in 2011 and 2012 measurements were also made at 5 °C above and below ambient leaf temperature, and covered a range from 15-38ºC. The climatic conditions among the 2010-2012 growing seasons varied widely from extremely wet in 2010 to severe drought in 2012 (Sanford et al. 2016), thereby allowing for evaluation of photosynthetic light responses under varying levels of plant water stress.

To generalize leaf-level net photosynthesis across varying environmental conditions, the light response photosynthesis data were fit to non-linear models. We first selected the most appropriate model by fitting the photosynthetic light response data from each crop type and canopy level to five candidate model types: rectangular hyperbola, hyperbolic tangent, nonrectangular hyperbola, exponential, and the Ye model (Ye 2007; Lobo et al. 2013). The exponential model resulted in the lowest Akaike information criterion (AIC) values for all crop types and canopy levels (Table 2.S.1) and thus was selected for further use:

$$A_{\text{net,leaf}}(Q) = \left\{A_{\text{g,max}}\left[1 - \exp\left(\frac{-\phi_{(Q_0)}Q}{A_{\text{g,max}}}\right)\right]\right\} - R_D \quad (2.7a)$$

where $A_{net,leaf}$ is measured net leaf photosynthesis, Q is the measured PAR quantum flux, $A_{g,max}$ is the estimated maximum gross leaf photosynthesis, $\phi_{(Q0)}$ is the estimated quantum yield at zero Q, and R_D is the estimated dark respiration rate. Next, the effects of leaf temperature (T_{leaf}, °C) and leaf vapor pressure deficit (VPD_{leaf}, kPa) were added to the model by allowing each light response model coefficient to vary as a function of T_{leaf} and VPD_{leaf}. We tested all combinations of T_{leaf}, VPD_{leaf}, T_{leaf} + VPD_{leaf}, and neither T_{leaf} nor VPD_{leaf} for all model coefficients and selected the most appropriate combination based on lowest median AIC value among crops and canopy levels (Table 2.S.2). The final leaf-level photosynthetic model terms were:

$$A_{\text{g,max}}\,(T_{\text{leaf}}, VPD_{\text{leaf}}) = aT_{\text{leaf}} + bVPD_{\text{leaf}} \quad (2.7b)$$

$$\phi_{(Q_0)} = c \quad (2.7c)$$

$$R_{\text{D}}(T_{\text{leaf}}) = dT_{\text{leaf}} \quad (2.7.d)$$

where *a*, *b*, *c*, and *d* are coefficients fitted for each crop type and canopy level. We assessed the leaf-level net photosynthesis model performance using a Monte Carlo cross-validation procedure. For each crop type and canopy level, the original photosynthetic light response data were randomly split into training and testing subsets consisting of 70% and 30% of the light response curves, respectively. The leaf net photosynthesis model was fit using the training dataset, predictions were made based on the independent variables of the testing dataset, and the predicted values were then compared to the measured photosynthesis values of the testing dataset. This procedure was repeated 10,000 times, each time recording the median absolute error (MAE) of the linear-regression between the predicted and measured testing dataset values.

The effects of T_{leaf} and VPD_{leaf} on leaf-level photosynthesis parameters were generally more prominent in maize than switchgrass and more pronounced in the upper canopy than the lower canopy (Table 2.S.3). The positive effect of temperature on $A_{g,max}$ (a) was greater in maize than in switchgrass and greater in the upper canopy compared to the lower canopy (Table 2.S.3). VPD_{leaf} had a negative effect on $A_{g,max}$ (b), but the effect was more prominent in maize than switchgrass and greater in the upper canopy than the lower canopy. Quantum yield at 0 ($\phi_{(Q0)}$ = c) was slightly greater in maize than switchgrass, but was consistent between upper and lower canopy layers. Similar to $A_{g,max}$ (a), the effect of temperature on R_D (d) was greater in maize than switchgrass and greater in the upper canopy than the lower canopy.

Leaf-level model residuals showed no significant linear relationship with PAR nor VPD_{leaf} (Table 2.S.4). However, T_{leaf} showed a marginally significant positive relationship with residuals from the maize lower leaf model ($p = 0.065$) and a negative relationship with residuals from the switchgrass upper leaf model ($p = 0.042$; Table 2.S.4). The magnitude of these residual relationships (0.094 and -0.067 μmol CO_2 m^{-2} s^{-1} °C^{-1} for maize lower and switchgrass upper, respectively) would result in an overall error of ±1.75 and ±1.25 μmol CO_2 m^{-2} s^{-1} at the measured seasonal temperature extremes for maize upper and switchgrass lower canopies, respectively. However, the inconsistency of the residual T_{leaf} effect among models (i.e. two models with no effect, one model with a positive effect, and one model with a negative effect) suggests that the marginal relationships could be statistical artifacts (i.e. type I errors). Irrespectively, the median absolute error was not inflated for the two models with the residual T_{leaf} relationships (Table 2.S.3), thereby indicating comparable overall predictive performance among crops and canopy layers.

Above-canopy beam and diffuse PAR were measured during the 2015 and 2016 growing seasons using a shadowband apparatus consisting of an LI-190 quantum sensor (LI-COR Inc., Lincoln, Nebraska, USA) and a rotating metal band that completely blocked beam PAR once every five minutes (Cruse et al. 2015). Flux densities of beam (Q_{ob}) and diffuse (Q_{od}) PAR radiation above the plant canopy were partitioned with equations presented in Cruse et al. (2015). Total PAR (Q_{ot} i.e. $Q_{ob} + Q_{od}$) was annually calibrated to an unblocked LI-190 quantum sensor using a linear model. The calibration coefficients were 0.99 and 1.04 in 2015 and 2016, respectively. Leaf area index (L_t), leaf zenith angle distribution (LAD), and apparent vegetation clumping (Ω) were measured approximately weekly during the growing season with an LAI-2000 plant canopy analyzer (LI-COR Inc., Lincoln, Nebraska, USA). Plant canopy measurements were made in ten locations per plot with one above-canopy and four below-canopy measurements per location. The four below-canopy measurements were stratified across local canopy heterogeneity (e.g. row and inter-row) to ensure adequate spatial representation. Percent green vegetation was visually estimated on the day of each plant canopy measurement. All plant canopy measurements were linearly interpolated to a one-hour frequency that was necessary for modeling canopy photosynthesis. Hourly air temperature and relative humidity were measured at weather station adjacent to our study site (AWON 2017), and occasional missing data were gap-filled using data from the Dane County Regional Airport located 18 km from the study site.

Photosynthetic (green) and non-photosynthetic (brown, senesced) leaf reflectance and transmittance were measured on one occasion using an ASD integrating sphere with an ASD FieldSpec 4 spectroradiometer (ASD Inc., Longmont, CO, USA). Reflectance and transmittance were averaged from 400-700 nm, and absorptance was calculated as 1-(reflectance +

transmittance). Green leaf PAR absoprtance was 0.908 for maize and 0.866 for switchgrass. Raw spectral data is shown in Fig. 2.S.1 and a summary of all leaf optical properties is given in Table 2.S.5.

Light attenuation model

The attenuation of direct radiation was described by a solar zenith angle-dependent beam radiation extinction coefficient, $K_b(\theta_S)$, which quantifies the area of foliage projected onto a horizontal surface (Anderson 1966; Campbell & Norman 1989):

$$K_b(\theta_S) = \frac{G(\theta_S)}{\cos\theta_S} \quad (2.8)$$

where θ_S is the solar zenith angle in radians and $G(\theta_S)$ is the projection of foliage area perpendicular to beam radiation. Assuming that leaf azimuth angle is uniformly distributed, then $G(\theta_S)$ can be computed as (Warren Wilson 1960; Nilson 1971; Wang et al. 2007):

$$G(\theta_S) = \int_0^{\pi/2} A(\theta_S, \theta_L)\ f(\theta_L)\ d\theta_L \quad (2.9)$$

where $f(\theta_L)$ is the LAD function at (θ_L) expressed in radians and $A(\theta_S, \theta_L)$ is:

$$A(\theta_S, \theta_L) = \begin{cases} \cos\theta_S \cos\theta_L, & \cot\theta_S \cot\theta_L \geq 1 \\ \cos\theta_S \cos\theta_L \{1 + [2/\pi][\tan\psi(\theta_{S,}\theta_L) - \psi(\theta_{S,}\theta_L)]\}, & \cot\theta_S \cot\theta_L < 1 \end{cases} \quad (2.10a)$$

$$\psi(\theta_{S,}\theta_L) = \cos^{-1}(\cot\theta_S \cot\theta_L) \quad (2.10b)$$

Both beta (Goel & Strebel 1984) and ellipsoidal (Campbell 1986) LAD functions can be estimated based on the LAI-2000 plant canopy measurements. We chose to use the beta LAD function for our light attenuation model because the beta LAD function has shown better

agreement with true LADs compared to the ellipsoidal function (Wang et al. 2007). The probability density of a given leaf angle for the beta function is (Goel & Strebel 1984):

$$f(\theta_L) = \frac{1}{\beta(\mu,\nu)} [1 - t(\theta_L)]^{\mu-1} [t(\theta_L)]^{\nu-1} \quad (2.11a)$$

$$t(\theta_L) = 2\theta_L/\pi \quad (2.11b)$$

$$\beta(\mu,\nu) = \frac{\Gamma(\mu)\,\Gamma(\nu)}{\Gamma(\mu+\nu)} \quad (2.11c)$$

where Γ is the gamma function, and μ and ν are derived from the LAI-2000 (Welles & Norman 1991). Probability density functions were standardized so that the area was equal to unity.

Vegetation clumping (i.e. non-random horizontal spatial distribution) affects light attenuation by decreasing the efficiency of radiation interception (Campbell & Norman 1998). As such, an apparent canopy clumping factor (Ω) for each LAI-2000 view angle (θ) was calculated as (Ryu et al. 2010, Pisek et al. 2011):

$$\Omega(\theta) = \frac{\ln[\overline{P(\theta)}]}{\overline{\ln[P(\theta)]}} \quad (2.12)$$

where $P(\theta)$ is the probability of beam radiation penetration at view angle θ. Following Kucharik et al. (1999), the dependency of Ω on solar zenith angle was fit to measured data with an exponential function:

$$\Omega(\theta_S) = y0 + g[1 - \exp(-h\,\theta_S)] \quad (2.13)$$

where θ_S is the solar zenith angle in radians and *y0*, *g*, and *h* are coefficients fitted via non-linear least squares regression, and $\Omega(\theta_S)$ is constrained to < 1. The probability of transmitted beam radiation through the canopy was calculated as (Monsi & Saeki 1953; Anderson 1966; Campbell & Norman 1998):

$$P_{\mathrm{b}}(\theta_{\mathrm{S}}) = \exp[-K_{\mathrm{b}}(\theta_{\mathrm{S}})\, \Omega(\theta_{\mathrm{S}})\, L_{\mathrm{t}}] \quad (2.14)$$

Similarly, the probability of transmitted beam plus scattered beam radiation was calculated as (Goudriaan 1977; Norman & Campbell 1998):

$$P_{\mathrm{b+sb}}(\theta_{\mathrm{S}}) = \exp\left[-\sqrt{\alpha}\, K_{\mathrm{b}}(\theta_{\mathrm{S}})\, \Omega(\theta_{\mathrm{S}})\, L_{\mathrm{t}}\right] \quad (2.15)$$

where α is the leaf PAR absorptivity. Effective leaf absorptivity was calculated as the average absorptivity of green and brown leaves weighted by the percentage of canopy greenness.

Unlike beam radiation, diffuse radiation occurs from all directions. Assuming isotropic hemispherical diffuse radiation, the probability of transmitted diffuse radiation was calculated by (Monsi & Saeki 1953; Welles & Norman 1991):

$$P_{\mathrm{d}} = \frac{\int_0^{\pi/2} P_{\mathrm{b+sb}}(\theta_{\mathrm{S}})\, \sin\theta_{\mathrm{S}} \cos\theta_{\mathrm{S}}\, d\theta_{\mathrm{S}}}{\int_0^{\pi/2} \sin\theta_{\mathrm{S}} \cos\theta_{\mathrm{S}}\, d\theta_{\mathrm{S}}} \quad (2.16)$$

The sunlit leaf area (L_{sl}) was calculated as (Warren Wilson 1967; Campbell & Norman 1998):

$$L_{\mathrm{sl}}(\theta_{\mathrm{S}}) = \frac{[1-P_{\mathrm{b}}(\theta_{\mathrm{S}})]}{K_{\mathrm{b}}(\theta_{\mathrm{S}})} \quad (2.17)$$

By difference, the shaded leaf area (L_{sh}) was (Warren Wilson 1967):

$$L_{\mathrm{sh}}(\theta_{\mathrm{S}}) = L_{\mathrm{t}} - L_{\mathrm{sl}}(\theta_{\mathrm{S}}) \quad (2.18)$$

To estimate downward scattered beam radiation (Q_{sb}) and upward leaf reflected radiation ($Q_{leaf\ refl}$), we first divided the canopy into ten equal layers, L_1-L_{10}, each of depth $L_t/10$. Q_{sb} at each depth i was calculated as (Campbell & Norman 1998):

$$Q_{\mathrm{sb},i} = Q_{ob}[P_{\mathrm{b+sb}}(\theta_{\mathrm{S}})_i - P_{\mathrm{b}}(\theta_{\mathrm{S}})_i] \quad (2.19)$$

where transmittances probabilities are calculated to cumulative canopy depth i. The average downward scattered beam radiation was then calculated by averaging $Q_{sb,i}$ throughout all layers:

$$\overline{Q_{\mathrm{sb}}} = \frac{\sum_{i=1}^{10} Q_{\mathrm{sb},i}}{10} \tag{2.20}$$

Assuming isotropic PAR reflection from leaves, the flux of leaf-reflected PAR above each canopy layer resulting from the initial downward solar fluxes Q_{od} and Q_{ob} was calculated following Flerchinger et al. (2009):

$$Q_{\mathrm{leaf\ refl},i} = P_{\mathrm{d,l}} Q_{\mathrm{leaf\ refl},i+1} + \rho_{\mathrm{leaf}}\left[1 - P_{\mathrm{d,l}}\right] Q_{\mathrm{d},i} + \rho_{\mathrm{leaf}}\left[1 - P_{\mathrm{b+sb,l}}(\theta_{\mathrm{S}})\right] Q_{\mathrm{b+sb},i} \tag{2.21}$$

where ρ_{leaf} is leaf albedo, $P_{d,l}$ and $P_{b+sb,l}(\theta S)$ are transmittance probabilities for a single layer, and $Q_{d,i}$ and $Q_{b+sb,i}$ are downward diffuse and beam plus scattered radiation fluxes at canopy depth i. Leaf albedo was calculated as the average reflectance of green and brown leaves weighted by the canopy greenness. The canopy average upwards leaf reflected radiation resulting from the initial solar flux was calculated as:

$$\overline{Q_{\mathrm{leaf\ refl}}} = \frac{\sum_{i=1}^{10} Q_{\mathrm{leaf\ refl},i}}{10} \tag{2.22}$$

Total reflected PAR from the soil surface resulting from the initial downward Q_{ob} and Q_{od} solar fluxes was calculated as:

$$Q_{\mathrm{soil\ refl}} = \rho_{\mathrm{soil}}\left[Q_{\mathrm{ob}} P_{\mathrm{b+sb}}(\theta_{\mathrm{S}}) + Q_{od} P_{\mathrm{d}}\right] \tag{2.23}$$

where ρ_{soil} is the albedo of the soil surface, assumed to be 0.15 (e.g. Coulson & Reynolds 1971). The canopy average PAR flux resulting from soil-reflected radiation is:

$$\overline{Q_{\mathrm{soil\ refl}}} = \frac{Q_{\mathrm{soil\ refl}}\left(1 - P_{\mathrm{d}}\right)}{-\ln(P_{\mathrm{d}})} \tag{2.24}$$

For simplicity, the mean canopy PAR resulting from additional reflections within the canopy was modelled as an exponential decrease of the canopy average initial reflected radiation:

$$\overline{Q_{\text{refl}}(n)} = \{\overline{Q_{\text{leaf refl}}} + \overline{Q_{\text{soil refl}}}\} \exp\{\ln[(1 - P_{\text{d}})\rho_{\text{leaf}}]n\} \quad (2.25)$$

where *n* is the additional reflection number. After three additional reflections, the remaining reflected PAR is negligible. Therefore, the average total re-reflected radiation was calculated as:

$$\overline{Q_{\text{refl}}} = \sum_{n=1}^{3} \overline{Q_{\text{refl}}(n)} \quad (2.26)$$

Diffuse radiation resulting from Q_{od} averaged throughout the entire canopy is given by (Campbell & Norman 1998):

$$\overline{Q_{\text{d}}} = \frac{Q_{\text{od}}(1 - P_{\text{d}})}{-\ln(P_{\text{d}})} \quad (2.27)$$

Average beam radiation on the sunlit leaf fraction is given by:

$$\overline{Q_{\text{b}}} = \frac{Q_{\text{ob}}[1 - P_{\text{b}}(\theta_{\text{S}})]}{L_{\text{sl}}} \quad (2.28)$$

Occasional errors at high zenith angles due to the reciprocal cosine response of $K_b(\theta_S)$ to θ_S were addressed by setting maximum $\overline{Q_b}$ to 2000 µmol photons m^{-2} s^{-1}. Average PAR in the shaded fraction was calculated as:

$$\overline{Q_{\text{sh}}} = \overline{Q_{\text{d}}} + \overline{Q_{\text{sb}}} + \overline{Q_{\text{leaf refl}}} + \overline{Q_{\text{soil refl}}} + \overline{Q_{\text{refl}}} \quad (2.29)$$

Average PAR in the sunlit fraction was calculated as (Campbell & Norman 1998):

$$\overline{Q_{\text{sl}}} = \overline{Q_{\text{b}}} + \overline{Q_{\text{sh}}} \quad (2.30)$$

Scaling net photosynthesis from leaf to canopy

For each hour of the growing season, net canopy photosynthesis ($A_{\text{net,canopy}}$) was calculated as:

$$A_{\text{net ,canopy}} = \begin{cases} A_{\text{net,leaf,sl}}(\overline{Q_{\text{sl}}}, T_{\text{air}}, VPD_{\text{air}})L_{\text{sl}} + A_{\text{net,leaf,sh}}(\overline{Q_{\text{sh}}}, T_{\text{air}}, VPD_{\text{air}})L_{\text{sh}}, & \theta_{\text{S}} < 90 \\ A_{\text{net,leaf,sh}}(T_{\text{air}}, VPD_{\text{air}})L_{\text{t}}, & \theta_{\text{S}} \geq 90 \end{cases} \quad (2.31)$$

We thus assumed that T_{air} and VPD_{air} were representative of leaf conditions. Night respiration was modelled using the response of shaded leaves to T_{air} and VPD_{air} in the absence of light, as measured shaded leaves were typically exposed to low ambient PAR levels and thus were closer to nighttime conditions than sunlit leaves. Hourly $A_{net,canopy}$ (μmol CO_2 m^{-2} hr^{-1}) was converted to g C m^{-2} hr^{-1} and then summed to daily and annual timescales.

2.9.2 Canopy net photosynthesis sensitivity analyses

Leaf zenith angle distributions

The beta distribution parameters given by the LAI-2000 are obtained from a series of idealized empirical relationships which have particularly high error for leaf angles < 25° and > 65° (Lang et al. 1986; Welles and Norman 1991). As such, we evaluated the effect of leaf zenith angle distribution on annual canopy photosynthesis by substituting the measured distribution with several theoretical distributions. The theoretical leaf zenith angle distributions used were (de Wit 1965; Goel & Strebel 1984):

$$f(\theta_{\text{L}})_{\,Erectophile} = [1 - \cos(2\theta_{\text{L}})]\,2/\pi \quad (2.32)$$

$$f(\theta_{\text{L}})_{\,Spherical} = \sin\theta_{\text{L}} \quad (2.33)$$

$$f(\theta_L)_{Plagiophile} = [1 - \cos(4\theta_L)]\,2/\pi \quad (2.34)$$

$$f(\theta_L)_{Uniform} = 2/\pi \quad (2.35)$$

$$f(\theta_L)_{Extremophile} = [1 + \cos(4\theta_L)]\,2/\pi \quad (2.36)$$

$$f(\theta_L)_{Planophile} = [1 + \cos(2\theta_L)]\,2/\pi \quad (2.37)$$

where θ_L is the leaf zenith angle. These distributions are shown in Fig. 2.S.2a.

Non-uniform leaf azimuth distribution

Since maize is known to exhibit non-uniform, bimodal azimuthal distribution of leaves (Girardin & Tollenaar 1994), we performed a sensitivity analysis to evaluate our assumption that leaf azimuth was uniformly distributed. When leaf azimuth is non-uniform, *G* becomes dependent on both zenith and azimuth (Nilson 1971; Kimes 1984):

$$G(\theta_S, \phi_S) = \int_0^{2\pi}\int_0^{\pi/2} |\cos\psi|\, g(\theta_L, \phi_L)\; d\theta_L d\phi_L \quad (2.38a)$$

$$\cos\psi = \cos\theta_L \cos\theta_S + \sin\theta_L \sin\theta_S \cos(\phi_L - \phi_S) \quad (2.38b)$$

where θ_L and θ_S are leaf and solar zenith, respectively, ϕ_L and ϕ_S are leaf and solar azimuth, respectively, and $g(\theta_L, \phi_L)$ is the joint probability density function for leaf zenith and azimuth. If leaf zenith and azimuth are independently distributed, then:

$$g(\theta_L, \phi_L) = f(\theta_L) f(\phi_L) \quad (2.39)$$

where $f(\theta_L)$ and $f(\phi_L)$ are the probability density functions for leaf zenith and leaf azimuth, respectively. We used the beta distribution values obtained from the LAI-2000 to determine

$f(\theta_L)$. For $f(\phi_L)$, we used the undistorted probability distribution function presented in Teh et al. (2000):

$$f(\phi_L) = \frac{1}{2\pi I_0(T)} exp\{T \cos[S(R - \phi_L)]\} \quad (2.40)$$

where I_0 is the modified Bessel function of the first kind and zero order, T is the elongation index, S is the shape index, and R is the rotation index. When leaf azimuth follows a uniform distribution, $T = 0$, $S = 1$, and R has no influence on the probability density (Fig. 2.S.3a). For maize growing in rows running southwest to northeast, Teh et al. (2000) found on average that $T = 1.35$, $S = 2.15$, and $R = 2.4$ (radians). We used these values of T and S and rotated the function ($R = 1.66$ radians) so that the maximum probability density occurred perpendicular to the maize rows (which ran south to north in our study; Fig. 2.S.3b). We standardized the area of the probability density functions to unity.

Leaf area index and environmental variables

Sensitivity analyses of L_t and above canopy PAR were performed by adjusting the measured values of each parameter from -20% to +20% of the measured value. We performed two sensitivity analyses for above canopy PAR: one for total PAR (Q_{ot}) and one for diffuse PAR (Q_{od}). For the Q_{od} analysis, Q_{ot} was maintained at the measured value so that the results only reflect differences in the partitioning of Q_{ot} between Q_{ob} and Q_{od}.

For the leaf temperature (T_{leaf}) sensitivity analysis, we adjusted the measured temperature value from -5 °C to +5 °C. This range corresponds to the approximate range of divergence between T_{leaf} and air temperature when air temperature is between 15 °C and 35 °C (Campbell & Norman 1998). We performed separate sensitivity analyses for daytime and nighttime T_{leaf}, as

the divergence between air temperature and leaf temperature likely varies between day and night. Since saturation vapor pressure deficit is temperature-dependent, we calculated the saturation vapor pressure deficit at each adjusted T_{leaf} and calculated the resulting VPD_{leaf}. Thus, T_{leaf} sensitivity analysis reflects the combined response of T_{leaf} and $VPD_{leaf.}$

2.9.3 Heterotrophic respiration correction

A correction was applied to measured values of heterotrophic soil respiration (R_H), to account for soil moisture differences between inside and outside of the root exclusion collar (Prolingheuer et al. 2014). To isolate the effect of soil moisture on R_H, we first fit measured R_H values to non-linear model that considers the interactive effects of soil moisture and soil temperature:

$$R_{\mathrm{H}}(T_{\mathrm{soil}}, M_{\mathrm{soil}}) = R_{10}\exp\left[E_0\left(\frac{1}{283.15-T_0}-\frac{1}{T_{\mathrm{soil}}-T_0}\right)\right]D^{\left(M_{\mathrm{opt}}-M_{\mathrm{soil,in}}\right)^2} \quad (2.41)$$

where T_{soil} is measured 2 cm soil temperature (°K), $M_{soil,in}$ is measured soil volumetric water content inside of the collar (%), R_{10} is estimated R_H at 10 °C, E_0 is estimated activation energy coefficient in (°K), T_0 is the estimated minimum temperature for R_H (°K), M_{opt} is the estimated optimal volumetric soil moisture (%), and D is an estimated coefficient describing the relative intensity of the soil moisture response (Luo & Zhou 2006; Savage et al. 2009). The full model is thus a combination of a Lloyd-Taylor temperature response (Lloyd & Taylor 1994) and a parabolic soil moisture response (Savage et al. 2009). While the model is empirical in nature, it effectively captures the decreasing Q_{10} with increasing temperature (Davidson et al. 2006), the intermediate optimal soil moisture (Linn & Doran 1984), and the interactive effects of soil moisture and soil temperature (Lellei-Kovács et al. 2011).

Since we were not able to measure soil moisture when soils were frozen, the initial R_H temperature and moisture response model was fitted using only the data which was collected when soils were not frozen. To better quantify the R_H temperature response, we set the soil moisture for frozen soils to the model-estimated M_{opt}, then re-fitted the model using both frozen and non-frozen data. Setting the frozen soil moisture levels to optimal ensured that the frozen soil data points had minimal influence on the estimation of M_{opt} while also allowing for the temperature effect to be estimated across the full temperature range. Final model R^2 for maize and switchgrass R_H were 0.63 and 0.73, respectively. Moisture-corrected R_H was then calculated as:

$$R_{\mathrm{H}_{\mathrm{corrected}}} = R_{\mathrm{H}_{\mathrm{measured}}} + R_{\mathrm{H}}\left(T_{\mathrm{soil}}, M_{\mathrm{soil,out}}\right) - R_{\mathrm{H}}\left(T_{\mathrm{soil}}, M_{\mathrm{soil,in}}\right) \quad (2.42)$$

where $M_{soil,out}$ and $M_{soil,in}$ are the volumetric soil moisture measurements inside and outside of the root exclusion collar, respectively.

2.10 Supplemental references

Anderson, M. C. 1966. Stand structure and light penetration. II. A theoretical analysis. Journal of Applied Ecology 3:41–54.

Automated Weather Observation Network (AWON). 2017. University of Wisconsin-Extension. http://agwx.soils.wisc.edu.

Campbell, G. 1986. Extinction coefficients for radiation in plant canopies calculated using an ellipsoidal inclination angle distribution. Agricultural and Forest Meteorology 36:317–321.

Campbell, G., Norman, J. 1989. The description and measurement of plant canopy structure. In: Plant Canopies: Their Growth, Form and Function. Russel, G., Marshall, B., and Jarvis, P. G. (eds). Cambridge University Press, Cambridge, England.

Campbell, G. S., Norman, J. M. 1998. An Introduction to Environmental Biophysics, 2nd ed. Springer, New York, USA.

Coulson, K. L., Reynolds, D. W. 1971. The spectral reflectance of natural surfaces. Journal of Applied Meteorology 10:1285–1295.

Cruse, M. J., Kucharik, C. J., Norman, J. M. 2015. Using a simple apparatus to measure direct and diffuse photosynthetically active radiation at remote locations. PLoS ONE 10:e0115633.

Davidson, E. A., Janssens, I. A., Luo, Y. Q. 2006. On the variability of respiration in terrestrial ecosystems: moving beyond Q(10). Global Change Biology 12:154–164.

de Wit, C. T. 1965. Photosynthesis of leaf canopies. Agricultural Research Report No. 663. Center for Agricultural Publications and Documentation, Wageningen, The Netherlands.

Flerchinger, G. N., Xiao, W., Sauer, T. J., Yu, Q. 2009. Simulation of within-canopy radiation exchange. Wageningen Journal of Life Sciences 57:5–15.

Girardin, P., Tollenaar, M. 1994. Effects of intraspecific interference on maize leaf azimuth. Crop Science 34:151–155.

Goel, N. S., Strebel, D. E. 1984. Simple beta distribution representation of leaf orientation in vegetation canopies. Agronomy Journal 76:800–802.

Goudriaan, J. 1977. Crop micrometeorology: a simulation study. Simulation Monographs. Pudoc, Center for Agricultural Publishing and Documentation, Wageningen, The Netherlands.

Kimes, D. S. 1984. Modeling the directional reflectance from complete homogeneous vegetation canopies with various leaf-orientation distributions. Journal of the Optical Society of America A 1:725–737.

Kucharik, C. J., Norman, J. M., Gower, S. T. 1999. Characterization of radiation regimes in nonrandom forest canopies: Theory, measurements, and a simplified modeling approach. Tree Physiology 19:695–706.

Lellei-Kovács, E., Kovács-Láng, E., Botta-Dukát, Z., Kalapos, T., Emmett, B., Beier, C. 2011. Thresholds and interactive effects of soil moisture on the temperature response of soil respiration. European Journal of Soil Biology 47:247–255.

Linn, D. M., Doran, J. W. 1984. Effect of water-filled pore space on carbon dioxide and nitrous oxide production in tilled and nontilled soils. Soil Science Society of America Journal 48:1267–1272.

Lloyd, J., Taylor, J. A. 1994. On the temperature dependence of soil respiration. Functional Ecology 8:315–323.

Lobo, F. d. A., de Barros, M. P., Dalmagro, H. J., Dalmolin, Â. C., Pereira, W. E., de Souza, É. C., Vourlitis, G. L., Rodríguez Ortíz, C. E. 2013. Fitting net photosynthetic light-response curves with Microsoft Excel – a critical look at the models. Photosynthetica 51:445–456.

Luo, Y., Zhou, X. 2006. Soil Respiration and the Environment. Academic Press. Cambridge, MA, USA.

Monsi, M., Saeki, T. 1953. Über den lichtfaktor in den pflanzengesellschaften und seine bedeutung für die stoffproduktion. Japanese Journal of Botany 14:22–52.

Nilson, T. 1971. A theoretical analysis of the frequency of gaps in plant stands. Agricultural Meteorology 8:25–38.

Pisek, J., Lang, M., Nilson, T., Korhonen, L., Karu, H. 2011. Comparison of methods for measuring gap size distribution and canopy nonrandomness at Järvselja RAMI (RAdiation transfer Model Intercomparison) test sites. Agricultural and Forest Meteorology 151:365–377.

Prolingheuer, N., Scharnagl, B., Graf, A., Vereecken, H., Herbst, M. 2014. On the spatial variation of soil rhizospheric and heterotrophic respiration in a winter wheat stand. Agricultural and Forest Meteorology 195-196:24–31.

Ryu, Y., Nilson, T., Kobayashi, H., Sonnentag, O., Law, B. E., Baldocchi, D. D. 2010. On the correct estimation of effective leaf area index: Does it reveal information on clumping effects? Agricultural and Forest Meteorology 150:463–472.

Sanford, G. R., Oates, L. G., Jasrotia, P., Thelen, K. D., Robertson, G. P., Jackson, R. D. 2016. Comparative productivity of alternative cellulosic bioenergy cropping systems in the North Central USA. Agriculture, Ecosystems & Environment 216:344–355.

Savage, K., Davidson, E. A., Richardson, A. D., Hollinger, D. Y. 2009. Three scales of temporal resolution from automated soil respiration measurements. Agricultural and Forest Meteorology 149:2012–2021.

Teh, C. B. S., Simmonds, L. P., Wheeler, T. R. 2000. An equation for irregular distributions of leaf azimuth density. Agricultural and Forest Meteorology 102:223–234.

Wang, W.-M., Li, Z.-L., Su, H.-B. 2007. Comparison of leaf angle distribution functions: Effects on extinction coefficient and fraction of sunlit foliage. Agricultural and Forest Meteorology 143:106–122.

Warren Wilson, J. 1960. Inclined point quadrats. New Phytologist 59:1–8.

Warren Wilson, J. 1967. Stand structure and light penetration. III. Sunlit foliage area. Journal of Applied Ecology 4:159–165.

Welles, J. M., Norman, J. M. 1991. Instrument for indirect measurement of canopy architecture. Agronomy Journal 83:818–825.

Ye, Z.-P. 2007. A new model for relationship between irradiance and the rate of photosynthesis in Oryza sativa. Photosynthetica 45:637–640.

2.11 Supplemental tables and figures

Table 2.S.1 – Relative quality, as indicated by Akaike information criterion (AIC), of statistical models for the light response of leaf-level net photosynthesis. Bracketed numbers refer to the full model equations as presented in Lobo et al. (2013).

	Akaike information criterion (AIC)				
	Maize		*Switchgrass*		
Model Name	***Upper***	***Lower***	***Upper***	***Lower***	***Median***
Exponential [8]	3336	2292	2924	2441	2683
Ye (2007) [11]	3337	2293	2926	2443	2684
Nonrectangular hyperbola [6]	3338	2294	2926	2444	2685
Hyperbolic tangent [4]	3338	2293	2930	2443	2687
Rectangular hyperbola [1]	3343	2297	2928	2446	2687

Table 2.S.2 – Relative quality (AIC) of the leaf-level light exponential response model with all combinations of leaf temperature (T_{leaf}) and leaf vapor pressure deficit (VPD_{leaf}) considered.

Model variables			Akaike information criterion (AIC)				
			Maize		*Switchgrass*		
$A_{g,max}$ (x)	$\phi_{(Q0)}$ (x)	R_D (x)	***Upper***	***Lower***	***Upper***	***Lower***	***Median***
T_{leaf} + VPD_{leaf}		T_{leaf}	2998	2166	2840	2317	2579
T_{leaf} + VPD_{leaf}		T_{leaf} + VPD_{leaf}	2999	2168	2842	2319	2580
T_{leaf} + VPD_{leaf}		VPD_{leaf}	3010	2167	2843	2317	2580
T_{leaf} + VPD_{leaf}			3004	2163	2855	2319	2587
T_{leaf} + VPD_{leaf}	T_{leaf} + VPD_{leaf}	T_{leaf}	3065	2159	2885	2320	2603
T_{leaf} + VPD_{leaf}	T_{leaf} + VPD_{leaf}	T_{leaf} + VPD_{leaf}	3066	2160	2887	2322	2604
T_{leaf} + VPD_{leaf}	T_{leaf}	VPD_{leaf}	3076	2165	2889	2320	2605
T_{leaf} + VPD_{leaf}	T_{leaf} + VPD_{leaf}	VPD_{leaf}	3074	2160	2890	2321	2605
T_{leaf} + VPD_{leaf}	T_{leaf}	T_{leaf} + VPD_{leaf}	3075	2167	2890	2322	2606
T_{leaf} + VPD_{leaf}	T_{leaf}	T_{leaf}	3076	2166	2891	2323	2607
T_{leaf} + VPD_{leaf}	T_{leaf} + VPD_{leaf}		3100	2158	2911	2325	2618
	T_{leaf} + VPD_{leaf}	VPD_{leaf}	3158	2240	2866	2384	2625
	T_{leaf} + VPD_{leaf}	T_{leaf}	3152	2241	2864	2386	2625
	T_{leaf} + VPD_{leaf}	T_{leaf} + VPD_{leaf}	3152	2242	2866	2385	2625
T_{leaf} + VPD_{leaf}	T_{leaf}		3119	2169	2921	2330	2626
	T_{leaf} + VPD_{leaf}		3150	2239	2869	2384	2627
	T_{leaf}	T_{leaf} + VPD_{leaf}	3245	2253	2882	2383	2632
T_{leaf} + VPD_{leaf}	VPD_{leaf}	T_{leaf} + VPD_{leaf}	3187	2208	2941	2340	2640
T_{leaf} + VPD_{leaf}	VPD_{leaf}	VPD_{leaf}	3196	2213	2945	2343	2644
		T_{leaf} + VPD_{leaf}	3299	2271	2895	2401	2648
	T_{leaf}	VPD_{leaf}	3284	2276	2892	2415	2653
	VPD_{leaf}	T_{leaf} + VPD_{leaf}	3344	2274	2927	2382	2655
T_{leaf} + VPD_{leaf}	VPD_{leaf}	T_{leaf}	3229	2223	2966	2353	2659
T_{leaf}		T_{leaf} + VPD_{leaf}	3246	2252	2931	2389	2660
		VPD_{leaf}	3313	2283	2898	2423	2661
T_{leaf}	T_{leaf} + VPD_{leaf}	T_{leaf} + VPD_{leaf}	3139	2230	2938	2383	2661
T_{leaf}	T_{leaf} + VPD_{leaf}	VPD_{leaf}	3149	2230	2937	2387	2662
T_{leaf}	T_{leaf} + VPD_{leaf}	T_{leaf}	3140	2233	2937	2391	2664
T_{leaf}	T_{leaf} + VPD_{leaf}		3160	2234	2957	2395	2676
T_{leaf}	T_{leaf}	T_{leaf} + VPD_{leaf}	3324	2250	2971	2392	2682
		T_{leaf}	3344	2294	2922	2442	2682
			3336	2292	2924	2441	2683
T_{leaf} + VPD_{leaf}	VPD_{leaf}		3281	2229	3001	2365	2683
	T_{leaf}	T_{leaf}	3342	2292	2930	2440	2685
T_{leaf}			3297	2287	2956	2437	2696
T_{leaf}		VPD_{leaf}	3297	2287	2956	2437	2696
	T_{leaf}		3366	2294	2951	2445	2698
T_{leaf}	VPD_{leaf}	T_{leaf} + VPD_{leaf}	3427	2270	3007	2398	2703
	VPD_{leaf}	VPD_{leaf}	3446	2320	2971	2441	2706
T_{leaf}	T_{leaf}	VPD_{leaf}	3402	2300	3005	2448	2726
T_{leaf}		T_{leaf}	3354	2307	2996	2466	2731
	VPD_{leaf}	T_{leaf}	3542	2347	3037	2480	2759
T_{leaf}	T_{leaf}	T_{leaf}	3472	2324	3054	2482	2768

Table 2.S.2 [continued]

Model variables			Akaike information criterion (AIC)				
			Maize		*Switchgrass*		
$A_{g,max}$ (x)	$\phi_{(Q0)}$ (x)	R_D (x)	***Upper***	***Lower***	***Upper***	***Lower***	***Median***
VPD_{leaf}	T_{leaf} + VPD_{leaf}	T_{leaf} + VPD_{leaf}	3304	2338	3072	2477	2775
	VPD_{leaf}		3575	2353	3065	2489	2777
VPD_{leaf}	T_{leaf} + VPD_{leaf}	VPD_{leaf}	3302	2346	3074	2490	2782
VPD	T_{leaf} + VPD_{leaf}	T_{leaf}	3302	2343	3077	2488	2783
T_{leaf}	VPD_{leaf}	VPD_{leaf}	3575	2349	3083	2484	2783
VPD_{leaf}	T_{leaf} + VPD_{leaf}		3307	2342	3082	2486	2784
T_{leaf}	T_{leaf}		3506	2331	3085	2493	2789
VPD_{leaf}		T_{leaf} + VPD_{leaf}	3490	2385	3107	2510	2808
VPD	T_{leaf}	T_{leaf} + VPD_{leaf}	3583	2394	3164	2518	2841
T_{leaf}	VPD_{leaf}	T_{leaf}	3678	2385	3155	2530	2842
T_{leaf}	VPD_{leaf}		3718	2394	3190	2543	2866
VPD_{leaf}	VPD_{leaf}	T_{leaf} + VPD_{leaf}	3762	2418	3212	2523	2867
VPD_{leaf}			3597	2452	3185	2605	2895
VPD_{leaf}		T_{leaf}	3598	2454	3186	2609	2897
VPD_{leaf}		VPD_{leaf}	3591	2463	3181	2617	2899
VPD_{leaf}	T_{leaf}		3708	2483	3276	2638	2957
VPD_{leaf}	T_{leaf}	T_{leaf}	3719	2490	3281	2645	2963
VPD_{leaf}	T_{leaf}	VPD_{leaf}	3722	2500	3277	2652	2964
VPD_{leaf}	VPD_{leaf}	VPD_{leaf}	4029	2577	3404	2698	3051
VPD_{leaf}	VPD_{leaf}		4035	2576	3431	2703	3067
VPD_{leaf}	VPD_{leaf}	T_{leaf}	4046	2581	3432	2708	3070

Table 2.S.3 – Parameter estimates and median absolute error (MAE) for leaf level photosynthesis models fit using equations 2.7a-d. Parameter estimates are from non-linear least squares regressions, while MAE is from Monte Carlo cross-validation procedures. The *p*-value for all parameter estimates was < 0.00001.

	Parameter estimate (standard error)				**Median absolute error (± 95%)**
Crop, canopy layer	*a*	*b*	*c*	*d*	(μmol CO_2 m^{-2} s^{-1})
Maize, upper	2.61 (0.072)	-15.6 (0.74)	0.054 (0.0018)	0.099 (0.0086)	1.29 (1.02, 1.56)
Maize, lower	1.77 (0.078)	-9.83 (0.78)	0.055 (0.0037)	0.057 (0.013)	1.06 (0.73, 1.56)
Switchgrass, upper	1.61 (0.067)	-8.92 (0.70)	0.044 (0.0024)	0.084 (0.0094)	1.11 (0.85, 1.46)
Switchgrass, lower	1.25 (0.058)	-7.53 (0.59)	0.048 (0.0039)	0.056 (0.011)	1.08 (0.71, 1.56)

Table 2.S.4 – Parameter estimates and *p*-values from linear regressions between final leaf-level net photosynthesis model residuals and the model independent variables (PAR, T_{leaf}, and VPD_{leaf}).

Variable	Crop, layer	Estimate	*p*
PAR			
	Maize, upper	-0.000017	0.934
	Maize, lower	-0.000006	0.985
	Switchgrass, upper	-0.000010	0.965
	Switchgrass, lower	0.000011	0.966
T_{leaf}			
	Maize, upper	0.0151	0.596
	Maize, lower	0.0937	0.065
	Switchgrass, upper	-0.0673	0.042
	Switchgrass, lower	0.0061	0.871
VPD_{leaf}			
	Maize, upper	0.081	0.629
	Maize, lower	0.204	0.417
	Switchgrass, upper	-0.236	0.230
	Switchgrass, lower	-0.067	0.744

Table 2.S.5 – Summary of optical properties for fully photosynthetic (green) and non-photosynthetic (brown) leaves.

	Maize		**Switchgrass**	
Leaf type	*Green*	*Brown*	*Green*	*Brown*
Reflectance	0.071	0.231	0.097	0.188
Transmittance	0.021	0.079	0.037	0.014
Absorptance	0.908	0.689	0.866	0.798

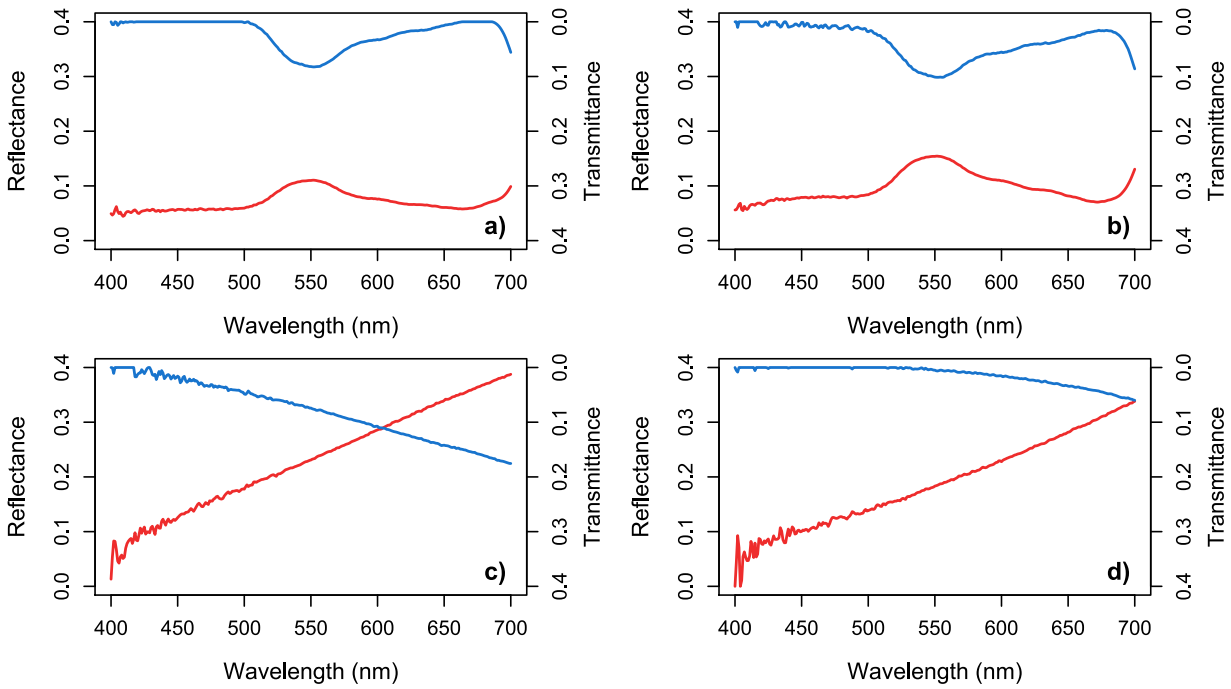

Figure 2.S.1 – Leaf PAR reflectance (red) and transmittance (blue) for (a) maize photosynthetic (green) leaves, (b) switchgrass photosynthetic (green) leaves, (c) maize non-photosynthetic (brown) leaves, and (d) switchgrass non-photosynthetic (brown) leaves.

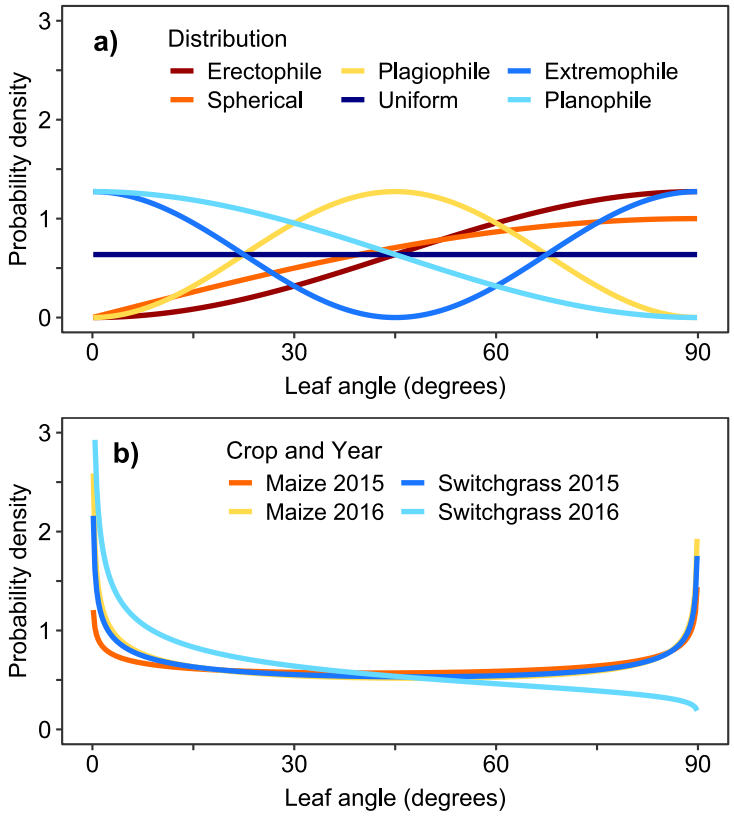

Figure 2.S.2 - Probability density functions for (a) theoretical and (b) LAI-2000 estimated leaf zenith angle distributions. Estimated leaf zenith angle distributions are based on seasonal median parameters for the beta distribution.

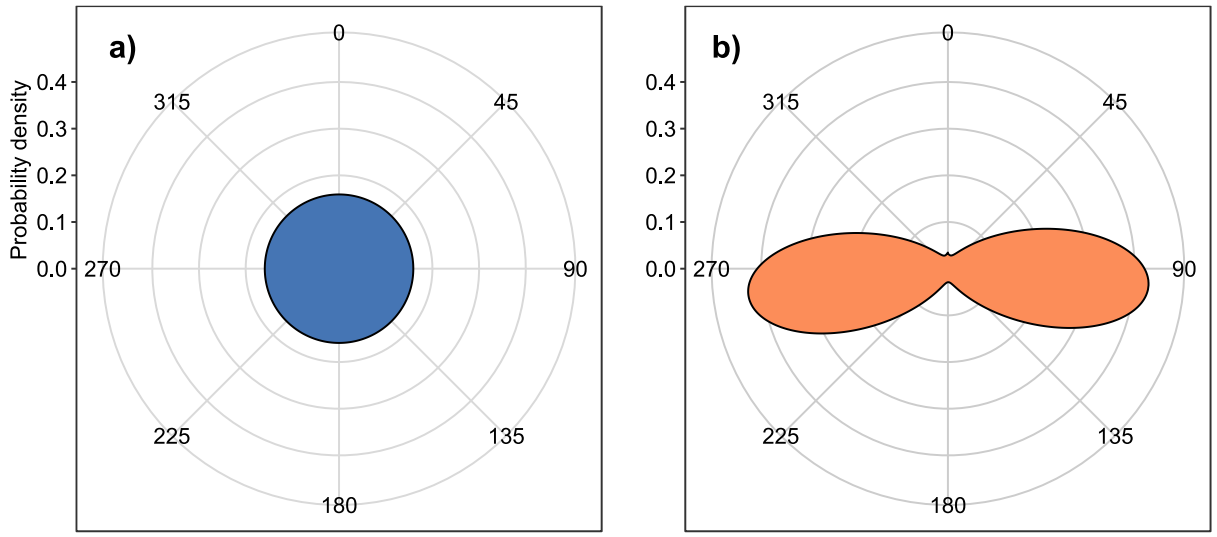

Figure 2.S.3 – Probability density functions for (a) uniform (b) non-uniform leaf azimuth angles in maize. North is 0° and east is 90°.

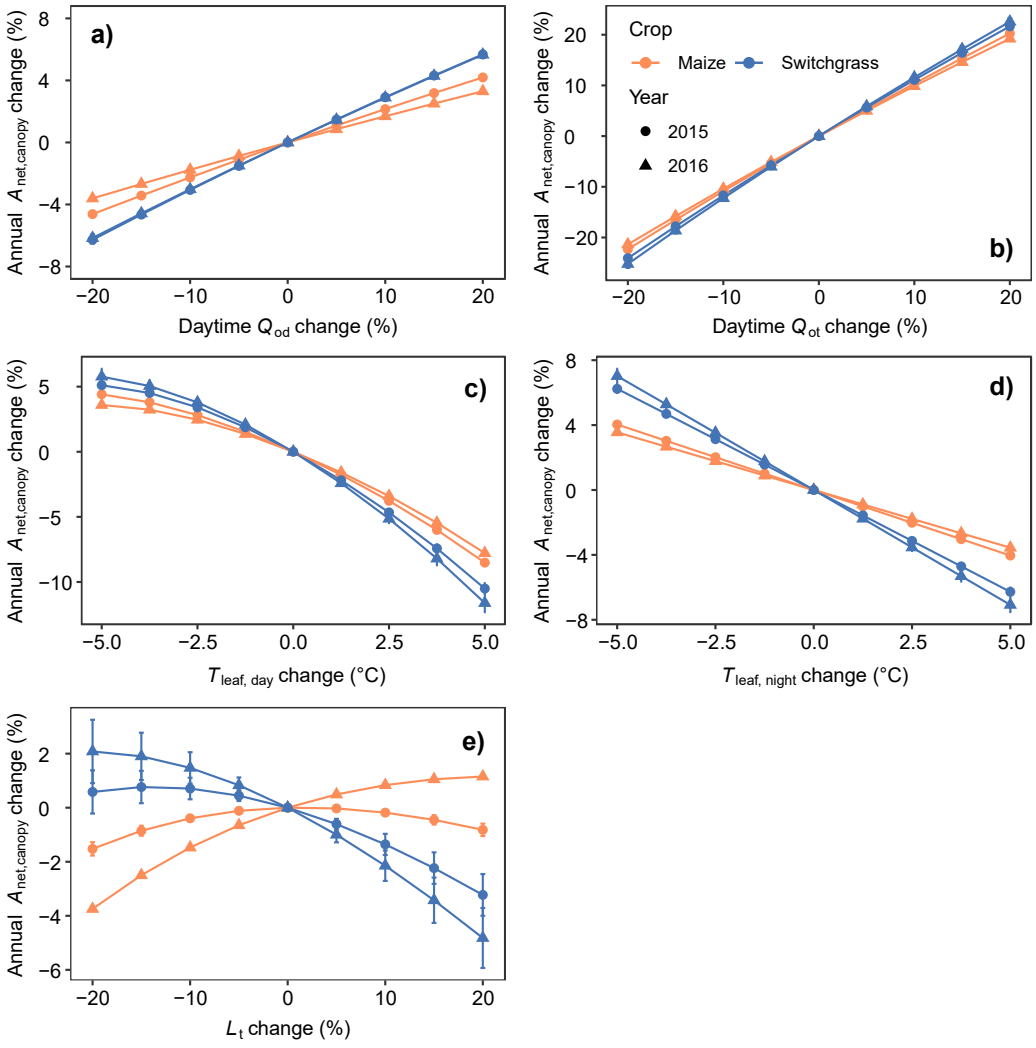

Figure 2.S.4 – Percent change in annual net canopy photosynthesis as a function of (a) daytime above-canopy diffuse PAR (Q_{od}) with no change in total PAR, (b) daytime above-canopy total PAR (Q_{ot}), (c) daytime leaf temperature ($T_{leaf,day}$), (d) nighttime leaf temperature ($T_{leaf,night}$), and (e) leaf area index (L_t).

Chapter 3

Autotrophic soil respiration in maize and switchgrass bioenergy cropping systems: an assessment of the growth-maintenance respiration framework at the ecosystem level

von Haden, A.C., Marín-Spiotta, E., Jackson, R.D., Kucharik, C.J.

Target journal: Global Change Biology

Abstract

Root respiration consumes a substantial fraction of plant fixed C and thus has a significant effect on the net C balance of plants and ecosystems. Studies dividing root respiration into growth and maintenance components have revealed physiological differences among plant species and growth types, but these studies have rarely been scaled to ecosystems and validated. We used *in situ* diel autotrophic soil respiration (R_A) measurements in maize and switchgrass to parameterize growth-maintenance models that also accounted for influence of temperature and photosynthesis. To account for the temperature effect on R_A, we implemented a method to directly estimate root temperature throughout the soil profile and account for lags between root respiration and soil surface R_A. We found that specific growth respiration, which likely included ion uptake costs, was about two times higher in switchgrass than maize. Contrarily, the specific maintenance respiration rates were about four times higher in maize than switchgrass, probably due to the greater concentrations of structural tissues in switchgrass roots and rhizomes. The diel influence of photosynthesis on maize R_A was apparent at a lag time of 14 to 16 hours, but the signal was too weak to detect in switchgrass. The R_A temperature sensitivity and temperature acclimation responses could not be statistically separated, and thus further work is needed to constrain those parameters. Predictions from the diel-based models simulated independently

measured seasonal trends of R_A reasonably well. Thus, the growth-maintenance respiration framework provides insight into the physiology of root respiration that translates adequately to the ecosystem level.

3.1 Introduction

Net ecosystem carbon balance is largely determined by the difference between gross photosynthetic C fixation by plants and ecosystem respiration by plants and heterotrophs (Chapin et al. 2006). Whole plant respiration typically consumes about half of daily fixed C, with roots respiring approximately 10 to 50% (Lambers et al. 2008). Therefore, root respiration accounts for a substantial fraction of the gross C loss from terrestrial ecosystems. However, the proportion of plant-fixed C respired by roots can vary greatly by species and growing conditions (Poorter et al. 1990; Poorter et al. 1995). For example, von Haden (2017) found that the annual proportion of net photosynthesis consumed by root respiration was approximately 20% and 40% in two C4 grasses, maize and switchgrass, respectively. A more mechanistic understanding of the underlying physiology of root respiration would therefore help to better predict plant and ecosystem C balances.

The growth respiration-maintenance respiration paradigm provides a simple, pragmatic construct for modeling plant root respiration physiology (Lambers et al. 1983; Thornley & Cannell 2000). In its basic form, root respiration is divided into two primary components: a growth component accounting for the respiratory CO_2 requirement of root growth and a maintenance component accounting for the respiratory CO_2 requirement of root biomass maintenance (Amthor 2000). Growth respiration is therefore proportional to root growth and maintenance respiration is proportional to root biomass (Johnson 1990). In addition, a growth

respiration coefficient quantifies the total respiration per unit growth, and a maintenance respiration coefficient quantifies the respiration rate per unit root biomass (Amthor 2000). Since the respiration coefficient is a biological rate, it varies with temperature, but the growth respiration coefficient is effectively temperature independent (Amthor 2000).

Growth and maintenance root respiration coefficients have been experimentally determined for a considerable number of species and growth conditions (Amthor 1984; Cannell & Thornley 2000). These studies have provided insight into the physiology of root respiration among functional groups, such as fast- and slow-growing species (Poorter et al. 1991). As a result, many ecosystem-level models have adapted the growth respiration-maintenance respiration framework (Thornley & Cannell 2000). However, few studies have attempted to directly scale root growth and maintenance respiration coefficients, as typically measured in a controlled setting, to the field. The few studies that have done so have either been unreliable without additional adjustments (Reekie & Redmann 1987) or have not been validated (Cannell & Thornley 2000; M'Bou et al. 2010). Thus, there is considerable uncertainty regarding the performance of the growth respiration-maintenance respiration framework at an ecosystem level.

At a diel timescale, root respiration is coupled to photosynthesis through the transport of photosynthates in the phloem from leaves to roots (Mencuccini & Hölttä 2010). The transport of photosynthates from leaves to roots, combined with the transport of root-respired CO_2 from the roots to the soil surface, creates a time lag between photosynthesis and realized autotrophic soil respiration (R_A) at the soil surface (Kuzyakov & Gavrichkova 2010; Mencuccini & Hölttä 2010). Since temperature exerts a strong influence on diel root respiration (Amthor 2000), the influence of photosynthesis on diel root respiration may be difficult to detect *in situ* (Mencuccini & Hölttä 2010). If the effect of temperature on R_A is accounted for, then the effect of photosynthesis can

be assessed. However, *in situ* temperature is often measured at a single soil depth, which can create an artifactual hysteresis between respiration and measured temperature that may be misattributed to the photosynthesis influence on R_A (Phillips et al. 2011). In addition, since there is a lag time between CO_2 generation and soil surface efflux, the soil profile temperature measured at the time of surface R_A efflux is unlikely to be representative of the temperatures when the CO_2 was generated, particularly at greater soil depths. These issues require mitigation to control for the effect of temperature on R_A and thus adequately determine the coupling of photosynthesis and R_A.

The primary objective of this study was to better understand the temporal patterns of root respiration in maize and switchgrass cropping systems. To meet this objective, we aimed to parameterize and validate root growth respiration-maintenance respiration models using *in situ* observations collected at diel and seasonal periods, respectively. As a secondary objective, we sought to assess the effect of photosynthesis on diel patterns of R_A and determine the lag time between the two processes. A third objective, which was necessary to meet the first two objectives, was to devise and implement a method to estimate *in situ* root temperature at the time of root respiration.

3.2 Methods

3.2.1 Study site

The study was conducted at the DOE-Great Lakes Bioenergy Research Center's Biofuel Cropping Systems Experiment (BCSE) in Arlington, WI, USA (43.296° N, 89.380° W). The thirty-year normal temperature and precipitation are 6.9 °C and 869 mm, respectively (NOAA

2017). Soils at the site are primarily Plano silt loams: Fine-silty, mixed, superactive, mesic Typic Argiudolls (Soil Survey Staff 2017). The larger BCSE was initiated in 2008 and contains five completely randomized blocks of twelve treatments with individual plots of 27.4 x 42.7 m (Sanford et al. 2016). Our study was undertaken in continuous no-till maize and "Cave-In-Rock" variety switchgrass within three replicated blocks. Switchgrass stands were established in June 2008, while maize was planted every Spring. On average, maize received 167 kg N ha^{-1} yr^{-1} and switchgrass received 56 kg N ha^{-1} yr^{-1} (Sanford et al. 2016). Further agronomic specifications are given in Sanford et al. (2016).

3.2.2 Autotrophic soil respiration

Soil respiration components were measured during the 2015 and 2016 using an LI-6400XT portable photosynthesis system with an LI-6400-09 soil CO_2 flux chamber (LI-COR Inc., Lincoln, NE, USA). Total soil respiration (R_T) and heterotrophic soil respiration (R_H) were measured, and autotrophic respiration (R_A) was calculated as the difference between R_T and R_H. For R_T, six 10.2 cm inner diameter, 5 cm tall PVC collars were inserted 2 cm into the soil within each plot. The R_T collars were stratified among the plant spaces (e.g. row and interrow) to capture small-scale spatial variability. Two root exclusion collars per plot were used to measure R_H (Vogel & Valentine 2005). A 12.7 cm diameter bucket auger was used to excavate 10 cm soil sections down to approximately 100 cm. The soil sections were kept separate and sieved on a 5 mm mesh screen to remove live roots; dead roots were kept in the soil. A 10.2 cm PVC tube was cut to approximately 103 cm and placed into the hole made with the bucket auger. The sieved soil was then serially backfilled into the PVC tube and packed to approximate the original soil

bulk density. Decagon 5TM soil moisture sensors (Decagon Devices Inc., Pullman, WA, USA) were placed inside and outside of each root exclusion collar at the 0-5 cm depth.

A soil moisture correction factor was applied to the measured R_H values to account for differences between soil moisture inside ($M_{soil,in}$) the root exclusion collar and soil moisture outside ($M_{soil,out}$) the root exclusion collars (Prolingheuer et al. 2014). A complete description is given in von Haden (2017). In short, a non-linear empirical model containing 2 cm soil temperature and $M_{soil,in}$ was fit to measured R_H values. For each R_H measurement timepoint, the model was used to estimate R_H at $M_{soil,in}$ and $M_{soil,out}$. The correction factor for each timepoint was the difference between predicted R_H at $M_{soil,out}$ and $M_{soil,in}$. The correction factor was applied to the corresponding R_H measurement.

Autotrophic soil respiration was measured at diel and seasonal timescales. The diel measurement campaigns occurred in late June, July, and August of 2015 and 2016 for a total of six diurnal cycles. During the diel campaigns, measurements were made in one set of plots, and each collar within the set of plots was measured once per hour for 24 contiguous hours. The seasonal survey measurements occurred approximately twice per week during the 2015 and 2016 growing seasons. The seasonal survey measurements were targeted between the hours of 0900 and 1300, and all collars within all three sets of plots were measured on each survey date.

3.2.3 Belowground growth and biomass

Belowground cumulative growth and growth phenology were estimated with the root ingrowth method (Persson et al. 1979). A complete description of the method is provided in von Haden (2017). In brief, six 50 cm long, 7.4 cm outer diameter plastic mesh ingrowth cores per

plot were used to estimate root growth at approximately monthly intervals during the two growing seasons. Prior to the insertion of the six ingrowth cores, soil was extracted in 10 cm depth increments to 40 cm deep using a 7.6 cm diameter bucket auger. The extracted soil was serially sieved over a 5 mm mesh screen, all belowground biomass that appeared live based on appearance was saved (Hayes & Seastedt 1987), and dead roots were discarded. The ingrowth cores were placed into the holes created by the bucket auger, the soil was serially backfilled into the holes, and each layer was packed to approximate the original bulk density. At the end of each ingrowth period, the ingrowth cores were removed and new ingrowth cores were inserted into new holes. The final set of ingrowth cores was removed when plants were near complete senescence. Belowground biomass and ingrowth biomass were washed with water over an 800 μm sieve and dried at 65 °C. We did not observe any rhizomes in the ingrowth cores, but rhizomes were present in the switchgrass belowground biomass samples. For convenience, we hereafter refer to belowground growth as root growth and belowground biomass as root biomass.

Model fitting was used to characterize root growth phenology and the vertical distribution of root biomass at smaller time and depth intervals, respectively. Cumulative seasonal root growth was fit to a logistic growth curve:

$$RG(t) = \frac{RG_{max}}{1+\exp[-k_G(t-t_m)]} \quad (3.1)$$

where RG(t) is accumulated root growth (g m^{-2}) at t days after plant emergence, RG_{max} is the maximum cumulative root growth (asymptote), t_m is the day of maximum root growth rate, and k_G affects the shape of the growth curve (Archontoulis & Miguez 2015). The first derivative is then:

$$RG'(t) = \frac{RG_{max}\, k_G \exp[k_G(t_m+t)]}{[\exp(k_G t_m)+\exp(k_G t)]^2} \quad (3.2)$$

where RG'(t) is the root growth rate (g m^{-2} d^{-1}) on day t. RG'(t) thus provides a daily estimate of root growth.

The vertical distribution of root biomass was fitted to an exponential decay function:

$$RB(d) = RB_{max}[1 - \exp(-k_B d)] \quad (3.3)$$

where RB(d) is cumulative root biomass at depth d (cm), RB_{max} is the maximum root biomass (asymptote), and k_B adjusts the shape of the curve. The first derivative is then:

$$RB'(d) = RB_{max} k_B \exp(-k_B d) \quad (3.4)$$

where RB'(d) is the instantaneous root biomass (g m^{-2} cm^{-1}) at depth d. To convert the absolute instantaneous root biomass [RB'(d)] to relative instantaneous root biomass [RB_R'(d)], the area under the RB'(d) function from d=0 to 40 cm was standardized to unity.

Since small temporal changes in root biomass are difficult to detect when the overall root biomass stock is large, we assumed that switchgrass root biomass was constant and equal to the measured average value for each plot. For maize, root biomass at time t was equal to the cumulative seasonal root growth at time t. Finally, we assumed that the vertical distribution of root biomass was temporally constant in switchgrass (equal to the plot average), but that the vertical distribution of root biomass in maize was temporally dynamic (equal to the plot measured values). It was therefore necessary to linearly interpolate maize root biomass quantity and vertical distributions to daily intervals.

3.2.4 Soil temperature, moisture, and soil properties

Soil temperature was measured with thermocouples, and soil moisture was measured with Campbell CS616 and CS640 moisture probes (Campbell Scientific, Logan, UT, USA). Soil temperature was measured at 15 min intervals and stored as hourly averages, and soil moisture was measured at either 15 min or hourly intervals and stored at hourly intervals, both using Campbell CR10X and CR1000 dataloggers. In addition to the three replicated blocks used in the other portions of the study, soil temperature and moisture were measured in a fourth block. The systems for measuring soil temperature and moisture varied among blocks, but all plots included at a pair of soil temperature thermocouples at 2 cm, 10 cm, and 20/30 cm each and soil moisture probes at a minimum of two depths (2/15 cm and 20/30 cm). Two of the blocks contained soil temperature and moisture probes at seven depths from 2 cm to 125 cm deep. For the two blocks with limited measurement depths (i.e. 20 or 30 cm), deeper soil temperature and moisture were set to the treatment averages among the other blocks. Where possible, missing data were gap-filled by using the treatment average of the other blocks. All volumetric water content measurements were standardized to a Delta-T SM150 TDR (Delta-T Devices Ltd., Cambridge, England) based on over 200 concurrent probe measurements spanning from 15 to 47% volumetric soil moisture. Hourly soil temperature [$T_{Soil}(d)$] and soil moisture [$M_{Soil}(d)$] depth profiles were estimated from 0.5 to 39.5 cm at 1 cm intervals using a natural cubic spline.

Soil physical and chemical properties were measured as a part of routine inventories in 2008 and 2013. A hydraulic probe was used to collect three 7.6 cm diameter, 100 cm deep soil cores per plot. The cores were split into 0-10, 10-25, 25-50, and 50-100 cm sections. Soil particle size analysis for soil texture was determined using the hydrometer method (Gee & Bauder 1986) on the 2008 soil samples. Bulk density and SOC were measured on the 2013 soil samples.

Percent C was determined using a Flash EA 1112 elemental analyzer (Thermo Electron Corp., Milan, Italy), and organic matter content was estimated by assuming that organic matter is 58% C by weight (Howard 1966). Soil properties were interpolated from 0.5 to 39.5 cm at 1 cm intervals using a natural cubic spline.

3.2.5 CO_2 diffusion time lag

The time lag between CO_2 production and diffusion to the soil surface was estimated using a 40-layer (0.5 to 39.5 cm) model based upon the soil properties of each layer. The one-dimensional mean diffusion time at a given distance can be calculated as (Monteith & Unsworth 2008):

$$t_d = \frac{d^2}{2D_s} \tag{3.5}$$

where d is the one-dimensional distance (depth, cm) and D_s is the soil diffusion coefficient (cm^2 s^{-1}). The soil diffusion coefficient was estimated using (Moldrup et al. 1999):

$$D_s = D_a \phi^2 \left(\frac{\varepsilon}{\phi}\right)^{\beta F_{cp}} \tag{3.6}$$

where D_a is CO_2 diffusivity in free air, ϕ is the total porosity, ε is the volumetric soil air content, F_{cp} is the fraction of silt plus sand, and β is an empirically-derived parameter of 2.9 (Moldrup et al. 1999; Vargas & Allen 2008). To account for diffusion in water-saturated soil ($\varepsilon = 0$), the minimum D_s was set at four orders of magnitude below diffusivity in free air (Jähne et al. 1987). The CO_2 diffusivity in free air was (Massman 1998; Monteith & Unsworth 2008):

$$D_a = \left(\frac{P_0}{P}\right)\left(\frac{T}{T_0}\right)^{1.81} 0.1381\ cm^2 s^{-1} \tag{3.7}$$

where P_0 is 101.325 kPa, T_0 is 273.15 °K, P is the time-specific air pressure (kPa), and T is the time- and depth-specific temperature (°K). The total porosity was calculated as (Brady & Weil 1999):

$$\phi = 1 - \left(\frac{\rho_b}{\rho_p}\right) \quad (3.8a)$$

$$\rho_p = [(F_{SOM})\ 1.40\ g\ cm^{-1}] + [(1 - F_{SOM})\ 2.65\ g\ cm^{-1}] \quad (3.8b)$$

where ρ_d is the bulk density, F_{SOM} is the fraction of soil organic matter, and 1.4 and 2.65 g cm^{-1} are the assumed densities of organic matter and mineral soil, respectively (Brady & Weil 1999; Ruhlman et al. 2006). Volumetric soil air content was calculated as (Vargas & Allen 2008):

$$\varepsilon = \phi - \theta \quad (3.9)$$

where θ is the time-and depth-specific volumetric soil moisture content. Since each depth increment had different physical properties, a partial diffusion time (tp) was calculated for each depth increment, d_i:

$$tp(d_i) = \frac{{d_i}^2 - {d_{i-1}}^2}{2D_{s_i}} \quad (3.10)$$

The total diffusion time to depth increment d was then:

$$t(d) = \sum_{d_i=0.5}^{d} tp(d_i) \quad (3.11)$$

The lagged soil temperature at each depth and hour was:

$$T_{Soil,lag}[d, h + t(d)] = T_{Soil}[d, h] \quad (3.12)$$

where d is the depth, h is the current hour, and t(d) the diffusion time at depth d (hours). Considering the multiple sources of potential error in the diffusion time estimate (e.g. bulk density, volumetric soil water content, soil diffusivity model), we used the treatment median

diffusion times to calculate lagged temperature profiles in each plot (Fig. 3.S.1). The lagged soil temperature profiles were then combined with relative root biomass distributions to estimate the soil profile average root temperature:

$$\overline{T_{Root}} = \sum_{d=0.5}^{39.5} RB_R'(d)\, T_{Soil,lag}(d) \quad (3.13)$$

Thus, the average root temperature is the lagged soil temperature profile weighted by the relative depth-distribution of roots.

3.2.6 Photosynthesis

Net canopy photosynthesis (A_n) was estimated at hourly timescales by scaling leaf-level light response curves to the canopy-level with light attenuation models. A complete description is given in von Haden 2017. In summary, leaf-level photosynthetically active radiation (PAR) photosynthesis response curves were made at our study site on upper- and lower-level canopy leaves through the 2010-2012 growing seasons using a LI-6400XT portable photosynthesis system (LI-COR Inc., Lincoln, NE, USA). Crop and canopy-specific net photosynthesis responses were fit to non-linear models which accounted for the effects of PAR, air temperature, and vapor pressure deficit. A light attenuation model was assembled following Campbell & Norman (1998). The light attenuation model used leaf area index, leaf angle distribution, solar zenith angle, and direct/diffuse solar PAR to estimate mean canopy light levels in the sunlit and shaded canopy fractions. The full canopy-level photosynthesis model coupled the light-response models to the light attenuation models, and the model was run at hourly timesteps using locally-collected input data from the 2015 and 2016 growing seasons.

3.2.7 Autotrophic soil respiration model

Diurnal R_A data was fit to a model which accounted for the effects of growth respiration, temperature sensitive maintenance respiration with temperature acclimation, and photosynthesis with time lag:

$$R_A = R_{maint} + R_{growth} + m_{A \rightarrow RA} A_n(h)\left(R_{maint} + R_{growth}\right) \quad (3.14a)$$

$$R_{growth} = R_{s,g} RG' \quad (3.14b)$$

$$R_{maint} = \left(AC_b - AC_m \overline{T_{Root,a}}\right)\left(Q_b - Q_m \overline{T_{Root}}\right)^{[(\overline{T_{Root}} - 20)/10]} RB \quad (3.14c)$$

where R_{maint} is total root maintenance respiration, R_{growth} is total root growth respiration, $m_{A \rightarrow RA}$ describes the relationship between diel net photosynthesis and R_A, $A_n(h)$ is net canopy photosynthesis at h hours of lag, $R_{s,g}$ is the specific root growth respiration (i.e. the growth respiration coefficient), and $T_{Root,a}$ is the average root temperature over the previous 24 hours, and T_{Root} is the current root temperature. The coefficients AC_b and AC_m describe the temperature acclimation response (Kattage & Knorr 2007) and the coefficients Q_b and Q_m describe the variable temperature sensitivity response (Tjoelker et al. 2001) of root maintenance respiration. The specific root maintenance respiration rate (i.e. the root maintenance coefficient; $R_{s,m}$) can thus be calculated as function of the temperature and acclimation responses. The photosynthetic lag time (h) was determined by fitting separate models with h ranging from 0 to 24 hours and selecting the lag time which produced all positive model coefficients and the lowest Akaike information criterion (AIC). For comparison to other studies, a growth efficiency (or yield) can be calculated from the specific root growth respiration (Thornley 1970; Reekie & Redman 1987):

$$Y_g = \frac{1}{1 + R_{s,g}} \quad (3.15)$$

where $R_{s,g}$ is converted to C equivalents by assuming that root C content is 43%. With the final model parameters, R_A predictions were made at hourly timesteps using data collected during the 2015 and 2016 growing seasons. For our purposes, we define the growing season as the time between plant aboveground emergence and complete senescence (i.e. the time during which root growth and leaf area index data were collected). The temperature acclimation response was limited to the range of measured values from which the model was parameterized (Lombardozzi et al. 2015). The model R_A output was then compared against field survey R_A measurements made throughout the 2015 and 2016 growing seasons.

Model fitting was performed with the 'nlsLM' non-linear least squares function (Elzhov et al. 2016) in R version 3.4.1 (R Core Team 2017).

3.3 Results

3.3.1 Seasonal and diel patterns

Growing season temperature and precipitation during 2015 and 2016 were warmer and wetter than normal, with 2016 being more extreme than 2015 (Table 3.1). Annual cumulative root growth was greater in 2016 than 2015 in both maize and switchgrass (Fig. 3.1). Switchgrass root growth began several weeks earlier than maize, but peak daily root growth rate occurred several weeks earlier in maize than switchgrass. However, the peak daily root growth rate in maize was nearly twice that of switchgrass. Maize root growth effectively ceased in mid-August, whereas switchgrass root growth continued appreciably into mid-September. Mean growing season root biomass stocks were 115 g m^{-2} and 829 g m^{-2} in maize and switchgrass, respectively.

Switchgrass R_A was greater than maize R_A on nearly all survey measurement dates during the 2015 and 2016 growing seasons (Fig. 3.2). Maize R_A peaked in early July in both years, and switchgrass R_A peaked in mid-July in 2016. However, in 2015 switchgrass R_A showed an early peak during May and then declined slightly into June and July. Root temperature (T_{Root}) showed similar seasonal patterns in both maize and switchgrass, with maize T_{Root} being slightly warmer than switchgrass for most of the growing season. The differences in T_{Root} between maize and switchgrass were more prominent in 2016 than 2015. Owing to an earlier plant emergence date, canopy net photosynthesis (A_n) began earlier in switchgrass compared to maize. Peak A_n also occurred earlier in switchgrass than maize, but the A_n peak values were greater in maize than switchgrass.

Diurnal cycles of R_A were moderately noisy, but temporal trends were nonetheless apparent, with R_A often peaking during the evening hours (Fig. 3.3). Similar to the seasonal survey measurements, R_A in switchgrass was typically greater than maize, although the difference was more prominent in 2015 than 2016. Diel patterns of T_{Root} tended to peak near or slightly before R_A, whereas diel A_{net} peaked much earlier than diel R_A.

3.3.2 Diel R_A models

Maize R_A models with peak net photosynthesis to peak R_A lag times between 14 and 16 h showed the best overall fit based on the AIC (Table 3.2). For switchgrass, the four best fitting models had negative parameter estimates for $m_{A \rightarrow RA}$ (Table 3.S.1), in which case the lag describes the time between peak photosynthesis and base (i.e. lowest) R_A. For consistency and interpretability, we chose to use only models with positive $m_{A \rightarrow RA}$, where the lag thus describes the peak net photosynthesis to peak R_A. Importantly, the parameters other than $m_{A \rightarrow RA}$ were

similar in the best fitting models with positive and negative $m_{A \rightarrow RA}$ (Table 3.S.1). The three best fitting switchgrass models with positive parameters indicated a lag time of 22 to 24 h between peak net photosynthesis and R_A. The overall best fitting R_A models for maize and switchgrass had peak-to-peak lag times of 16 and 23 h, respectively. The model estimated relationship between net canopy photosynthesis and R_A was strong in maize, but the relationship was not statistically significant in switchgrass (Table 3.2). Full overall model fits were good, with R^2 of 0.89 and 0.71 for maize and switchgrass, respectively (Fig. 3.4).

The specific growth respiration rate was 1.8 times greater in switchgrass than maize (Table 3.3). Contrarily, the calculated specific maintenance respiration rate at T_{Root} and $T_{Root,a}$ of 20 °C was more than 4 times greater in maize than switchgrass. The Q_m parameters were not statistically significant for either crop model, which is likely attributable to the limited number of observations and the multicollinearity between T_{Root} and $T_{Root,a}$. While the combination of the acclimation and temperature sensitivity responses adequately describe the overall temperature response of R_A in our data (Fig. 3.4), the multicollinearity prevents the interpretation of the individual acclimation and sensitivity coefficients.

3.3.3 Seasonal predictions

Modelled growth and maintenance R_A showed markedly different seasonal patterns in maize and switchgrass (Fig. 3.5). Growth R_A followed root growth phenology, with an earlier, shorter peak in maize. Despite the lower daily root growth rates in switchgrass than maize, the modelled peak growth R_A rates were similar between crops due to the greater specific growth respiration in switchgrass. Over the course of the growing season, growth R_A in switchgrass was more than double that of maize (Table 3.4). Seasonal patterns of maintenance R_A were also

contrasting in maize and switchgrass, with maize maintenance respiration peaking in mid-to-late August and switchgrass maintenance respiration showing no clear peaking trend (Fig. 3.5). Despite lower specific maintenance respiration in switchgrass than maize, seasonal maintenance R_A was approximately twice as high in switchgrass (Table 3.4) due to the much greater root biomass stock in switchgrass. Growth R_A accounted for about one-third of total growing season R_A for both crops (Table 3.4). The relatively greater R_A in maize in 2016 compared to 2015 was reflected in both growth and maintenance respiration components, which likely resulted from a higher root growth rate, greater cumulative root production, and higher root temperatures (Fig. 3.1; Fig. 3.3). There was reasonable agreement and minimal bias between seasonal survey R_A measurements and model predicted R_A, with R^2 of 0.52 and 0.41 in maize and switchgrass, respectively (Fig. 3.6).

3.4 Discussion

3.4.1 Growth and maintenance respiration differed between plant types

The estimated values of specific root growth respiration and subsequent root growth efficiency (Y_g, 0.54 for maize and 0.39 for switchgrass) were within the range of values reported for grasses in other studies. Depending on the specific growth conditions and methodology, Hansen & Jensen (1977) reported Y_g between 0.39 and 0.65 for *Lolium multiflorum* Lam. Similarly, Reekie & Redman (1987) reported Y_g of 0.54 for *Agropyron dasystachyum* (Hook.) Scribn. The fact that our Y_g estimates were in the low- to mid-range of reported values may stem from the fact that the root ingrowth method is thought to conservatively estimate root production (Milchunas 2009). If root growth was in fact slightly underestimated, the specific growth respiration rate would be overestimated, causing the growth efficiency parameter to be

underestimated. Nonetheless, given that both maize and switchgrass are C4 grasses, it was somewhat surprising that switchgrass growth efficiency was appreciably lower than maize. In addition, this finding contrasts a comparison of annual versus perennial grass species that showed no significant difference in root construction costs (Roumet et al. 2006). A potential explanation for the differences in growth efficiency observed in our study is that the cost of ion uptake by roots was implicitly included within the root growth respiration estimates (Lambers et al. 1983). The specific respiratory cost of ion uptake is inherently greater in species with lower specific root growth rates (Poorter et al. 1991), and thus switchgrass may allocate a greater proportion of total belowground carbon to ion (e.g. nitrate) uptake than maize. This phenomenon may have been exacerbated by the differences in fertilizer regimes between crops in our study (Poorter et al. 1995), with maize receiving three times more N than switchgrass each year.

Estimated values of specific root maintenance respiration at 20 °C were lower than values reported for grass species in other root studies, which have reported minimum values of 37 [(mg C respiration day^{-1}) (g C biomass)$^{-1}$] (Reekie & Redman 1987). However, specific maintenance respiration rates as low as 12 [(mg C respiration day^{-1}) (g C biomass)$^{-1}$] have been reported for grass shoots (Hansen & Jensen 1977). One key difference between this study and other root maintenance respiration studies is that we measured R_A *in situ*, whereas other studies have been performed in a controlled environment. Estimating live root biomass *in situ* is challenging, as senesced or non-functioning roots may appear intact and alive, particularly in perennial systems. If live root biomass was overestimated due to the inclusion of senesced roots, then we would expect the specific root maintenance rates to be underestimated. Other grass root maintenance respiration studies have typically measured young plants in the range of several weeks to several months old (Hansen & Jensen 1977; Reekie & Redman 1987), but the switchgrass stands used in

our study were in their 8th and 9th growing seasons during this study. Considering that specific growth maintenance declines with grass plant age as a result of decreasing root tissue protein content (Stahl & McCree 1988), it is likely that the older switchgrass plants in our study had inherently lower specific root growth maintenance compared to younger plants. For example, Reekie and Redman (1987) found that scaling specific root maintenance respiration from young grass plants to an older, established grassland severely overestimated annual root respiration rates. However, when the specific root respiration rates were adjusted to the lower non-structural tissue content of the established grassland, the estimated annual root respiration rates decreased by approximately 75% and thus were much more reasonable (Reekie and Redman 1987). This same phenomenon may explain the higher specific root maintenance respiration rates observed in maize compared to switchgrass. Fast growing plant species typically have greater root protein content than slow growing plants (Poorter et al. 1991), and annual species typically have greater root N concentration (e.g. protein) than perennial species (Roumet et al. 2006). This is especially relevant considering that switchgrass "root" biomass also contained rhizomes, which are typically lower in protein content than roots (e.g. Gallagher et al. 1984). Thus, we may expect maize to have higher specific root maintenance respiration rates than switchgrass.

When all belowground dynamics were considered, model estimated growing season R_A was 2.2 times greater in switchgrass compared to maize. This agrees well with Buyanovsky et al. (1987) who reported that the annual contribution of root respiration was approximately twice as great in native prairie than winter wheat (*Triticum aestivum* L.). Similarly, Anderson-Teixeira et al. (2013) reported consistently greater R_A in perennial compared to annual bioenergy cropping systems. Buyanovsky et al. (1987) speculated that higher R_A in the perennial system was a result of greater root biomass and longer active growing season. While our results agree with this

assessment, the R_A model provides additional physiological insight. For example, both greater annual root growth and greater specific root growth respiration (which likely includes ion uptake costs) contributed to the higher R_A in switchgrass compared to maize. In other words, a greater total quantity of substrates was allocated to root growth in switchgrass, but the conversion of that substrate to growth was much less efficient. While average root biomass was much greater in switchgrass than maize, the specific root maintenance respiration rate was lower in switchgrass than maize. However, the difference in root biomass outweighed the difference in specific root maintenance respiration rate such that total root maintenance R_A was 2.3 times greater in switchgrass than maize. These results highlight potential juxtapositions between the belowground carbon economies of annual versus perennial or fast-growing versus slow-growing species that may be more generalizable.

3.4.2 Lag times between photosynthesis and R_A were detectable in maize

The lag time between photosynthesis and R_A in maize was estimated at 14 to16 h based on the top three performing models. This estimate is in good agreement with other literature values that suggest a lag time of 12.5 ± 7.5 h for grasses (Kuzyakov & Gavrichkova 2010). In reality, the lag time from photosynthesis to CO_2 production by the root is probably not constant, but rather varies as a function of phloem transport time, and thus is related the distance between leaves and roots (Kuzyakov & Gavrichkova 2010). The full lag time from photosynthesis to soil surface efflux includes transport from the roots through the soil, and therefore is also not constant, but depends on upon the soil CO_2 diffusivity (Mencuccini & Hölttä 2010). Since both plant height and soil CO_2 diffusivity varied among our diel R_A measurement data, our estimated lag time for maize can be considered typical but not temporally constant.

For switchgrass, the model estimated lag time was not statistically significant and therefore cannot be regarded as reliable. The lack of a statistical relationship between switchgrass photosynthesis and R_A does not necessarily mean that the relationship does not exist, but most likely indicates that the signal was too weak to detect. For example, at an extreme canopy net photosynthetic rate of 65 µmol CO_2 m^{-2} s^{-1} in maize, the increase in R_A (compared to nil photosynthesis) is 30% over the baseline R_A. In contrast, for switchgrass the model estimated increase over baseline R_A is only 6% at the same photosynthetic rate. Thus, in switchgrass the photosynthesis signal appears very small compared to the baseline R_A. Measuring R_A *in situ* in switchgrass is also particularly challenging due to the irregular small-scale spatial variability (i.e. the plants are not equally spaced in rows). Increased spatial and temporal R_A measurement resolution would likely be necessary to adequately estimate the photosynthetic R_A lag in switchgrass.

3.4.3 Root temperature affected R_A

Root temperature ($T_{Root)}$ and ambient root temperature ($T_{Root,a}$) exerted a large influence on root maintenance respiration and thus largely shaped the temporal patterns of R_A. However, $T_{root,a}$ and T_{root} are inherently correlated at the seasonal scale, and therefore the model acclimation parameters are probably implicitly describing part of the temperature sensitivity response in addition to the acclimation response. This likely explains the lack of statistical significance of the temperature sensitivity response parameter Q_m and the weak statistical significance of Q_b. With such a small sample size (n = 144), the multicollinearity of $T_{root,a}$ and T_{root} strips the biological meaning of the acclimation and sensitivity parameters. In addition, it likely creates more error in the predictions made from the model, which may explain the flashiness of modelled maintenance

R_A. A larger sample size would reduce the influence of multicollinearity and improve the parameter estimation for both temperature sensitivity and temperature acclimation. In addition, the range of T_{Root} during the diel measurements was notably limited compared to the full growing season T_{Root} range, with an absence of diel T_{Root} below about 15 °C. Expanding the range of T_{Root} used to parameterize the diel R_A models would also improve the temperature sensitivity estimates (Q_b and Q_m) and therefore provide better predictions of seasonal R_A. In sum, proper estimation of the complex R_A response to T_{root} and $T_{root,a}$ will require substantially larger R_A datasets such as those obtained by high-frequency automated soil respiration systems.

3.4.4 Strengths and limitations of the approach

The direct estimation of T_{Root}, in lieu of using an arbitrary soil temperature depth, is a key strength of our approach. Numerous studies have documented the inherent limitations of using temperature at an arbitrary soil depth as an explanatory variable for soil respiration (Pavelka et al. 2007; Graf et al. 2008; Phillips et al. 2011). Essentially, while soil temperature at a given depth may correlate with soil respiration, there is a lack of causation between the variables because the processes controlling soil respiration are not occurring solely at the measured depth. Instead, the processes controlling soil respiration (e.g. root respiration) are occurring along a vertical distribution gradient which typically declines non-linearly with depth (e.g. roots). Likewise, soil temperatures are not typically constant with depth, but vary throughout the soil profile. By accounting for the vertical distribution of both soil temperature and roots, we calculated a profile-average root temperature, which is thus causally linked to root respiration. A related but separate issue stems from the fact that diffusion of CO_2 through the soil profile necessarily creates a lag time between root respiration and surface efflux, and temporal changes

in soil physical properties can alter the lag time (Phillips et al. 2011). If this lag is ignored, then the relationship between temperature and CO_2 generation becomes temporally disconnected, with the separation becoming more prominent with depth (i.e. the CO_2 diffusion time increases with depth). We addressed this issue by estimating the CO_2 diffusion times throughout the soil profile and then adjusting the root temperature profiles to represent the temperature when CO_2 was generated.

The mechanistic model, which partitioned R_A into growth and maintenance components, can be viewed as both a strength and a limitation. On the positive side, we gained a better understanding of physiological differences in root processes between maize and switchgrass cropping systems. In turn, we predicted reasonably well the seasonal patterns of R_A even outside of the conditions used to parameterize the model. The model also facilitated the estimation of the link between diel photosynthesis and R_A. However, the model did not explicitly account for root respiration associated with ion uptake and other plant processes (Thornley & Cannell 2000), and thus may be more susceptible to errors than a more complex model (Lambers et al. 1983). Other environmental factors such as plant water availability were not considered, although it is important note that the plants were unlikely to be water stressed during our two study years. The model did not account for the potential for the growth and maintenance respiration coefficients to vary with respect to plant ontogeny and subsequent changes in root tissue types, which may be particularly important for annual species such as maize (Stahl & McCree 1988). The model is also unrealistic in that it assumes that substrates are always available for root respiration (Thornley & Cannell 2000), which likely leads to errors in model predictions particularly during aboveground plant senescence. Finally, the R_A models were parametrized from six diel campaigns, and therefore the model parameter reliability is limited both by the number of

measurements and the range of measured values. This is especially true of the temperature acclimation and temperature sensitivity parameters.

The model parameter estimates are subject to the errors and uncertainty associated with the measurements used to parameterize the models. In particular, R_A itself is difficult to measure *in situ*, and all methods have drawbacks (Subke et al. 2006). The root exclusion method does not account for SOC priming in the R_H measurement (Kuzyakov 2006), so the R_A estimate likely includes SOC priming. However, other issues such as the diffusion of soil CO_2 from below the R_H collars causes an overestimate of R_H and an underestimate of R_A (Jassal & Black 2006). There is additional compounded error arising from the calculation of R_A as the difference between R_T and R_H. Although the use of T_{Root} provides more realistic R_A temperature responses and likely improves parameter estimation and model performance, there are several uncertainties associated with the T_{Root} calculation. Notably, the soil CO_2 diffusion model which was used to estimate the lag time between root CO_2 generation and surface efflux requires many input parameters which can be difficult to measure. For example, volumetric water content and bulk density are central for calculating the total pore space and volumetric soil air content, which in turn is necessary to estimate the soil CO_2 diffusivity parameter. Considering that the model used to estimate the CO_2 diffusivity parameter is a non-linear function, small errors in the input parameters could result in larger errors in the output parameter. Refining the input parameter estimates through greater measurement replication would likely help to improve the T_{Root} estimates and hence improve the model.

3.5 Conclusions

We used *in situ* diel R_A measurements to parameterize growth respiration-maintenance respiration models for maize and switchgrass cropping systems. The models indicated apparent physiological differences in root respiration between maize and switchgrass, with greater specific growth respiration in switchgrass and greater specific root maintenance respiration in maize. These differences are likely related to the relative root growth rates and root tissue types between the two species, and thus may be more generalizable. Seasonal R_A model simulations matched the measured patterns of R_A reasonably well, indicating that the growth respiration-maintenance respiration modelling approach is useful at the ecosystem level. However, the inability to independently characterize the temperature acclimation and sensitivity responses of maintenance respiration precludes the use of those model parameters estimates in other applications. Future *in situ* studies using the growth respiration-maintenance respiration framework will require significantly larger sample sizes to adequately estimate the temperature acclimation and temperature sensitivity responses.

The *in situ* approach required a direct estimate of root temperature in order to characterize the response of R_A to temperature and subsequently estimate the relationship between diel photosynthesis and R_A. The method to estimate root temperature accounted for the vertical distribution of roots, the vertical distribution of soil temperature, and lag time between CO_2 generation and soil surface efflux. While we believe that this approach mitigates the issues associated with single-depth soil temperature measurements, the method requires empirical validation. Nonetheless, the approach was seemingly successful as indicated by the estimated lag time of 14 to 16 h for maize, which agrees well with literature values. For switchgrass, the lag time could not be determined due to the apparently weak influence of photosynthesis on diel R_A.

Additional studies will require more spatial and temporal measurements to accurately assess this coupling.

3.6 Acknowledgements

This work was funded by the Great Lakes Bioenergy Research Center (DOE BER Office of Science DE-FC02-07ER64494 and DOE OBP Office of Energy Efficiency and Renewable Energy DE-AC05-76RL01830), the USDA National Institute of Food and Agriculture (Hatch project 0225417-WIS01586), and the National Science Foundation (grant DEB-1038759). L.G. Oates and G. Sanford provided logistical support. C. Cummings, M. Cruse, J. Sustachek, A. D'orlando, C. Menick, B. Le Sauz, H. Melampy, A. Henkel, C. King, B. Dvorak, and C. Cavadini provided field and lab assistance.

3.7 References

Amthor, J. S. 1984. The role of maintenance respiration in plant growth. Plant, Cell & Environment 7:561–569.

Amthor, J. S. 2000. The McCree–de Wit–Penning de Vries–Thornley respiration paradigms: 30 years later. Annals of Botany 86:1–20.

Anderson-Teixeira, K. J., Masters, M. D., Black, C. K., Zeri, M., Hussain, M., Bernacchi, C. J., DeLucia, E. H. 2013. Altered belowground carbon cycling following land-use change to perennial bioenergy crops. Ecosystems 16:508–520.

Brady, N. C., Weil, R. R. 1999. The Nature and Properties of Soils, 12th ed. Prentice Hall, New Jersey, USA.

Buyanovsky, G. A., Kucera, C. L., Wagner, G. H. 1987. Comparative analyses of carbon dynamics in native and cultivated ecosystems. Ecology 68:2023–2031.

Campbell, G. S., Norman, J. M. 1998. An Introduction to Environmental Biophysics, 2nd ed. Springer, New York, USA.

Cannell, M. G. R., Thornley, J. H. M. 2000. Modelling the components of plant respiration: Some guiding principles. Annals of Botany 85:45–54.

Chapin III, F. S., Woodwell, G. M., Randerson, J. T., Rastetter, E. B., Lovett, G. M., Baldocchi, D. D., Clark, D. A., Harmon, M. E., Schimel, D. S. et al. 2006. Reconciling carbon-cycle concepts, terminology, and methods. Ecosystems 9:1041–1050.

Elzhov, V. T., Mullen, K. M., Spiess, A.-N., Bolker, B. 2016. minpack.lm: R Interface to the Levenberg-Marquardt Nonlinear Least-Squares Algorithm Found in MINPACK, Plus Support for Bounds.

Gallagher, J. L., Wolf, P. L., Pfeiffer, W. J. 1984. Rhizome and root growth rates and cycles in protein and carbohydrate concentrations in Georgia *Spartina alterniflora* Loisel. plants. American Journal of Botany 71:165–169.

Gee, G. W., Bauder, J. W. 1986. Particle-size analysis. In: Methods of soil analysis. Part 1. Physical and mineralogical methods. Klute, A. (ed.). American Society of Agronomy, Madison, USA.

Graf, A., Weihermuller, L., Huisman, J. A., Herbst, M., Bauer, J., Vereecken, H. 2008. Measurement depth effects on the apparent temperature sensitivity of soil respiration in field studies. Biogeosciences 5:1175–1188.

Hansen, G. K., Jensen, C. R. 1977. Growth and maintenance respiration in whole plants, tops, and roots of *Lolium multiflorum*. Physiologia Plantarum 39:155–164.

Hayes, D. C., Seastedt, T. R. 1987. Root dynamics of tallgrass prairie in wet and dry years. Canadian Journal of Botany-revue Canadienne De Botanique 65:787–791.

Howard, P. J. A. 1966. The carbon-organic matter factor in various soil types. Oikos 15:229–236.

Jähne, B., Heinz, G., Dietrich, W. 1987. Measurement of the diffusion coefficients of sparingly soluble gases in water. Journal of Geophysical Research-oceans 92:10767–10776.

Jassal, R. S., Black, T. A. 2006. Estimating heterotrophic and autotrophic soil respiration using small-area trenched plot technique: Theory and practice. Agricultural and Forest Meteorology 140:193–202.

Kattage, J., Knorr, W. 2007. Temperature acclimation in a biochemical model of photosynthesis: a reanalysis of data from 36 species. Plant, Cell & Environment 30:1176–1190.

Kuzyakov, Y. 2006. Sources of CO_2 efflux from soil and review of partitioning methods. Soil Biology & Biochemistry 38:425–448.

Kuzyakov, Y., Gavrichkova, O. 2010. Time lag between photosynthesis and carbon dioxide efflux from soil: a review of mechanisms and controls. Global Change Biology 16:3386–3406.

Lambers, H., Chapin III, F. S., Pons, T. L. 2008. Plant Physiological Ecology, 2nd ed. Springer, New York, USA.

Lambers, H., Szaniawski, R. K., de Visser, R. 1983. Respiration for growth, maintenance and ion uptake. An evaluation of concepts, methods, values and their significance. Physiologia Plantarum 58:556–563.

Lombardozzi, D. L., Bonan, G. B., Smith, N. G., Dukes, J. S., Fisher, R. A. 2015. Temperature acclimation of photosynthesis and respiration: A key uncertainty in the carbon cycle-climate feedback. Geophysical Research Letters 42:8624–8631.

Massman, W. 1998. A review of the molecular diffusivities of H_2O, CO_2, CH_4, CO, O_3, SO_2, NH_3, N_2O, NO, and NO_2 in air, O_2 and N_2 near STP. Atmospheric Environment 32:1111–1127.

M'Bou, A. T., Saint-Andre, L., de Grandcourt, A., Nouvellon, Y., Jourdan, C., Mialoundama, F., Epron, D. 2010. Growth and maintenance respiration of roots of clonal Eucalyptus cuttings: scaling to stand-level. Plant and Soil 332:41–53.

Mencuccini, M., Hölttä, T. 2010. The significance of phloem transport for the speed with which canopy photosynthesis and belowground respiration are linked. New Phytologist 185:189–203.

Milchunas, D. G. 2009. Estimating root production: Comparison of 11 methods in shortgrass steppe and review of biases. Ecosystems 12:1381–1402.

Moldrup, P., Olesen, T., Yamaguchi, T., Schjonning, P., Rolston, D. E. 1999. Modeling diffusion and reaction in soils: IX. The Buckingham-Burdine-Campbell equation for gas diffusivity in undisturbed soil. Soil Science 164:542–551.

Monteith, J. L., Unsworth, M. H. 2008. Principles of Environmental Physics, 3rd ed. Academic Press, Massachusetts, USA.

National Oceanic and Atmospheric Administration (NOAA). 2017. National Centers for Environmental Information: Climate Data Online. www.ncdc.noaa.gov.

Pavelka, M., Acosta, M., Marek, M. V., Kutsch, W., Janous, D. 2007. Dependence of the Q10 values on the depth of the soil temperature measuring point. Plant and Soil 292:171–179.

Phillips, C. L., Nickerson, N., Risk, D., Bond, B. J. 2011. Interpreting diel hysteresis between soil respiration and temperature. Global Change Biology 17:515–527.

Poorter, H., Remkes, C., Lambers, H. 1990. Carbon and nitrogen economy of 24 wild species differing in relative growth rate. Plant Physiology 94:621–627.

Poorter, H., Van der Werf, A., Atkin, O. K., Lambers, H. 1991. Respiratory energy requirements of roots vary with the potential growth rate of a plant species. Physiologia Plantarum 83:469–475.

Poorter, H., van de Vijver, C. A. D. M., Boot, R. G. A., Lambers, H. 1995. Growth and carbon economy of a fast-growing and a slow-growing grass species as dependent on nitrate supply. Plant and Soil 171:217–227.

Prolingheuer, N., Scharnagl, B., Graf, A., Vereecken, H., Herbst, M. 2014. On the spatial variation of soil rhizospheric and heterotrophic respiration in a winter wheat stand. Agricultural and Forest Meteorology 195–196:24–31.

R Core Team. 2017. R: A language and environment for statistical computing.

Reekie, E. G., Redmann, R. E. 1987. Growth and maintenance respiration of perennial root systems in a dry grassland dominated by *Agropyron dasystachyum* (Hook.) Scribn. New Phytologist 105:595–603.

Roumet, C., Urcelay, C., Díaz, S. 2006. Suites of root traits differ between annual and perennial species growing in the field. New Phytologist 170:357–367.

Rühlmann, J., Korschens, M., Graefe, J. 2006. A new approach to calculate the particle density of soils considering properties of the soil organic matter and the mineral matrix. Geoderma 130:272–283.

Sanford, G. R., Oates, L. G., Jasrotia, P., Thelen, K. D., Robertson, G. P., Jackson, R. D. 2016. Comparative productivity of alternative cellulosic bioenergy cropping systems in the North Central USA. Agriculture, Ecosystems & Environment 216:344–355.

Soil Survey Staff. 2017. Natural Resources Conservation Service, U.S. Department of Agriculture. Official Soil Series Descriptions. www.nrcs.usda.gov.

Stahl, R. S., McCree, J. 1988. Ontogenetic changes in the respiration coefficients of grain sorghum. Crop Science 28:111–113.

Subke, J. A., Inglima, I., Cotrufo, M. F. 2006. Trends and methodological impacts in soil CO2 efflux partitioning: A metaanalytical review. Global Change Biology 12:921–943.

Thornley, J. H. M. 1970. Respiration, growth and maintenance in plants. Nature 227:304–305.

Thornley, J. H. M., Cannell, M. G. R. 2000. Modelling the components of plant respiration: Representation and realism. Annals of Botany 85:55–67.

Tjoelker, M. G., Oleksyn, J., Reich, P. B. 2001. Modelling respiration of vegetation: evidence for a general temperature-dependent Q10. Global Change Biology 7:223–230.

Vargas, R., Allen, M. F. 2008. Dynamics of fine root, fungal rhizomorphs, and soil respiration in a mixed temperate forest: Integrating sensors and observations. Vadose Zone Journal 7:1055–1064.

Vogel, J. G., Valentine, D. W. 2005. Small root exclusion collars provide reasonable estimates of root respiration when measured during the growing season of installation. Canadian Journal of Forest Research 35:2112–2117.

von Haden, A.C. 2017. Annual ecosystem carbon balances in long-term no-till maize and mature switchgrass bioenergy cropping systems: evaluating methods and processes. In: Mechanisms of ecosystem carbon storage and stability in temperature bioenergy cropping systems. Doctoral Dissertation. University of Wisconsin-Madison, Madison, WI, USA.

3.8 Tables and figures

Table 3.1 – Growing season temperature and precipitation during the two study years compared to the 30-year mean (NOAA 2017).

	2015		**2016**		**30-year mean**	
	Temp (°C)	*Precip. (mm)*	*Temp (°C)*	*Precip. (mm)*	*Temp (°C)*	*Precip. (mm)*
May	14.8	112.0	14.3	87.6	13.2	93.7
Jun	18.6	79.8	20.3	104.1	18.7	118.9
Jul	20.3	80.3	21.8	164.8	20.8	105.7
Aug	19.8	110.0	21.4	138.7	19.6	99.1
Sep	18.9	144.8	17.9	156.7	15.2	89.9
Oct	10.4	49.8	11.3	85.6	8.6	64.8
Total	17.2	576.6	17.9	737.6	16.0	572.0

Table 3.2 – Parameter estimates for the top three diel R_A models (based on AIC), which also met the criteria of all positive parameters. *P*-values are denoted by *** < 0.0001, ** < 0.01, * < 0.05, and · < 0.1.

Lag (h)	AIC	$m_{A \rightarrow RA}$	$R_{r,g}$	AC_b	AC_m	Q_b	Q_m
Maize							
16	23.2	4.65E-3***	0.355***	5.43E-2***	2.26E-3***	91.3*	2.48
15	23.8	4.15E-3***	0.360***	5.07E-2***	2.08E-3***	90.1*	2.88·
14	24.8	3.80E-3***	0.363***	4.69E-2***	1.90E-3***	83.5**	2.89*
Switchgrass							
23	128.1	8.56E-4	0.650***	1.77E-2***	7.79E-4***	15.5*	0.520
24	128.3	7.89E-4	0.651***	1.75E-2***	7.73E04***	16.1*	0.563
22	128.3	8.32E-4	0.649***	1.78E-2***	7.85E-4***	14.9·	0.476

Table 3.3 – Specific growth respiration ($R_{s,g}$), growth efficiency (Y_g), and the specific maintenance respiration rate at 20 °C ($R_{s,m}$).

	$R_{s,g}$	Y_g	$R_{s,m}$ (20 °C)
Units	(g C respiration) (g C growth)$^{-1}$	(g C growth) (g C growth + g C respiration)$^{-1}$	(mg C respiration day^{-1}) (g C biomass)$^{-1}$
Maize	0.86 (0.02)	0.54 (0.01)	22.0 (0.40)
Switchgrass	1.57 (0.11)	0.39 (0.02)	5.0 (0.05)

Table 3.4 – Growing season root growth (R_{growth}) and root maintenance (R_{maint}) respiration as predicted by the R_A model.

		2015		2016	
	Units	R_{growth}	R_{maint}	R_{growth}	R_{maint}
Maize	g C m^{-2}	58.8 (5.2)	112.5 (9.6)	71.8 (7.3)	152.9 (14.7)
	% of R_A	34.3 (0.34)	65.7 (0.34)	31.9 (0.34)	68.1 (0.34)
Switchgrass	g C m^{-2}	127.5 (11.7)	314.4 (20.5)	155.9 (21.3)	288.5 (24.0)
	% of R_A	28.9 (2.9)	71.1 (2.9)	35.1 (4.6)	64.9 (4.6)

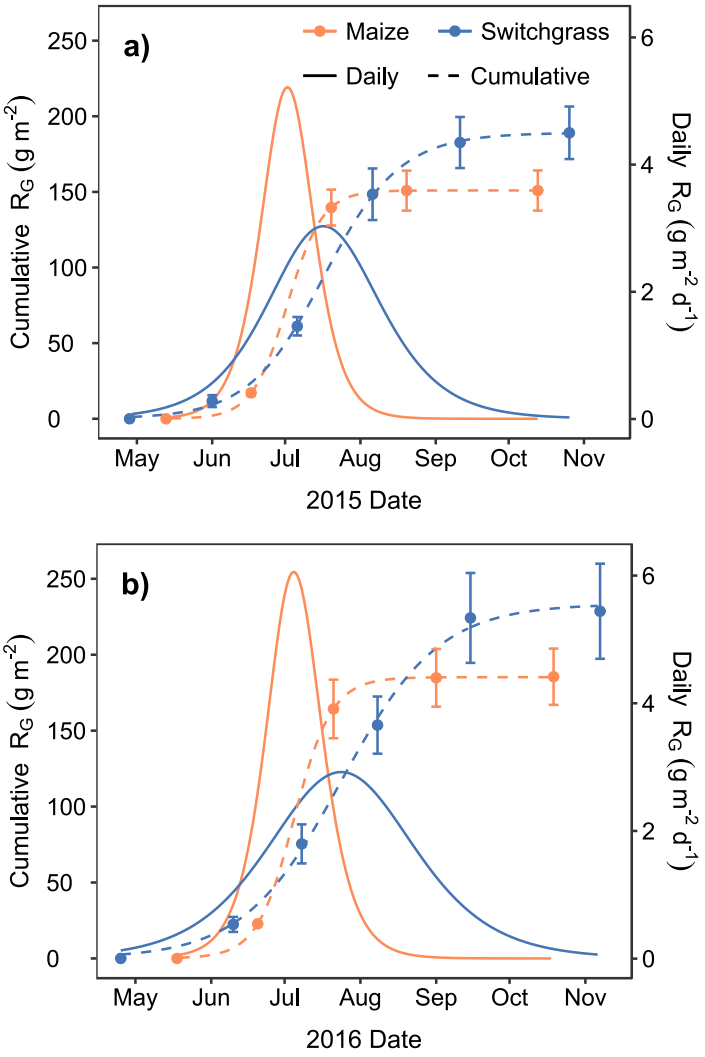

Figure 3.1 – Cumulative and daily root growth (R_G) for maize and switchgrass during the (a) 2015 and (b) 2016 growing seasons. Measured cumulative root growth is shown as points with standard error, and the growth model curves are presented as dashed lines.

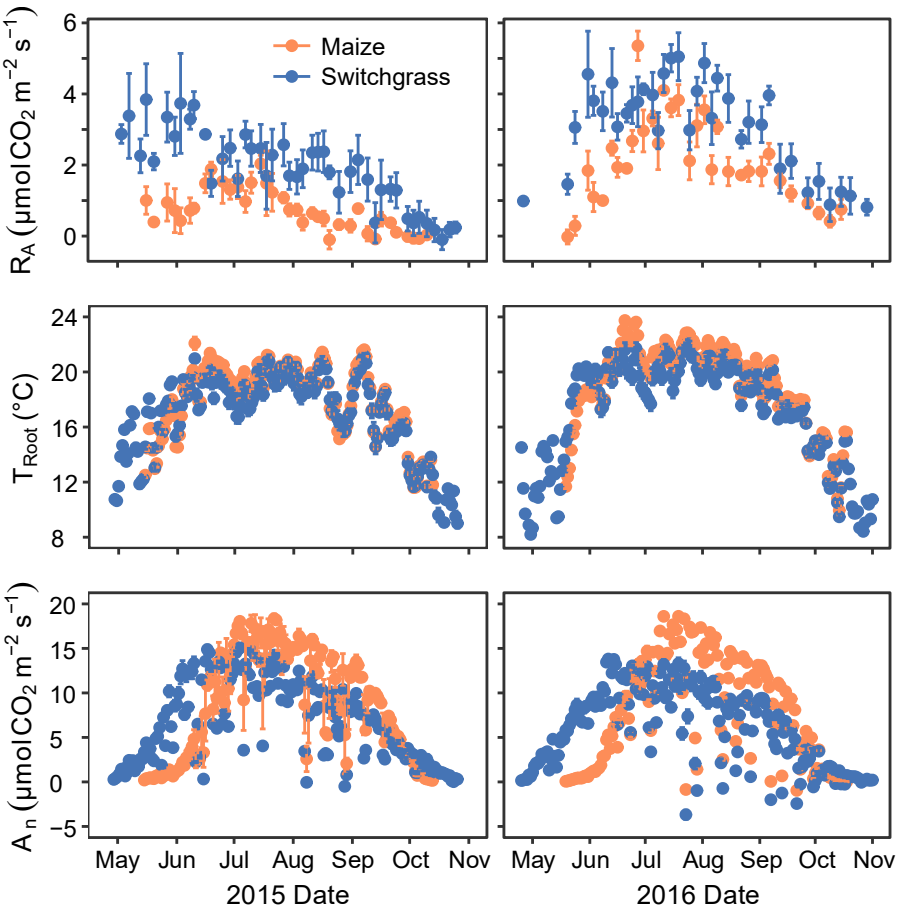

Figure 3.2 – Seasonal patterns of autotrophic root respiration (R_A) from the survey measurements, daily average root temperature (T_{Root}), and net canopy photosynthesis (A_n).

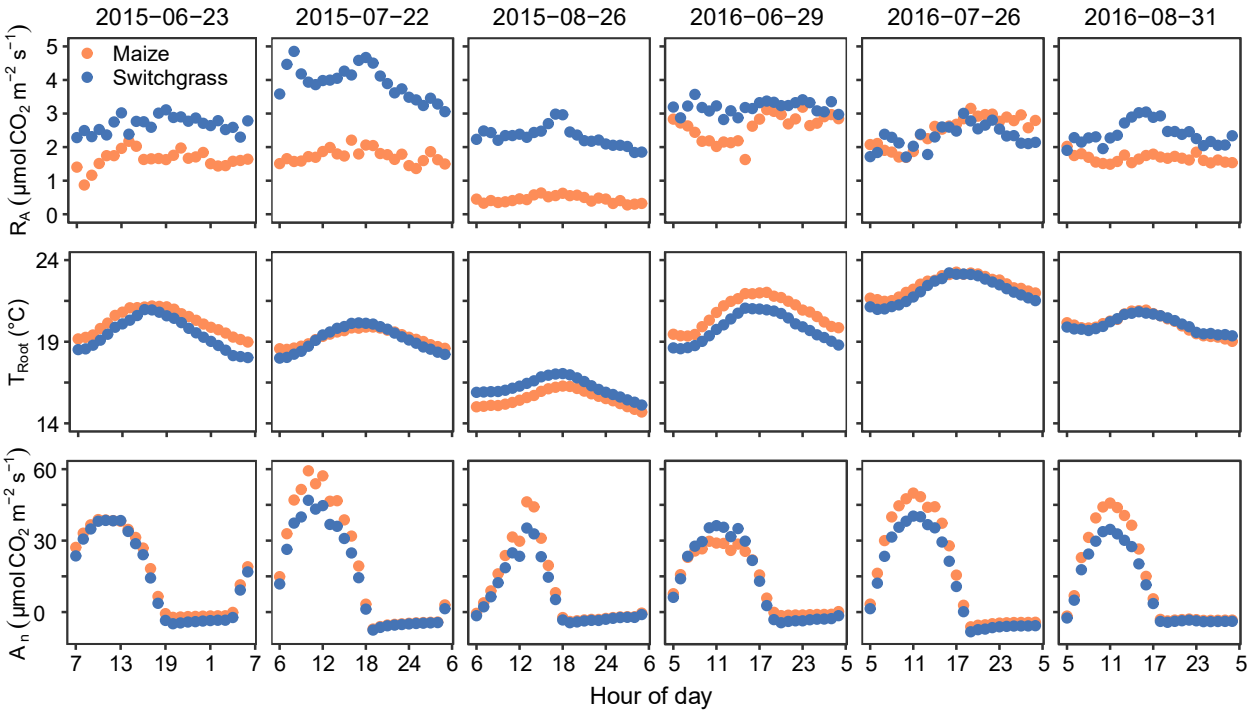

Figure 3.3 – Diel patterns of hourly autotrophic root respiration (R_A), root temperature (T_{Root}), and net canopy photosynthesis (A_n) during six campaigns in 2015 and 2016. Time 0 is midnight local standard time. Dates indicate the day on which respiration measurements began.

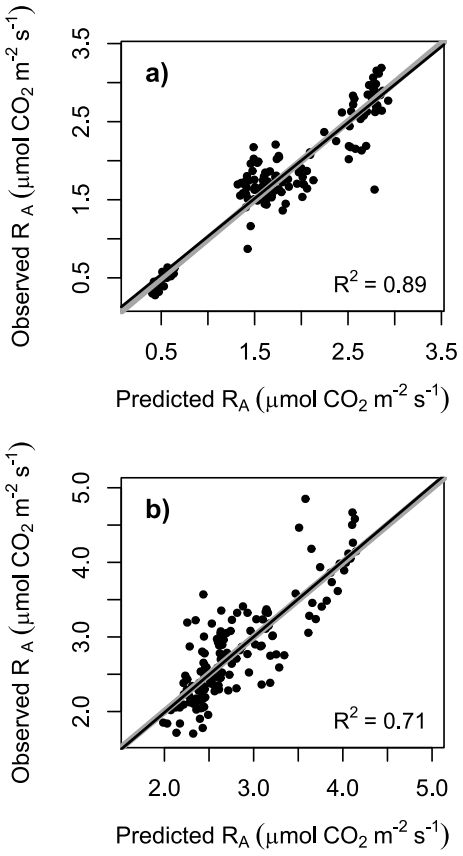

Figure 3.4 – Predicted versus observed diel autotrophic root respiration (R_A) for (a) maize and (b) switchgrass. The black line is the linear regression between the two variables, and the gray line shows 1:1.

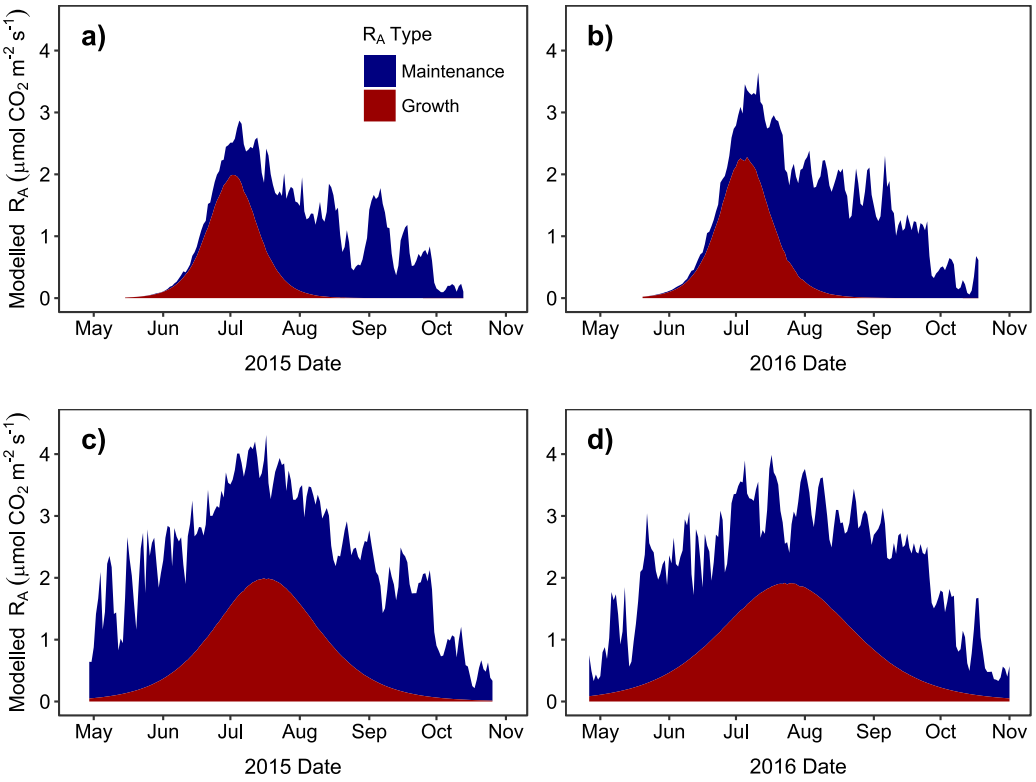

Figure 3.5 – Modelled seasonal patterns of daily average maintenance and growth autotrophic root respiration (R_A) in maize (a, b), and switchgrass (c, d). The R_A types are stacked such that total R_A is represented as the sum of maintenance and growth respiration.

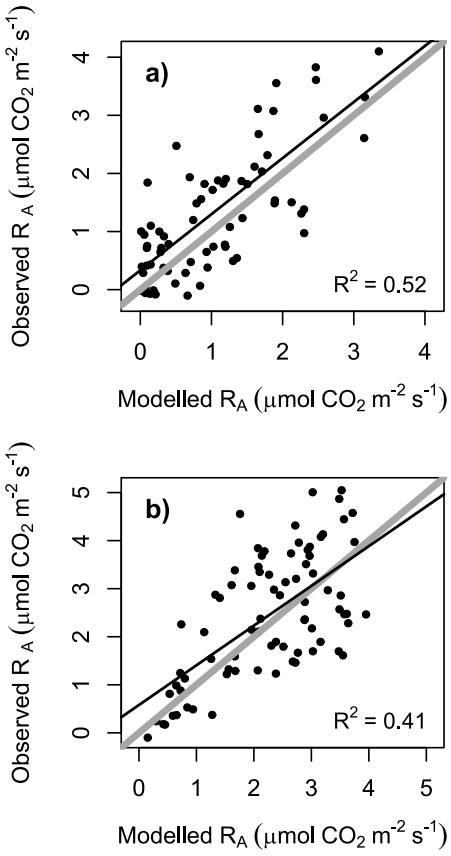

Figure 3.6 – Model predicted hourly autotrophic root respiration (R_A) versus observed R_A from the seasonal survey measurements for (a) maize and (b) switchgrass. Each point is the mean of three plots. The black line is the regression between observed and modelled R_A, and the gray line is 1:1.

3.9 Supplemental tables and figures

Table 3.S.1 – Parameters for 0-24 h lags between net photosynthesis and autotrophic respiration.

	Lag (h)	AIC	R^2	$m_{A \rightarrow RA}$	$R_{r,g}$	AC_b	AC_m	Q_b	Q_m
Maize									
	16	23.23	0.894	4.651E-03	0.355	5.426E-02	2.257E-03	91.3	2.48
	15	23.78	0.893	4.155E-03	0.360	5.070E-02	2.085E-03	90.1	2.88
	14	24.80	0.893	3.804E-03	0.363	4.689E-02	1.900E-03	83.5	2.89
	13	26.12	0.892	3.613E-03	0.366	4.304E-02	1.714E-03	74.3	2.69
	17	27.68	0.890	4.939E-03	0.352	5.702E-02	2.391E-03	86.2	1.77
	12	28.78	0.889	3.512E-03	0.369	3.898E-02	1.519E-03	64.3	2.40
	1	32.43	0.887	-2.960E-03	0.400	4.670E-02	1.852E-03	76.2	2.79
	11	33.21	0.886	3.441E-03	0.371	3.486E-02	1.319E-03	54.2	2.07
	2	33.26	0.886	-2.962E-03	0.397	5.098E-02	2.057E-03	86.0	3.03
	3	34.47	0.885	-3.078E-03	0.395	5.519E-02	2.258E-03	94.1	3.13
	0	34.87	0.885	-2.914E-03	0.402	4.206E-02	1.629E-03	65.0	2.44
	24	37.52	0.883	-2.795E-03	0.396	4.237E-02	1.646E-03	66.9	2.49
	18	39.29	0.881	4.364E-03	0.354	5.741E-02	2.405E-03	85.9	1.82
	4	39.55	0.881	-3.039E-03	0.393	5.814E-02	2.399E-03	97.2	3.01
	23	40.62	0.880	-2.791E-03	0.398	3.796E-02	1.433E-03	56.6	2.15
	10	41.32	0.879	3.109E-03	0.374	3.222E-02	1.190E-03	47.5	1.83
	5	45.19	0.876	-2.883E-03	0.391	5.948E-02	2.465E-03	95.6	2.79
	22	47.31	0.874	-2.482E-03	0.399	3.529E-02	1.306E-03	50.2	1.92
	9	48.69	0.873	2.575E-03	0.376	3.199E-02	1.176E-03	45.9	1.77
	19	50.63	0.871	2.740E-03	0.365	5.415E-02	2.242E-03	87.1	2.54
	6	52.91	0.869	-1.906E-03	0.388	5.518E-02	2.265E-03	88.1	2.79
	21	53.86	0.868	-1.627E-03	0.395	3.740E-02	1.413E-03	53.5	2.03
	8	54.81	0.867	1.392E-03	0.381	3.711E-02	1.417E-03	54.5	2.06
	20	56.46	0.866	4.919E-04	0.381	4.673E-02	1.874E-03	73.5	2.59
	7	56.54	0.866	-3.711E-04	0.385	4.679E-02	1.873E-03	73.0	2.59
Switchgrass									
	14	125.61	0.717	-1.282E-03	0.684	1.745E-02	7.690E-04	17.9	0.679
	13	125.63	0.717	-1.226E-03	0.682	1.766E-02	7.789E-04	17.6	0.649
	12	126.83	0.714	-1.021E-03	0.677	1.784E-02	7.872E-04	17.0	0.602
	15	127.56	0.713	-1.010E-03	0.678	1.735E-02	7.637E-04	17.7	0.674
	23	128.07	0.712	8.559E-04	0.650	1.767E-02	7.791E-04	15.5	0.520
	24	128.28	0.711	7.889E-04	0.651	1.753E-02	7.725E-04	16.1	0.563
	22	128.34	0.711	8.321E-04	0.649	1.779E-02	7.850E-04	14.9	0.476
	20	128.43	0.711	9.220E-04	0.645	1.799E-02	7.948E-04	13.7	0.385
	21	128.48	0.711	8.482E-04	0.647	1.790E-02	7.902E-04	14.3	0.432
	11	128.74	0.711	-6.284E-04	0.669	1.788E-02	7.889E-04	16.3	0.560
	0	128.74	0.711	6.363E-04	0.651	1.750E-02	7.712E-04	15.8	0.546
	7	128.96	0.710	7.921E-04	0.648	1.685E-02	7.390E-04	16.8	0.645
	1	128.98	0.710	5.679E-04	0.652	1.741E-02	7.665E-04	16.1	0.571
	6	129.03	0.710	7.951E-04	0.649	1.682E-02	7.376E-04	16.8	0.647
	19	129.13	0.710	6.752E-04	0.647	1.793E-02	7.915E-04	14.3	0.430
	16	129.20	0.710	-5.784E-04	0.670	1.741E-02	7.664E-04	17.3	0.642
	5	129.29	0.709	6.328E-04	0.651	1.701E-02	7.470E-04	16.8	0.634
	2	129.40	0.709	4.251E-04	0.654	1.738E-02	7.653E-04	16.3	0.587
	3	129.53	0.709	3.907E-04	0.654	1.734E-02	7.631E-04	16.5	0.598
	8	129.55	0.709	4.139E-04	0.653	1.727E-02	7.593E-04	16.6	0.611
	4	129.57	0.709	4.034E-04	0.654	1.727E-02	7.599E-04	16.6	0.609
	10	129.65	0.709	-2.746E-04	0.663	1.779E-02	7.846E-04	16.1	0.550
	18	129.66	0.709	3.457E-04	0.653	1.779E-02	7.847E-04	15.4	0.502
	17	129.79	0.708	-1.720E-04	0.662	1.755E-02	7.734E-04	16.6	0.593
	9	129.84	0.708	5.380E-05	0.658	1.759E-02	7.751E-04	16.3	0.571

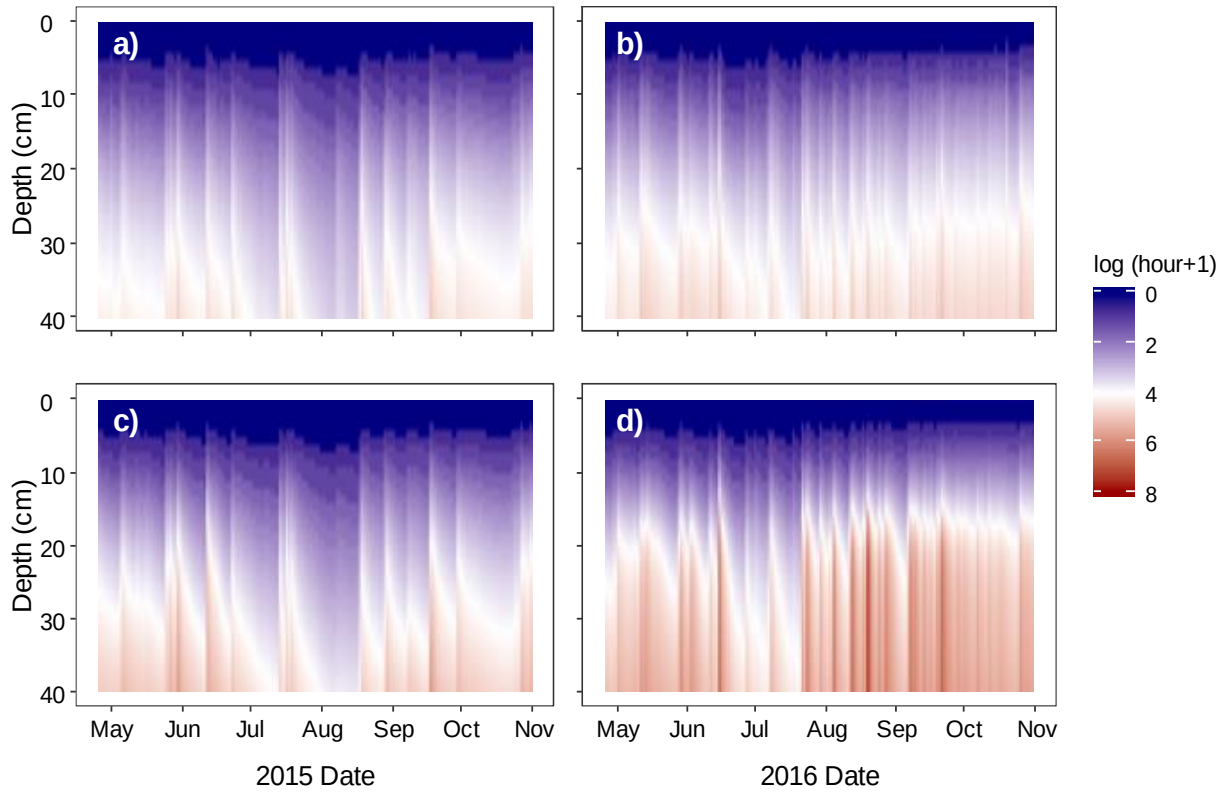

Figure 3.S.1 – Lag times [log (h + 1)] between CO_2 generation and soil surface efflux throughout the 0-40 cm soil profile for maize (a, b) and switchgrass (c, d) in 2015 and 2016.

Chapter 4

Soil microclimate in temperate bioenergy cropping systems: implications for C loss via heterotrophic soil respiration

von Haden, A.C., Marín-Spiotta, E., Jackson, R.D., Kucharik, C.J.

Target journal: Agricultural and Forest Meteorology

Abstract

Soil organic carbon (C) storage in biofuel cropping systems facilitates net C emissions reductions. Heterotrophic soil respiration (R_H) is the primary pathway of C loss from litter and soil organic carbon and thus R_H affects ecosystem C storage. Since R_H is sensitive to soil temperature and moisture, soil microclimates resulting from plant and management factors may influence C loss via R_H. We examined multiyear soil microclimate differences among no-till maize, switchgrass, and hybrid poplar bioenergy cropping systems in Wisconsin, USA. In addition, we measured R_H in maize and switchgrass and parameterized models to predict the direct effects of altered soil microclimate on annual R_H. Summertime soil temperatures were typically warmer in maize compared to poplar and switchgrass, likely caused in part by earlier leaf-out and greater peak LAI in the latter systems. Due to spatially-limited vertical plant stubble, snow depths were consistently shallow in maize, leading to the coldest wintertime soil temperatures among the systems. Differences in soil moisture, which was only available for maize and switchgrass, varied by depth. Maize was relatively drier near the surface, but switchgrass was relatively drier below 50 cm. Modelled scenarios indicated that annual maize R_H would decrease by 3 to 6% under the cooler and wetter switchgrass soil microclimate, but annual switchgrass R_H would increase by 8 to 17% under the warmer and drier maize soil microclimate.

Our simple model suggested that R_H could be moderately influenced by management practices that alter the soil microclimate. However, soil microclimate effects on plant productivity, N mineralization, and other greenhouse gas emissions need to be weighed against the potential C storage benefit.

4.1 Introduction

As demand for bioenergy grows, further conversion of land to biofuel cropping systems will be necessary (Lark et al. 2015). For biofuels to provide the potential for immediate climate change mitigation, conversion of lands to biofuel cropping systems must preserve or enhance biogeochemical cycling relative to baseline conditions (Robertson et al. 2011) and ecosystem carbon (C) debts must be avoided (Gibbs et al. 2008; Gelfand et al. 2011). Therefore, the ecosystem C balance is a key component of the overall sustainability of biofuel cropping systems (Robertson et al 2011). Fundamentally, the ecosystem C balance is a function of the difference between C inputs and C outputs (Chapin et al. 2006; Lambers et al. 2008), and thus decreasing the rate of C loss from biofuel cropping system could provide a means for maintaining or storing additional C (Whitmore et al. 2015).

Heterotrophic respiration (R_H) resulting from the decomposition of organic C is the primary pathway of C loss from soil organic carbon (SOC) and litter (Chapin et al. 2006; Lambers et al. 2008). Although R_H is facilitated by the decomposer community and depends upon the availability of C substrates, temperature and moisture strongly regulate the R_H rate (Lambers et al. 2008). Owing to greater enzyme activity, enzyme affinity for the substrate, and substrate diffusion rates (Davidson et al. 2006), R_H increases with greater temperatures within typical soil temperature ranges (Lloyd & Taylor 1994). At low soil moisture, R_H is limited by

substrate transport and microbial physiology, whereas at high soil moisture, R_H is limited through oxygen diffusion and availability (Moyano et al. 2013). Therefore, R_H is typically highest at intermediate soil moisture levels (Linn & Doran 1984).

At the landscape level, soil temperature and soil moisture are regulated by seasonal patterns of solar radiation intensity, albedo, air temperature, and precipitation. However, at smaller scales, the soil microclimate is influenced by localized conditions such as the spatial and temporal patterns of plant structure and phenology (Flerchinger & Pierson 1997; Chen et al. 1999). For example, spatial differences in leaf area index or litter cover may facilitate differences in soil temperature or soil moisture among vegetation types (Hatfield & Prueger 1996; Wolkovich et al. 2009; Hardwick et al. 2015). Deep snow cover, which may be enhanced by tall, upright stubble which more effectively traps snow, can decouple the soil from air temperature fluctuations, leading to warmer soil temperatures during winter (Sharratt et al. 1998). Since management factors such as planting date, residue removal rates, and stubble properties are known to modify the soil microclimate (Hatfield & Prueger 1996; Flerchinger & Pierson 1997; Sharratt et al. 1998), it is plausible that management-induced soil microclimates affect R_H. Given that C storage is a central focus of biofuel cropping systems, reducing R_H by altering the soil microclimate may be viewed as a potential C management strategy (e.g. Whitmore et al. 2015). However, a better understanding of temporal dynamics of soil microclimates and the subsequent response of R_H is necessary to assess whether such a strategy is viable.

Our objectives were to evaluate soil microclimate differences among several candidate bioenergy cropping systems and to predict whether R_H would be significantly modified under alternate soil microclimate scenarios. We hypothesized that annual cropping systems would exhibit more extreme soil temperatures than perennial systems due to lower leaf area index

during the summer and shallower snow depth during the winter. We also hypothesized that soil moisture would be lower in annual than perennial systems due primarily to greater evaporative loss. Finally, we expected that the differences in soil microclimate between annual and perennial systems would be sufficient to facilitate substantial differences in R_H.

4.2 Methods

4.2.1 Study site

The research was conducted at the DOE-Great Lakes Bioenergy Research Center's Biofuel Cropping Systems Experiment (BCSE) in Arlington, WI, USA (43.296° N, 89.380° W). The thirty-year normal annual air temperature and precipitation are 6.9 °C and 869 mm, respectively (NOAA 2017). The site is dominated by Plano silt loam soils which are Fine-silty, mixed, superactive, mesic Typic Argiudolls (Soil Survey Staff 2017). The BCSE began in 2008 and consists of five completely randomize blocks of twelve treatments with plots measuring 27.4 m x 42.7 m each (Sanford et al. 2016). Our study was constrained to continuous no-till maize (*Zea mays* L.), 'Cave-In-Rock' switchgrass (*Panicum virgatum* L.), and hybrid poplar (*Populus nigra* × *P. maximowiczii* A. Henry 'NM6') cropping systems within four of the blocks.

Maize was planted every spring, switchgrass was planted in June 2008, and hybrid poplar cuttings were planted in May 2008. Maize received an average of 167 kg N ha^{-1} annually, switchgrass received 56 kg N ha^{-1} annually, and poplar received 210 kg N ha^{-1} in 2010 only (Sanford et al. 2016). Maize grain plus approximately 50% of the maize stover was harvested annually, while approximately 55% of switchgrass aboveground biomass was harvested each year (Sanford et al. 2016). Unharvested maize stover laid prostrate on the soil and was most

concentrated in the rows where the plants had stood. The remaining maize stubble was typically about 5 cm tall. Switchgrass was harvested at approximately 15 cm above the soil, leaving a tall, ubiquitous layer of stubble. In addition, some of the unharvested biomass in switchgrass consisted of plants that had lodged during the growing season and were laying prostrate on the soil surface. Poplars were in a six-year coppice rotation beginning in 2008. In 2010 the poplars were stricken with *Marssonina* spp. leaf spot fungus which impaired growth until the trees were coppiced in 2013 (Sanford et al. 2016). Poplar regeneration following coppicing was poor, and the treatment was therefore discontinued after 2013.

4.2.2 Soil temperature and moisture

Soil temperature and volumetric moisture content were measured in three blocks from 2011 through 2014 and in four blocks from 2015 through 2016. Details regarding the types of sensors and the depths at which they were installed are given in Table 4.1. At each depth, two temperature sensors and one soil moisture sensor were used, except in block C where two moisture sensors were used at each depth. Soil temperature data was collected at 15-minute intervals and averaged to hourly values, whereas soil moisture was collected either at hourly or 15-minute intervals and averaged to hourly intervals. Due to improper measurement settings used for the soil moisture probes and mechanical failure of the multiplexers, much of the soil moisture data collected from 2011 through 2014 was erratic and therefore was not used.

To account for potential differences between the responses of the two soil moisture probe types, the moisture measurements were standardized to a Delta-T SM150 TDR (Delta-T Devices Ltd., Cambridge, England) based on over 200 concurrent probe measurements from 15 to 47% volumetric moisture content. When possible, missing soil temperature and soil moisture data

were gap filled using the averages of the other blocks. Daily averages were then calculated for each plot and depth, and those values were interpolated from 0.5 to 99.5 cm at 1 cm intervals using a natural cubic spline. Cropping system averages were calculated at each depth and timepoint. To better illustrate differences among the cropping systems, an average was also calculated among crops for each depth and timepoint, and the deviation from that average was calculated for each crop.

4.2.3 Heterotrophic soil respiration

Heterotrophic soil respiration (R_H) was estimated in maize and switchgrass using root exclusion collars that were installed within three blocks (Vogel & Valentine 2005). Two root exclusion collars were installed within each plot in the beginning of each measurement year. Prior to each installation, a 12.7 cm diameter hole was excavated in 10 cm increments to 100 cm using a bucket auger. Each soil increment was sieved to remove living roots. A 10.2 cm inner diameter PVC pipe was placed in the hole and the soil sections were backfilled and packed to initial bulk density. A small hole was drilled in the soil at ground level to allow water to drain from inside, and Decagon 5TM soil moisture sensors (Decagon Devices Inc., Pullman, WA, USA) were installed inside and outside of the collars at the 0 to 5 cm depth.

Soil respiration measurements were made using a LI-COR 6400XT portable photosynthesis system with a LI-6400-09 soil CO_2 flux chamber (LI-COR Inc., Lincoln, NE, USA). All root exclusion collars were measured on each sampling date except during the winter months when only one collar per plot was typically measured. Soil temperature and soil moisture inside and outside of the collars were measured concurrent with soil respiration measurements. A correction for differences between the soil moisture inside and outside of the root exclusion

collars was applied (Prolingheuer et al. 2014) using the procedure described in von Haden (2017a).

Heterotrophic soil respiration data for each plot were fit to a model which accounted for the interactive effects of soil temperature and soil moisture (Savage et al. 2009):

$$R_H = R_{H,10} Q_{10}^{[(T_{SOC}-10)/10]} D^{\left(M_{\mathrm{SOC,opt}}-M_{SOC,meas}\right)^2} \quad (4.1)$$

where $R_{H,10}$ is the R_H at 10 °C, Q_{10} is proportional increase of R_H per 10 °C, T_{SOC} is the soil temperature profile weighted by the vertical distribution of soil organic carbon (SOC), $M_{SOC,opt}$ is the soil moisture profile (as weighted by the vertical SOC distribution) at which the optimal R_H occurs, $M_{SOC,opt}$ is the measured soil moisture as weighted by the SOC distribution, and D describes the shape of the soil moisture response curve. The soil temperature and moisture values used in the model replace the typical single-depth soil measurements with values that integrate the depth distributions of soil temperature and moisture with SOC (i.e. the primary substrate from which R_H is derived). In addition, the T_{SOC} and M_{SOC} values account for the time lag between when CO_2 is generated within the soil profile and when the flux is realized at the soil surface. These modifications are intended to avoid the parameter estimation errors associated with single-depth temperature/moisture measurements and CO_2 diffusion lags (Phillips et al. 2011). Details of this calculation are given in von Haden (2017b). Since approximately 80% of the 0 to 100 cm SOC occurs within the top 50 cm at our site, and because the uncertainty in the T_{SOC} and M_{SOC} calculations increases with depth, we chose to constraint T_{SOC} and M_{SOC} to 0-50 cm.

The R_H model fitting procedure required multiple steps to account for heteroscedasticity and to include measurements for which no soil moisture data were available. First, data collected

when soils were not frozen (i.e. when soil moisture data was available) were fit using ordinary least square (OLS) regression and residuals were calculated. The inverse square of the residuals were then used as weighting factors for a weighted least squares (WLS) regression using the same data (Savage et al. 2009). Soil moisture values that were missing due to frozen soils were then set to the model-estimated $M_{SOC,opt}$. The resulting data were then fit first using OLS, residuals were calculated, and the data were then fit using WLS. While assigning missing (frozen) soil moisture data points to optimal moisture values likely overestimates R_H at freezing temperatures (i.e. when R_H is very low), the error is very small compared to the range of R_H across all temperatures (Fig. 4.S.5) and thus is acceptable for the modelling exercise described below.

Since we did not directly manipulate the soil microclimate, we used simple model simulations to predict the direct effects of soil temperature and soil moisture on R_H under four soil microclimate scenarios: 1) actual soil temperature and soil moisture; 2) altered soil temperature and actual soil moisture; 3) actual soil temperature and altered soil moisture; 4) altered soil temperature and altered soil moisture. To ensure that the altered soil microclimate scenarios were plausible, we used the microclimate of the opposing cropping system as the altered soil microclimate scenarios. The models were run at hourly timesteps using crop average values and then summed to estimate annual R_H for each scenario.

4.2.4 Ancillary measurements

Leaf area index (LAI) was measured in three blocks using a LI-COR LI-2000/2200 plant canopy analyzer (LI-COR Inc., Lincoln, NE, USA) in 2011 through 2012 and 2014 through 2016. During 2011 through 2012, the number of LAI measurements varied by date, but typically

consisted of 10 to 40 measurements per plot per date. During 2014 through 2016, 40 LAI measurements were made per plot per date. To illustrate typical LAI seasonal patterns, the LAI data were interpolated using a natural spline and predicted at daily intervals, and the daily LAI values were then averaged by day of year separately for the 2011 through 2012 and 2014 through 2016 time periods.

Snow depths were periodically measured in switchgrass and maize during the winters of 2015 and 2016. During each measurement date, the snow depth was measured in six to eight locations per plot. Treatment differences in snow depth was assessed using a mixed model with cropping system as a fixed effect and block as a random effect in SAS 9.4 (SAS Institute, Cary, North Carolina, USA).

4.3 Results

4.3.1 Weather, leaf area index, and snow depth

Monthly average air temperature ranged from -14.6 °C during the winter months to 24.3 °C during the summer (Fig. 4.1a). Annual air temperatures were warmer than normal in 2012, 2015, and 2016, and cooler than normal during 2013 and 2014 (Fig. 4.1b). The winter months of 2013 and 2014 were much colder than normal, with February 2015 also being anomalously cold (Fig. 4.1b). Monthly precipitation was generally greatest in the summer and lowest in winter with an overall average of 72.5 mm month^{-1} (Fig 4.1c). Total annual precipitation was about 15% higher than normal in 2013, 2015, and 2016 and was approximately 15% and 35% lower than normal in 2011 and 2012, respectively (Fig. 4.1d). The 2012 growing season was notably dry,

with 7 mm of precipitation recorded in June of that year. The winter of 2013, early summer of 2014, fall of 2015, and summer of 2016 were generally wetter than normal.

In 2011 and 2012, poplar leaf area index (LAI) was greater than maize and switchgrass from April through June, with switchgrass LAI surpassing poplar in July (Fig 4.2a). Poplar LAI typically began to decrease by July, likely due to the fungal disease which caused premature leaf drop. Switchgrass emergence occurred prior to maize planting, and thus switchgrass LAI increased earlier in the growing season (Fig 4.2a, b). During the 2014 through 2016 growing seasons, the largest absolute differences between switchgrass and maize LAI occurred within June and July, with values becoming more similar later in season (Fig. 4.2b). Nonetheless, mean LAI was consistently greater in switchgrass than maize (Fig. 4.2b).

Measured snow depths ranged from 1.9 to 23.6 cm (Table 4.2). The mean measured snow depth was consistently greater in switchgrass than maize, but the difference was statistically significant on only four of the eight measurement dates ($\alpha = 0.05$).

4.3.2 Soil temperature and moisture

During 2011 through 2013, soil temperature variation within the surface 25 cm was most moderate in poplar and most extreme in maize, with switchgrass typically intermediate (Fig. 4.3). The most notable differences in soil temperatures within the surface 25 cm occurred during the summer and winter months when air temperatures were near the high and low extremes, respectively. For example, during the summer of 2012, soil surface temperatures were greater in maize than poplar, whereas during the winter of 2013, soil surface temperatures were greater in poplar than maize. From 2011 through 2013, mean daily maximum soil temperatures at 10 cm

were 11.21 °C, 10.68 °C, and 10.34 °C in maize, switchgrass, and poplar, respectively (Fig. 4.S.1). During that same time period, mean daily minimum soil temperatures at 10 cm were 8.27 °C, 8.35 °C, and 8.62 °C in maize, switchgrass, and poplar, respectively (Fig. 4.S.2). The resulting overall mean 10 cm soil temperatures from 2011-2013 were 9.64 °C, 9.45 °C, and 9.42 °C for maize, switchgrass, and poplar, respectively (Fig. 4.3).

Although the soil temperature regimes among the cropping systems were most variable near the soil surface, seasonal differences among cropping systems were apparent to 100 cm (Fig. 4.4). Soil profile temperatures during autumn and winter were warmest in poplar, during spring were warmest in switchgrass, and during summer were warmest in maize. Conversely, soil profile temperatures during autumn and winter were coolest in maize, during spring were coolest in poplar, and during summer were coolest in switchgrass.

Surface soil temperatures during 2014-2016 showed similar patterns to those in 2011-2013, with switchgrass temperatures being more moderated than maize (Fig. 4.S.3). Differences were most notable during the extremely frigid winter months of 2014 and 2015, when the cold temperatures propagated much deeper in maize than switchgrass. However, seasonal differences in soil temperature persisted throughout the soil profile, with warmer winter temperatures in switchgrass from mid-fall through spring and warmer temperatures in maize from summer to mid-fall (Fig. 4.S.4).

Volumetric soil moisture content was typically lower near the soil surface compared to deeper in the soil profile (Fig. 4.5). The pattern of soil drying after rainfall events varied between maize and switchgrass, with maize soils drying out more quickly, particularly in 2015 when about 20% less precipitation fell from May through September compared to 2016. With a few exceptions, volumetric soil moisture within the top 50 cm was lower in maize than switchgrass

(Fig. 4.6). The exceptions to this usually occurred following rainfall events which led to brief periods where maize volumetric moisture content was greater than switchgrass near the soil surface. However, volumetric soil moisture was consistently lower in switchgrass than maize deeper in the horizon. The depth at which maize and switchgrass had equal soil moisture was typically shallowest during July, but was nearly always below 50 cm.

4.3.3 Heterotrophic soil respiration

Heterotrophic respiration (R_H) showed clear seasonal oscillations, with peak rates occurring during summer and minimum rates during winter (Fig. 4.7a). Switchgrass R_H was nearly always greater than maize, and the absolute differences were greatest during the summer. Temporal patterns of R_H were closely related to T_{SOC} (Fig. 4.7b). Consistent with the soil temperature profiles, T_{SOC} was greater in switchgrass during the winter and greater in maize during the summer (Fig. 4.7b). The temporal variation in M_{SOC} was greater in 2015 than 2016, with a large decrease in M_{SOC} occurring during mid-summer in 2015 (Fig. 4.7c). In agreement with the soil moisture profiles, M_{SOC} was usually greater in switchgrass than maize.

The R_H models fit the data reasonably well, with R^2 of 0.71 and 0.80 for maize and switchgrass, respectively (Fig. 4.S.5). The model parameters indicated greater $R_{H,10}$, Q_{10}, and M_{opt} in switchgrass compared to maize (Table 4.3). However, the model D parameter was lower in switchgrass than maize indicating a more pronounced soil moisture effect in switchgrass. Soil microclimate scenario simulations showed the greatest divergence during the summer months (Fig. 4.S.6). Independently altered soil temperature and soil moisture reduced modelled R_H from 1 to 4% in maize and increased modelled R_H from 4 to 8% in switchgrass (Table 4.4). The combined modelled effects of altered soil temperature soil moisture decreased maize R_H by 3 to

6% and increased switchgrass R_H by 8-17%. The effects of altered soil moisture and temperature on R_H were greater in 2016 than 2015.

4.4 Discussion

4.4.1 Less extreme soil temperatures in perennial systems

Compared to the annual maize system, the perennial systems had several traits conferring less extreme soil temperature fluctuations near the soil surface. The earlier leaf-out in poplar and switchgrass compared to maize, and the generally higher LAI in switchgrass than maize, resulted in a relatively cool soil microclimate during spring and summer in the two perennial systems. Temporal differences between poplar and switchgrass were also apparent, with earlier leaf-out in poplar leading to cooler springtime soil temperatures than switchgrass, and higher peak LAI in switchgrass resulting in lower mid-summer soil temperatures than poplar. Greater LAI increases both the quantity of solar radiation reflected upwards and the amount of radiation absorbed by the plant canopy, thus leading to less radiation at the soil surface (Campbell & Norman 1998; Hardwick et al. 2015). In addition, greater LAI reduces the turbulent mixing of air from above the canopy, thereby reducing the influence of above canopy temperature on soil temperatures (Hardwick et al. 2015). In agreement with our results, several studies have reported the moderating effect of LAI on soil temperature in other ecosystems including temperate and tropical forests (Closa et al. 2010; Hardwick et al. 2015).

During winter, a warmer soil microclimate in the perennial systems likely resulted in part from greater snow accumulation and subsequently greater insulation from the cold air temperatures. In line with the findings of Sharratt et al. (1998), the ubiquitous upright stubble in

switchgrass was more efficient at trapping snow and thus led to warmer wintertime soil temperatures than maize, which had primarily prostrate litter. The depth of the litter and stubble layer, combined with differences in residue thermal properties, likely also contributed to the greater insulation of soils under switchgrass (e.g. Kucharik et al. 2013). During fall and spring, when snow was not present, the standing stubble in switchgrass may have also reduced the turbulent mixing of air between the soil and air (Campbell & Norman 1998), therefore limiting the influence of changes in air temperatures on the soil. Although we did not measure snow depth within the poplar systems, we expect that the herbaceous understory created similar conditions to the switchgrass system. In addition, the poplar leaf litter layer may have provided insulation between the soil and air, thus buffering soil temperatures from air temperature fluctuations. Differences in SOC, bulk density, and soil water holding capacity among cropping systems may have also contributed to differences in soil microclimates through their influence on soil thermal properties (Haruna et al. 2017).

While the management practices within a cropping system are constrained to an extent, there are certain choices that could cause changes to the soil temperature regime. For example, assuming similar plant growth dynamics, earlier maize planting would result in earlier peak LAI and thus would likely reduce the mid-summer soil temperatures. Contrarily, earlier harvest of maize or switchgrass (e.g. maize for silage or a double switchgrass harvest) would likely increase soil temperatures through the reduction of LAI. Increasing the upright stubble height in maize would likely increase the amount of snow trapped and therefore keep winter soil temperature warmer (Sharratt et al. 1998; Sharratt 2002). On the other hand, harvesting switchgrass closer to the soil surface would decrease the amount of snow trapped and permit colder soil temperatures. Similarly, harvesting the herbaceous understory or leaf litterfall in poplar would likely lead to a

more extreme soil temperature regime. Soil temperatures are also likely to be more extreme following poplar harvest when LAI and litterfall are reduced.

4.4.2 Soil moisture microclimate varies with depth

Unlike the soil temperature microclimate, which was generally consistent with depth, the soil moisture microclimate was generally drier in maize near the soil surface, but was drier in switchgrass deeper within the soil profile. Other studies have shown that perennial grasses deplete more deep soil moisture and less near-surface soil moisture when compared to annual grasses (Monti & Zatta 2009; Ferchaud et al. 2015). This effect is likely a result of the contrasting fine root distributions between perennial and annual rooting plant rooting systems, with fine roots typically extending deeper in perennial crops (Ferchaud et al. 2015). Species with deeper fine roots are known to extract more water from deeper horizons than shallowly rooted species (Craine et al. 2003), although the differences are most prominent when surface water becomes limiting (Nippert & Knapp 2007). The latter point is consistent with our finding that the largest difference in deep soil moisture between maize and switchgrass occurred during the summer months when water surface moisture was most depleted.

While divergent fine root distributions likely contribute to the differences in soil moisture regimes between maize and switchgrass, other factors are also important. In the springtime, greater surface soil moisture in switchgrass than maize could result from the greater water recharge from snowmelt (Sharratt et al. 1998). During late spring and summer, the greater solar energy reaching the soil in the low LAI maize system likely enhanced water evaporation from the soil surface relative to switchgrass, thus causing drier soil conditions (Ferchaud et al. 2015). Reciprocally, greater surface soil moisture in switchgrass would lead to a higher soil volumetric

heat capacity (Hillel 2003) and thus reduce the temperature fluctuations in switchgrass. Variation in the distribution of litter may also be important (Hatfield & Prueger 1996; Ferchaud et al. 2015), with the more ubiquitous stubble and litter layer in switchgrass reducing evaporation relative to maize. Overall, the soil moisture microclimate results from complex interactions among many factors (von Arx et al. 2013), and thus may not be easily predictable.

4.4.3 Soil microclimate affects modelled C loss

Considering that the altered microclimate scenarios represented extreme shifts in the soil microclimate (i.e. entirely different cropping systems), the predicted changes in R_H under the scenarios likely represent an upper limit to what is achievable through management practices within a cropping system. On the other hand, larger differences in soil microclimates during more extreme years (such as 2012) would likely have more significant effects on R_H than shown in our 2015 and 2016 model scenarios. The moderate changes in R_H predicted under the modelled soil microclimate scenarios were driven about equally by the changes in soil moisture and soil temperature. As expected, increased soil temperatures in switchgrass led to greater R_H, while decreased soil temperatures in maize resulted in lower R_H. However, since the model Q_{10} was greater in switchgrass than maize, the resulting soil temperature effect was greater in switchgrass. Due to the non-linear effect of soil temperature on R_H, the most prominent differences in R_H among the scenarios occurred during the summer months when soil temperature was highest. The effect of soil moisture was somewhat less predictable, owing to differences in the optimal soil moisture (M_{opt} parameter) and the strength of the moisture response (D parameter). Since the effect of soil moisture was interactive with temperature, the influence of soil moisture on R_H was also most prominent when soil temperature was high.

While it was beyond the scope of this study, understanding why there were differences in the soil temperature and soil moisture response parameters among cropping systems would be required to make more generalizable predictions in other cropping systems and at different locations.

In situations where C sequestration in soils is a management priority, reducing R_H may be a potential strategy for land managers. For example, implementing management practices that keep soil relatively cool would likely reduce R_H, although the indirect effects on soil moisture would also need to be considered. Due to the magnitude of summertime R_H, practices that reduce the extreme summer soil temperatures are likely to induce the greatest reduction of annual R_H. Management practices that alter soil moisture would be more difficult to implement, as they would require knowledge of the optimal soil moisture for R_H of a given system and a comprehensive understanding of how management practices effect soil moisture. In addition, the indirect effects on other ecosystem processes would also need to be considered. Importantly, reducing R_H would likely come at the cost of decreasing N mineralization (Rustad et al. 2001), which in turn could negatively affect plant productivity. Changes to the soil microclimate could also have implications for emissions of other greenhouse gases, such as N_2O, which are stimulated under wetter conditions (del Prado et al. 2006). These unintended changes would need to be weighed against the potential increases in C storage resulting from decreased R_H.

While our modelled scenarios illustrate the potential for plant and management factors to directly alter R_H through soil microclimate effects, there are several limitations to our modelling approach. First, our model does not explicitly represent substrate supply and therefore does not account for feedbacks between R_H and substrates. For example, our model indicated that R_H in switchgrass systems would be greater if the soils were relatively warmer. However, greater R_H would also deplete C substrates more quickly, thus likely reducing the R_H potential. Our model

also did not account for differences in the size and structure of the soil microbial community, both of which are known to differ between maize and switchgrass at this site (Jesus et al. 2015). It is possible, for example, that the microbial community could either enhance or decrease the temperature sensitivity of R_H under the altered soil microclimate (Karhu et al. 2014). A more comprehensive understanding of the effects of soil microclimates on R_H would require direct manipulation of the soil temperature and moisture under the existing cropping systems and would need to consider a range of potential mechanisms and feedbacks.

4.5 Conclusions

Seasonal differences in soil temperature among bioenergy cropping systems tracked patterns of leaf area index in the summer and differences in snow depth during the winter. Compared to annual systems, cooler summer soil temperatures and warmer winter soil temperatures in perennial systems were associated with higher leaf area index and deeper snow cover, respectively. Seasonal differences in soil moisture varied by depth, with drier surface soils in the annual maize system and drier deep soils in the perennial switchgrass system. Soil moisture differences between crops likely reflect multiple factors including fine root distribution and surface evaporation. Simple model simulations indicated that hypothetically altering the soil microclimates between maize and switchgrass systems could alter annual C losses from heterotrophic respiration by 3 to 17%. However, other mechanisms such as substrate depletion and soil microbial community responses need to be considered to provide a more comprehensive understanding of the effect of soil microclimate on heterotrophic respiration. Management for C sequestration via reduced heterotrophic soil respiration may be possible, but the resulting effects on plant productivity and non-CO_2 greenhouse gas emissions must also be weighed.

4.6 Acknowledgements

This research was funded by the Great Lakes Bioenergy Research Center (DOE BER Office of Science DE-FC02-07ER64494 and DOE OBP Office of Energy Efficiency and Renewable Energy DE-AC05-76RL01830), the USDA National Institute of Food and Agriculture (Hatch project 0225417-WIS01586), and the National Science Foundation (grant DEB-1038759). We extend thanks to M. Cruse and C. Cummings for help with field data collection.

4.7 References

Campbell, G. S., Norman, J. M. 1998. An Introduction to Environmental Biophysics, 2nd ed. Springer, New York, USA.

Chapin III, F. S., Woodwell, G. M., Randerson, J. T., Rastetter, E. B., Lovett, G. M., Baldocchi, D. D., Clark, D. A., Harmon, M. E., Schimel, D. S. et al. 2006. Reconciling carbon-cycle concepts, terminology, and methods. Ecosystems 9:1041–1050.

Chen, J., Saunders, S. C., Crow, T. R., Naiman, R. J., Brosofske, K. D., Mroz, G. D., Brookshire, B. L., Franklin, J. F. 1999. Microclimate in forest ecosystem and landscape ecology: Variations in local climate can be used to monitor and compare the effects of different management regimes. BioScience 49:288–297.

Closa, I., Irigoyen, J. J., Goicoechea, N. 2010. Microclimatic conditions determined by stem density influence leaf anatomy and leaf physiology of beech (*Fagus sylvatica* L.) growing within stands that naturally regenerate from clear-cutting. Trees 24:1029–1043.

Craine, J. M., Wedin, D. A., Chapin III, F. S., Reich, P. B. 2003. Relationship between the structure of root systems and resource use for 11 North American grassland plants. Plant Ecology 165:85–100.

Davidson, E. A., Janssens, I. A., Luo, Y. Q. 2006. On the variability of respiration in terrestrial ecosystems: moving beyond Q(10). Global Change Biology 12:154–164.

Ferchaud, F., Vitte, G., Bornet, F., Strullu, L., Mary, B. 2015. Soil water uptake and root distribution of different perennial and annual bioenergy crops. Plant and Soil 388:307–

322.

Flerchinger, G. N., Pierson, F. B. 1997. Modelling plant canopy effects on variability of soil temperature and water: model calibration and validation. Journal of Arid Environments 35:641–653.

Gelfand, I., Zenone, T., Jasrotia, P., Chen, J. Q., Hamilton, S. K., Robertson, G. P. 2011. Carbon debt of Conservation Reserve Program (CRP) grasslands converted to bioenergy production. Proceedings of the National Academy of Sciences of the United States of America 108:13864–13869.

Gibbs, H. K., Johnston, M., Foley, J. A., Holloway, T., Monfreda, C., Ramankutty, N., David 2008. Carbon payback times for crop-based biofuel expansion in the tropics: the effects of changing yield and technology. Environmental Research Letters 3:034001.

Hardwick, S. R., Toumi, R., Pfeifer, M., Turner, E. C., Nilus, R., Ewers, R. M. 2015. The relationship between leaf area index and microclimate in tropical forest and oil palm plantation: Forest disturbance drives changes in microclimate. Agricultural and Forest Meteorology 201:187–195.

Haruna, S. I., Anderson, S. H., Nkongolo, N. V., Reinbott, T., Zaibon, S. 2017. Soil thermal properties influenced by perennial biofuel and cover crop management. Soil Science Society of America Journal 81:1147–1156.

Hatfield, J., Prueger, J. 1996. Microclimate effects of crop residues on biological processes. Theoretical and Applied Climatology 54:47–59.

Hillel, D. 2003. Introduction to Environmental Soil Physics, 1st ed. Academic Press, Massachusetts, USA.

Jesus, E. d. C., Liang, C., Quensen, J. F., Susilawati, E., Jackson, R. D., Balser, T. C., Tiedje, J. M. 2016. Influence of corn, switchgrass, and prairie cropping systems on soil microbial communities in the upper Midwest of the United States. Global Change Biology Bioenergy 8:481–494.

Karhu, K., Auffret, M. D., Dungait, J. A. J., Hopkins, D. W., Prosser, J. I., Singh, B. K., Subke, J.-A., Wookey, P. A., Agren, G. I. et al. 2014. Temperature sensitivity of soil respiration rates enhanced by microbial community response. Nature 513:81–84.

Kucharik, C. J., VanLoocke, A., Lenters, J. D., Motew, M. M. 2013. Miscanthus establishment and overwintering in the Midwest USA: A regional modeling study of crop residue management on critical minimum soil temperatures. PLoS ONE 8:e68847.

Lambers, H., Chapin III, F. S., Pons, T. L. 2008. Plant Physiological Ecology, 2nd ed. Springer, New York, USA.

Lark, T. J., Salmon, J. M., Gibbs, H. K. 2015. Cropland expansion outpaces agricultural and biofuel policies in the United States. Environmental Research Letters 10:044003.

Linn, D. M., Doran, J. W. 1984. Effect of water-filled pore space on carbon dioxide and nitrous oxide production in tilled and nontilled soils. Soil Science Society of America Journal 48:1267–1272.

Lloyd, J., Taylor, J. A. 1994. On the temperature dependence of soil respiration. Functional Ecology 8:315–323.

Monti, A., Zatta, A. 2009. Root distribution and soil moisture retrieval in perennial and annual energy crops in Northern Italy. Agriculture, Ecosystems & Environment 132:252–259.

Moyano, F. E., Manzoni, S., Chenu, C. 2013. Responses of soil heterotrophic respiration to moisture availability: An exploration of processes and models. Soil Biology & Biochemistry 59:72–85.

Nippert, J. B., Knapp, A. K. 2007. Linking water uptake with rooting patterns in grassland species. Oecologia 153:261–272.

National Oceanic and Atmospheric Administration (NOAA). 2017. National Centers for Environmental Information: Climate Data Online. www.ncdc.noaa.gov.

Phillips, C. L., Nickerson, N., Risk, D., Bond, B. J. 2011. Interpreting diel hysteresis between soil respiration and temperature. Global Change Biology 17:515–527.

del Prado, A., Merino, P., Estavillo, J. M., Pinto, M., Gonzalez-Murua, C. 2006. N_2O and NO emissions from different N sources and under a range of soil water contents. Nutrient Cycling in Agroecosystems 74:229–243.

Prolingheuer, N., Scharnagl, B., Graf, A., Vereecken, H., Herbst, M. 2014. On the spatial variation of soil rhizospheric and heterotrophic respiration in a winter wheat stand. Agricultural and Forest Meteorology 195–196:24–31.

Robertson, G. P., Hamilton, S. K., Del Grosso, S. J., Parton, W. J. 2011. The biogeochemistry of bioenergy landscapes: carbon, nitrogen, and water considerations. Ecological Applications 21:1055–1067.

Rustad, L. E., Campbell, J. L., Marion, G. M., Norby, R. J., Mitchell, M. J., Hartley, A. E., Cornelissen, J. H. C., Gurevitch, J. 2001. A meta-analysis of the response of soil respiration, net nitrogen mineralization, and aboveground plant growth to experimental ecosystem warming. Oecologia 126:543–562.

Sanford, G. R., Oates, L. G., Jasrotia, P., Thelen, K. D., Robertson, G. P., Jackson, R. D. 2016. Comparative productivity of alternative cellulosic bioenergy cropping systems in the North Central USA. Agriculture, Ecosystems & Environment 216:344–355.

Savage, K., Davidson, E. A., Richardson, A. D., Hollinger, D. Y. 2009. Three scales of temporal resolution from automated soil respiration measurements. Agricultural and Forest Meteorology 149:2012–2021.

Sharratt, B. 2002. Corn stubble height and residue placement in the northern US Corn Belt: Part I. Soil physical environment during winter. Soil and Tillage Research 64:243–252.

Sharratt, B., Benoit, G., Voorhees, W. 1998. Winter soil microclimate altered by corn residue management in the northern Corn Belt of the USA. Soil and Tillage Research 49:243–248.

Soil Survey Staff. 2017. Natural Resources Conservation Service, U.S. Department of Agriculture. Official Soil Series Descriptions. www.nrcs.usda.gov.

Vogel, J. G., Valentine, D. W. 2005. Small root exclusion collars provide reasonable estimates of root respiration when measured during the growing season of installation. Canadian Journal of Forest Research 35:2112–2117.

von Haden, A.C. 2017a. Annual ecosystem carbon balances in long-term no-till maize and mature switchgrass bioenergy cropping systems: evaluating methods and processes. In: Mechanisms of ecosystem carbon storage and stability in temperature bioenergy cropping systems. Doctoral Dissertation. University of Wisconsin-Madison, Madison, WI, USA.

von Haden, A.C. 2017b. Autotrophic soil respiration in maize and switchgrass bioenergy cropping systems: an assessment of the growth-maintenance respiration framework at the ecosystem level. In: Mechanisms of ecosystem carbon storage and stability in temperature bioenergy cropping systems. Doctoral Dissertation. University of Wisconsin-Madison, Madison, WI, USA.

Whitmore, A. P., Kirk, G. J. D., Rawlins, B. G. 2015. Technologies for increasing carbon storage in soil to mitigate climate change. Soil Use and Management 31:62–71.

Wolkovich, E. M., Bolger, D. T., Cottingham, K. L. 2009. Invasive grass litter facilitates native shrubs through abiotic effects. Journal of Vegetation Science 20:1121–1132.

4.8 Tables and figures

Table 4.1 – Soil temperature and soil moisture equipment used within each experimental block. CS640 and CS616 are Campbell Scientific sensors (Campbell Scientific Inc., Logan, Utah, USA).

Block	Start year	Temperature sensor and depths (cm)		Moisture sensor and depths (cm)	
A	2011	Thermocouple	2, 10, 20, 35, 65, 95, 125	CS640	2, 20, 35, 50, 65, 95, 125
B	2011	Thermocouple	2, 10, 20, 35, 65, 95, 125	CS640	2, 20, 35, 50, 65, 95, 125
C	2011	Thermocouple	2, 10, 30, 95	CS616	15, 30
D	2015	Thermocouple	2, 10, 20	CS616	2, 20

Table 4.2 – Snow depths measured throughout the winter of 2015 and 2016 in maize and switchgrass. Bolded *p*-values indicate significant differences between cropping systems ($p < 0.05$).

Date	Snow depth (cm)		n	*F* value	*p* value
	Maize	*Switchgrass*			
11/22/2015	9.4 (0.6)	11.3 (0.3)	4	6.93	0.078
12/30/2015	7.3 (0.6)	23.6 (1.4)	4	114.16	**0.002**
1/20/2016	5.5 (1.0)	16.5 (0.6)	4	102.91	**0.002**
12/5/2016	8.9 (0.2)	9.8 (0.3)	4	6.76	0.080
12/22/2016	12.3 (1.4)	19.5 (2.2)	4	7.5	0.071
12/30/2016	4.9 (1.0)	10.9 (2.4)	3	6.7	0.122
1/28/2017	10.1 (0.4)	12.4 (0.1)	3	34.31	**0.028**
2/27/2017	1.9 (0.2)	5.3 (0.5)	3	40.67	**0.024**

Table 4.3 – Mean parameter estimates (with standard error among the plots) for heterotrophic respiration (R_H) models.

Parameter	**Maize**	**Switchgrass**
$R_{H,10}$	1.237 (0.151)	1.667 (0.118)
Q_{10}	2.308 (0.038)	3.033 (0.092)
M_{opt}	0.266 (0.029)	0.311 (0.014)
D	0.999 (0.003)	0.993 (0.002)

Table 4.4 – Modelled annual heterotrophic soil respiration (R_H) under actual and altered soil microclimate scenarios. The altered scenarios refer to modelled R_H under the soil temperature and/or soil moisture regimes of the opposing cropping system.

Crop	**Maize**		**Switchgrass**	
Year	2015	2016	2015	2016
Soil microclimate scenario	g C m^{-2} y^{-1} (% difference)			
Actual soil microclimate	527	567	709	687
Altered soil temperature	517 (-2%)	542 (-4%)	738 (+4%)	742 (+8%)
Altered soil moisture	520 (-1%)	557 (-2%)	740 (+4%)	744 (+8%)
Altered soil temperature and moisture	509 (-3%)	533 (-6%)	768 (+8%)	803 (+17%)

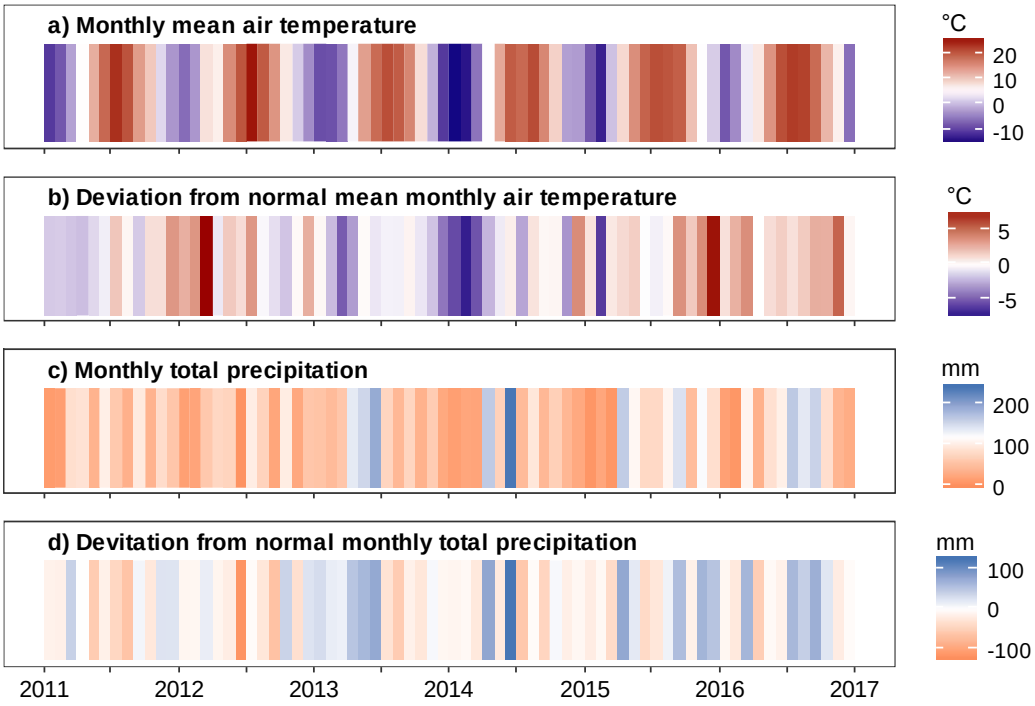

Figure 4.1 – Mean monthly air temperature (a), deviation from 30-year normal air temperature (b), total monthly precipitation (c), and deviation from normal precipitation (d) at Arlington, WI, USA (NOAA 2017).

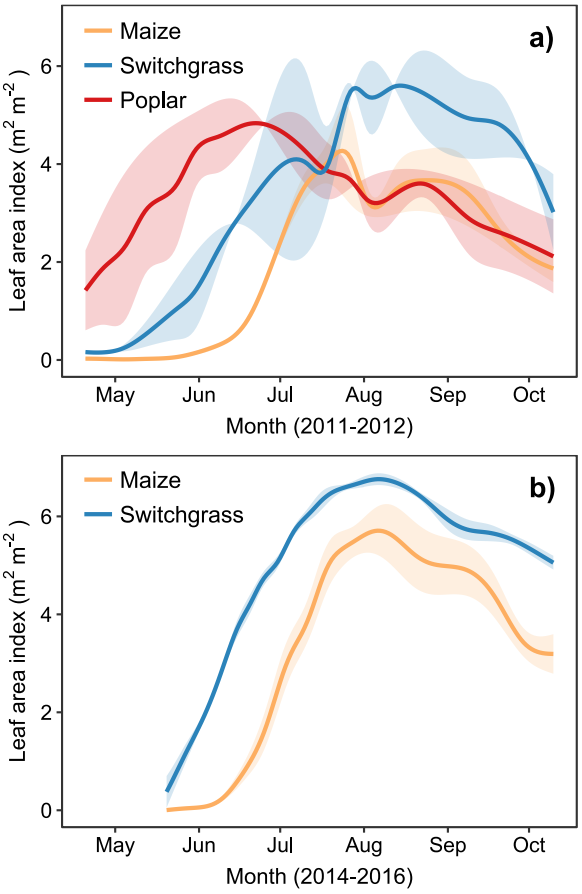

Figure 4.2 – Natural spline-interpolated mean leaf area index (LAI) during 2011-2012 (a) and 2014-2016 (b). Shaded areas indicate the standard error among years.

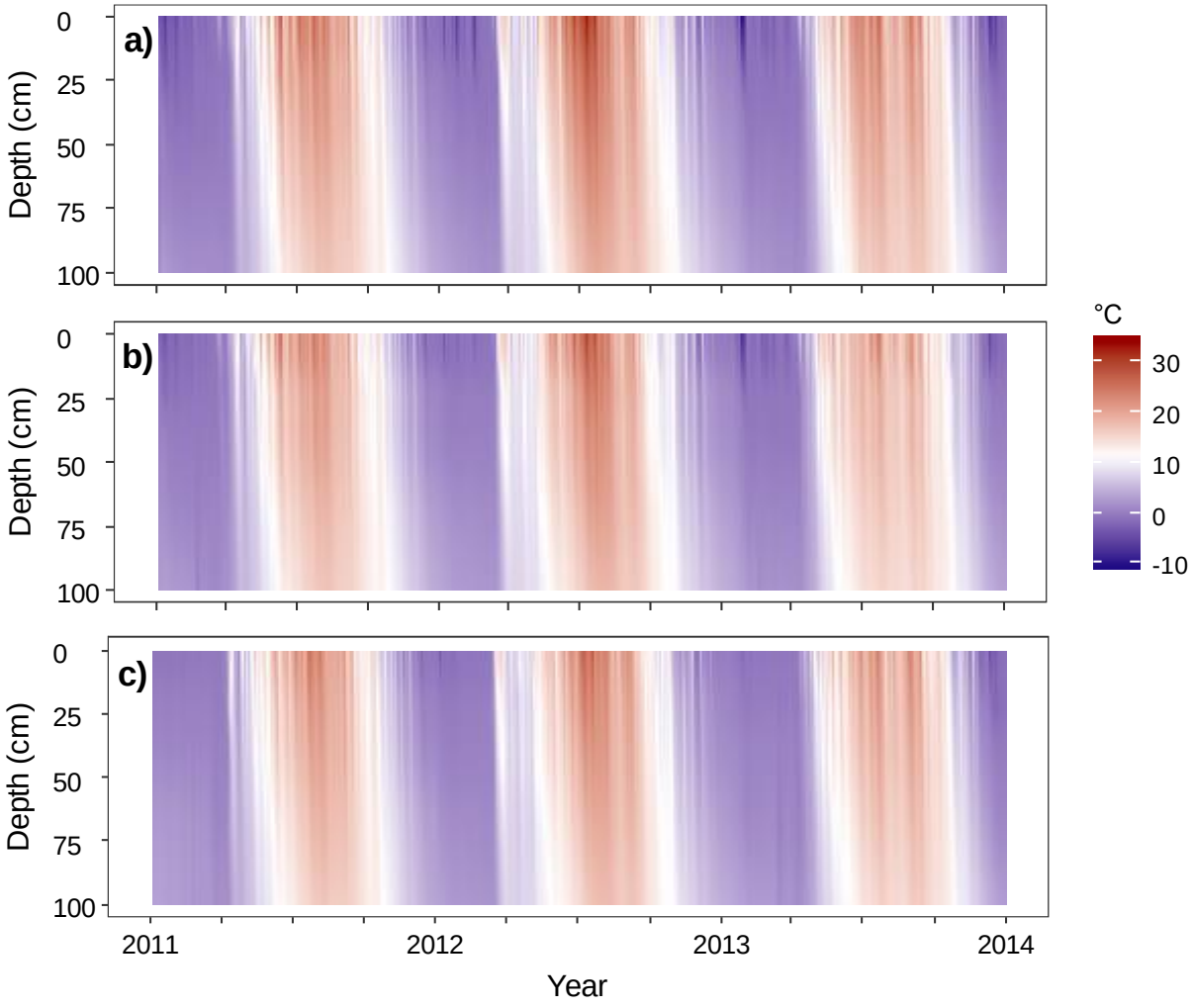

Figure 4.3 – Daily mean soil temperatures with depth for maize (a), switchgrass (b), and poplar (c) during 2011-2013.

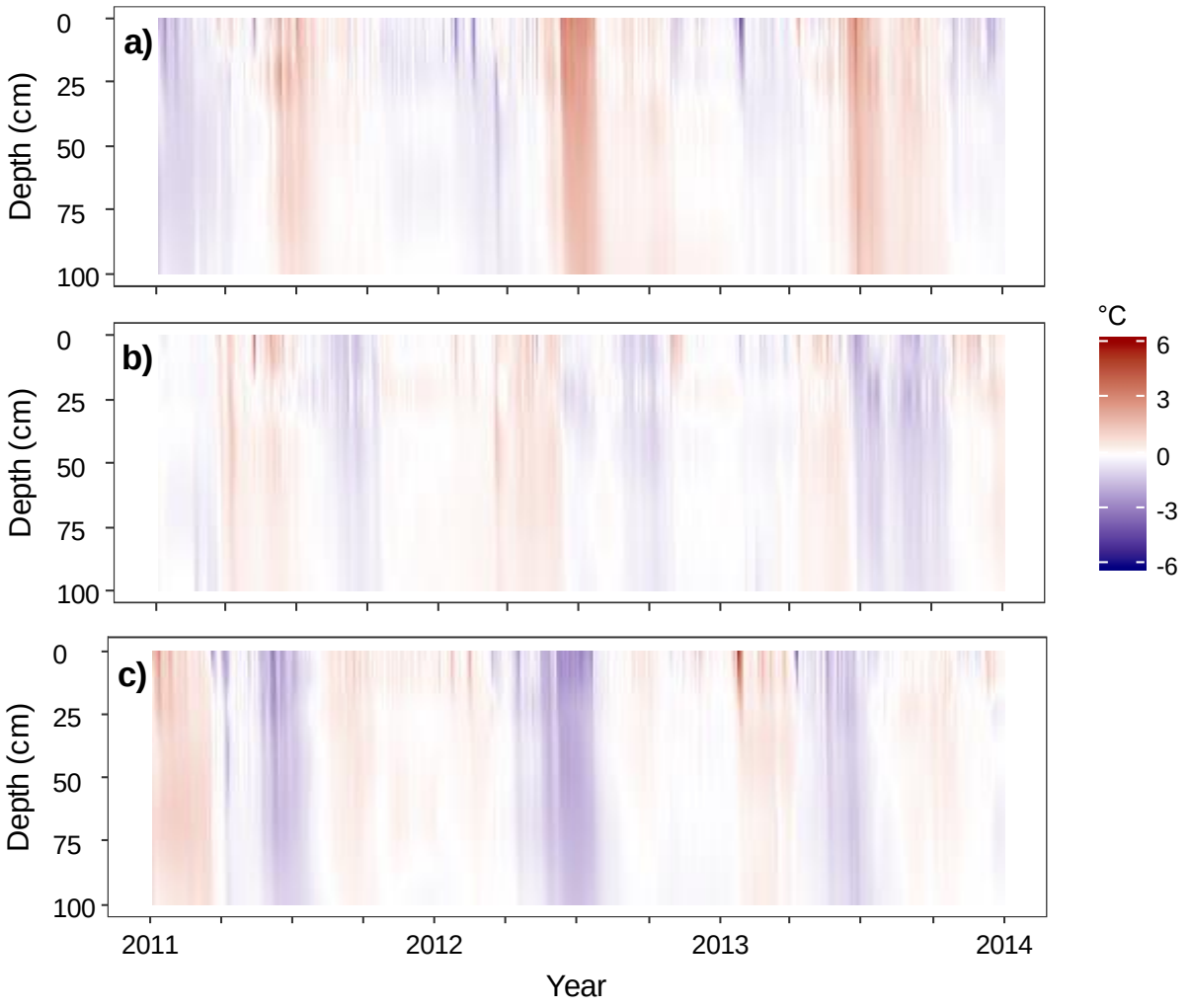

Figure 4.4 – Deviation from average daily mean soil temperature among the cropping systems for maize (a), switchgrass (b), and poplar (c) from 2011-2013.

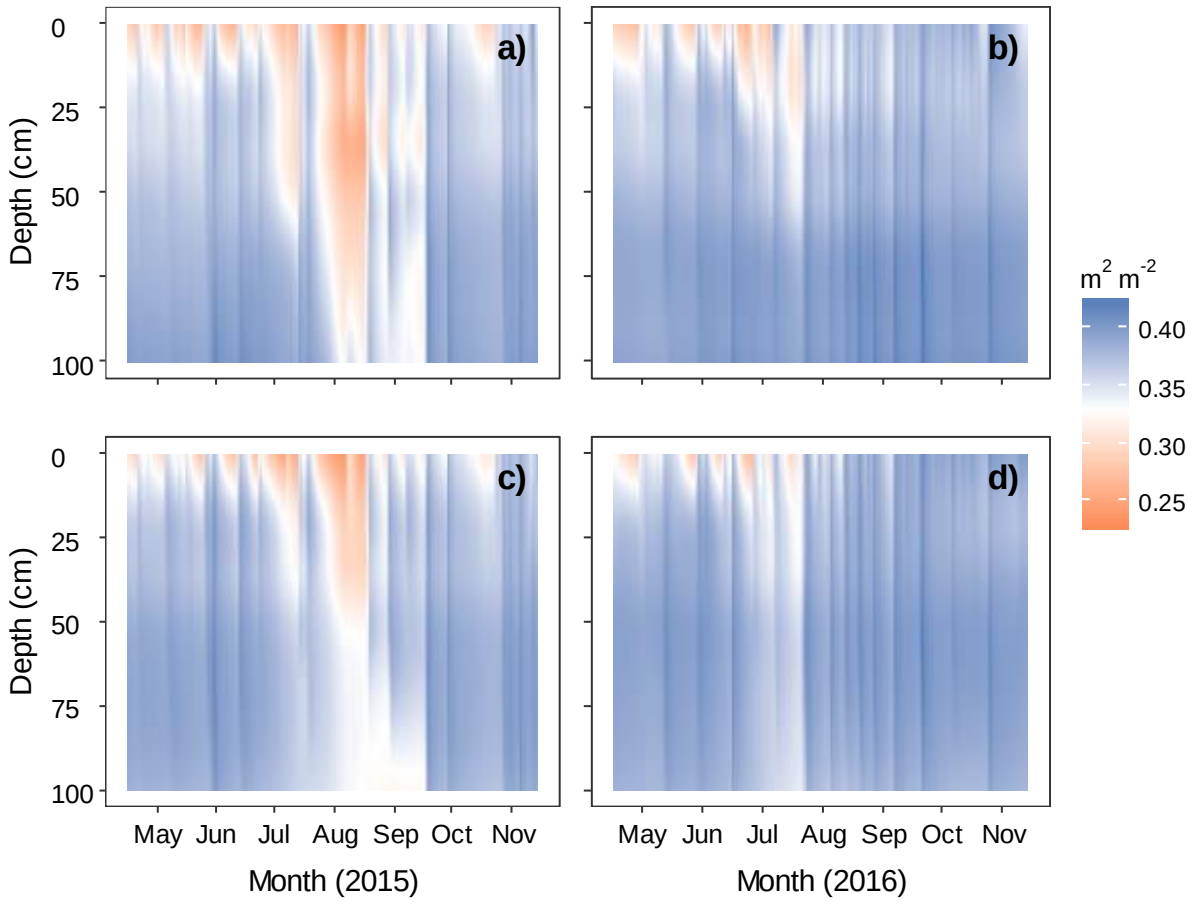

Figure 4.5 – Daily volumetric soil moisture by depth for maize (a and b) and switchgrass (c and d) during 2015 and 2016.

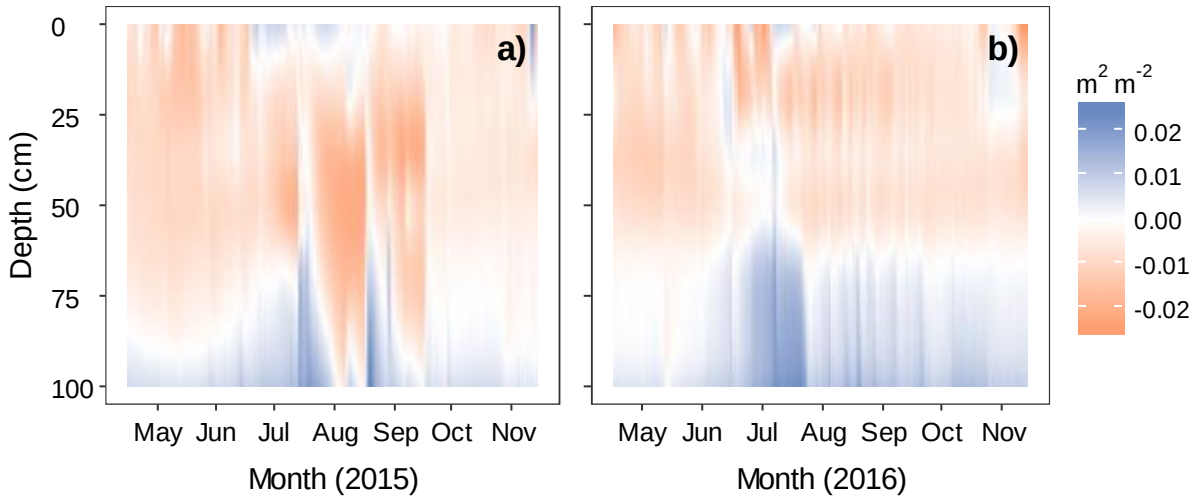

Figure 4.6 – Deviation from daily average volumetric soil moisture between cropping systems in (a) 2015 and (b) 2016. Orange indicates that maize is drier than switchgrass, and blue indicates that maize is wetter than switchgrass.

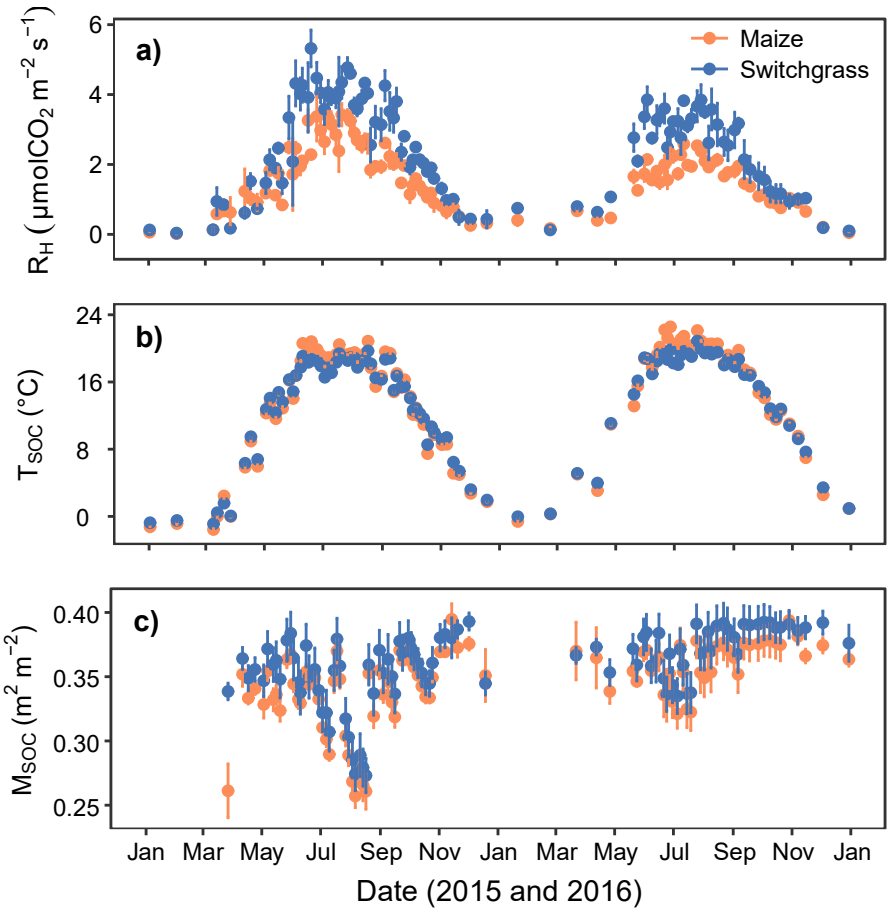

Figure 4.7 – Measured heterotrophic respiration (R_H) (a), soil profile SOC-weighted temperature (T_{SOC}) (b), and soil profile SOC-weighted volumetric soil moisture (M_{SOC}) (c).

4.9 Supplemental figures

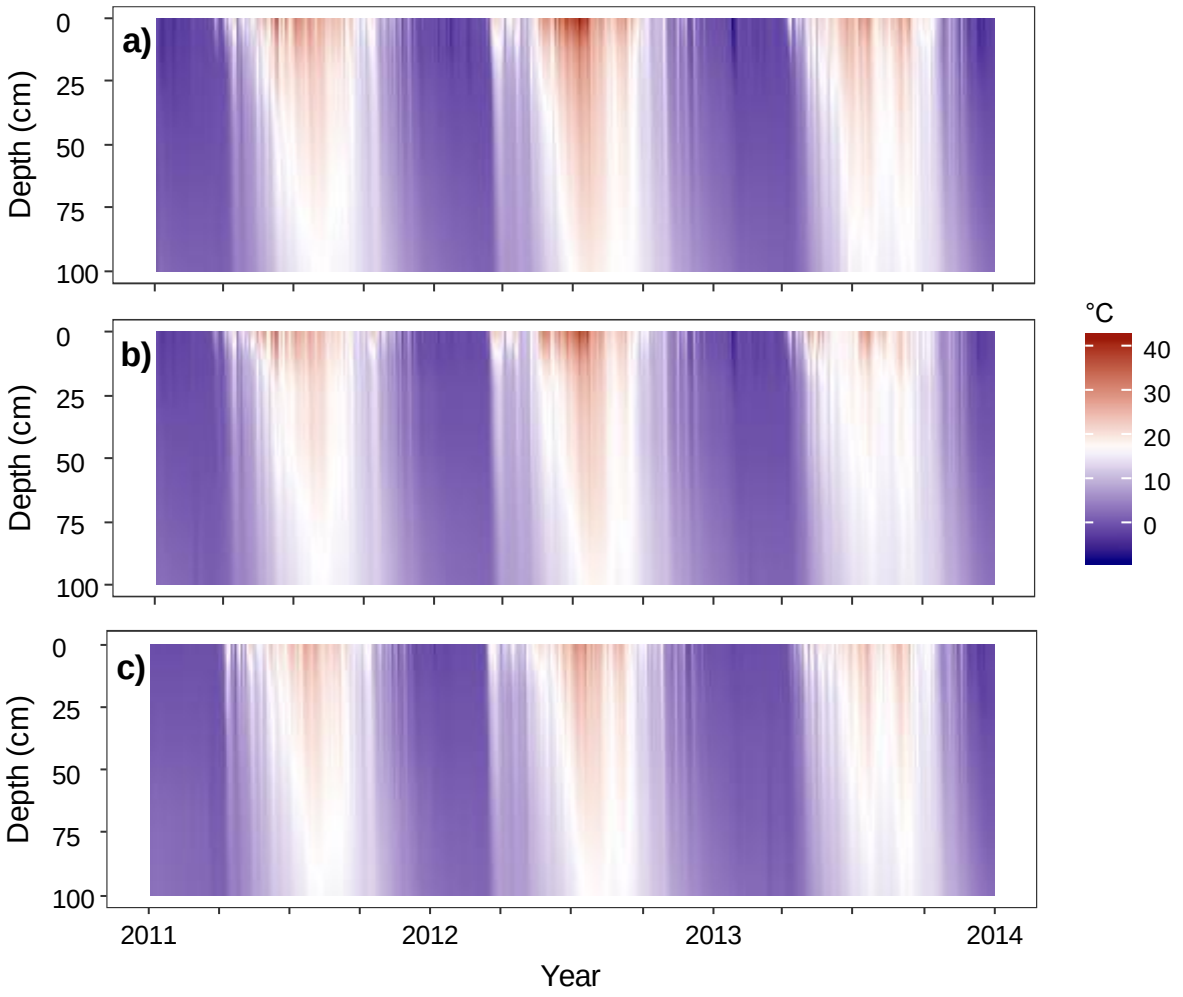

Fig 4.S.1 – Mean daily maximum soil temperatures from 2011 through 2013 in maize (a), switchgrass (b), and poplar (c).

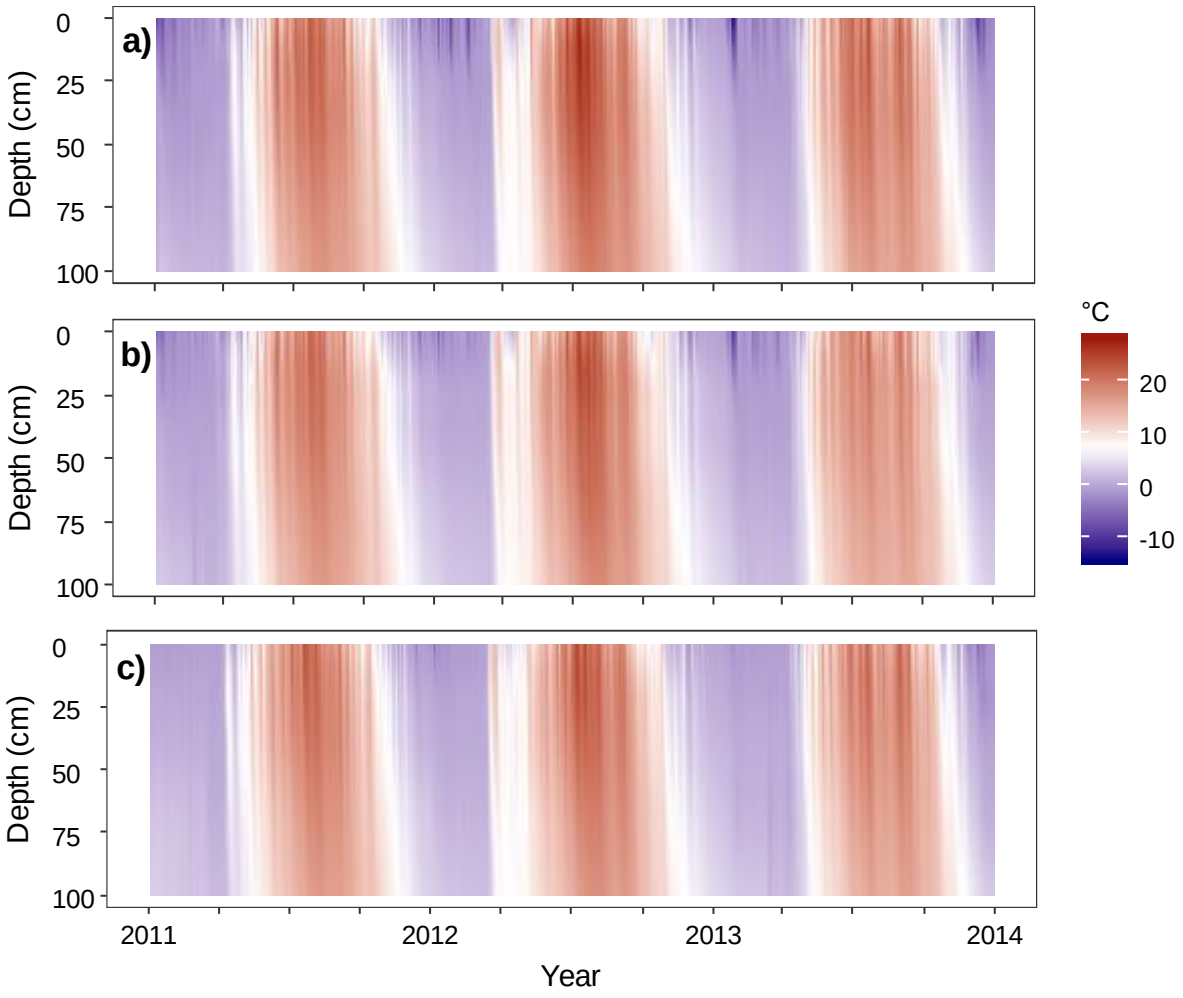

Figure 4.S.2 – Mean daily minimum soil temperatures from 2011 through 2013 in maize (a), switchgrass (b), and poplar (c).

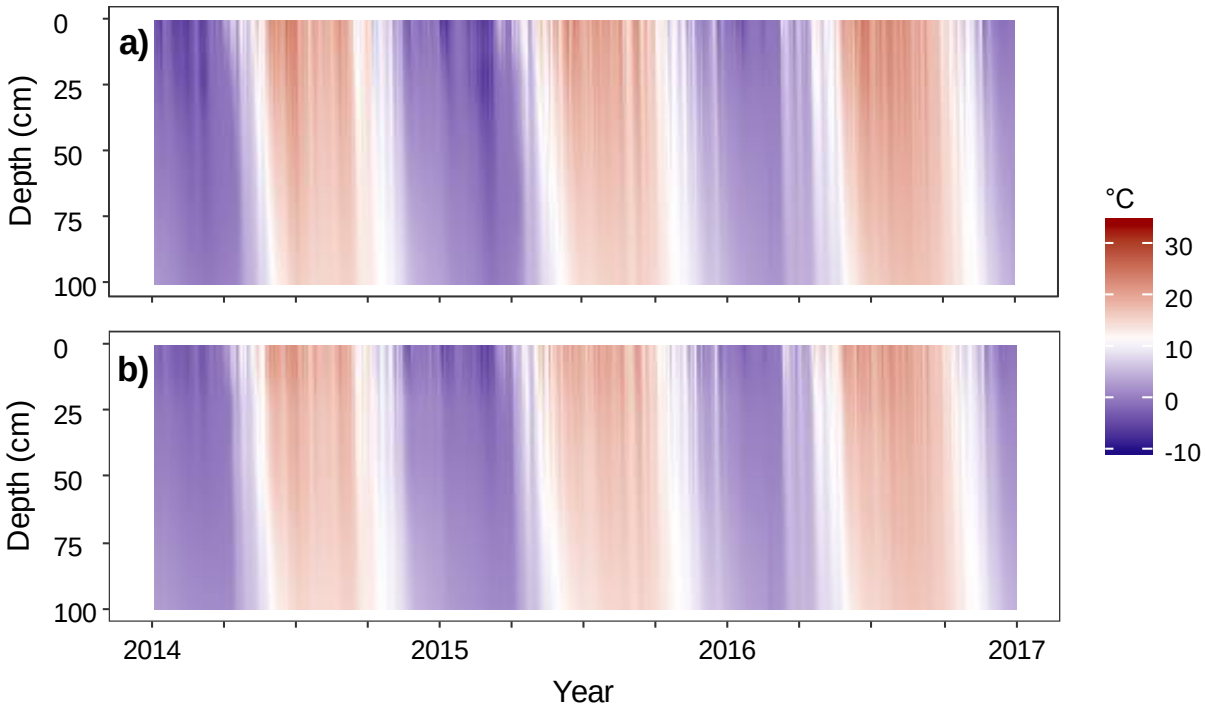

Figure 4.S.3 – Average daily soil temperature by depth during 2014-2016 for maize (a) and switchgrass (b).

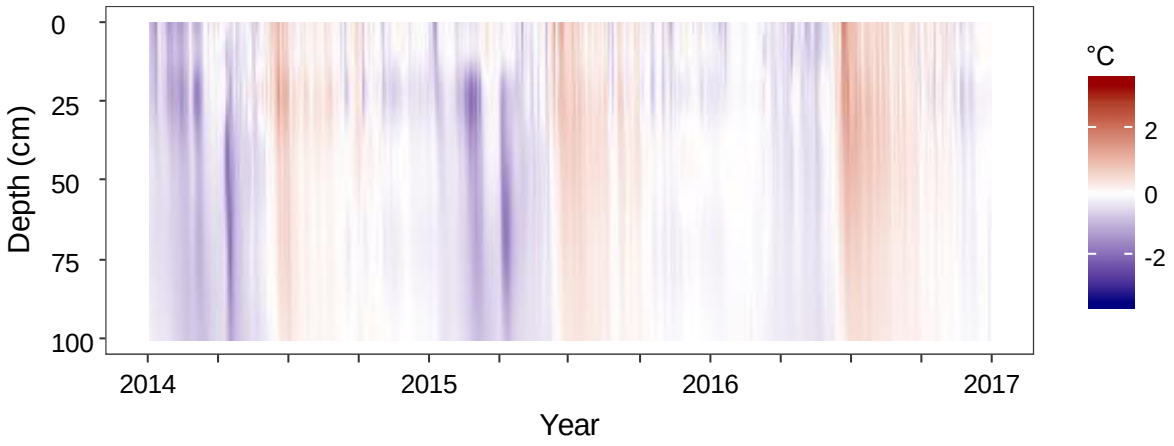

Figure 4.S.4 – Deviation from average daily soil temperature between maize and switchgrass. Red indicates that temperatures are warmer in maize than switchgrass, and blue indicates that temperatures are cooler in maize than switchgrass.

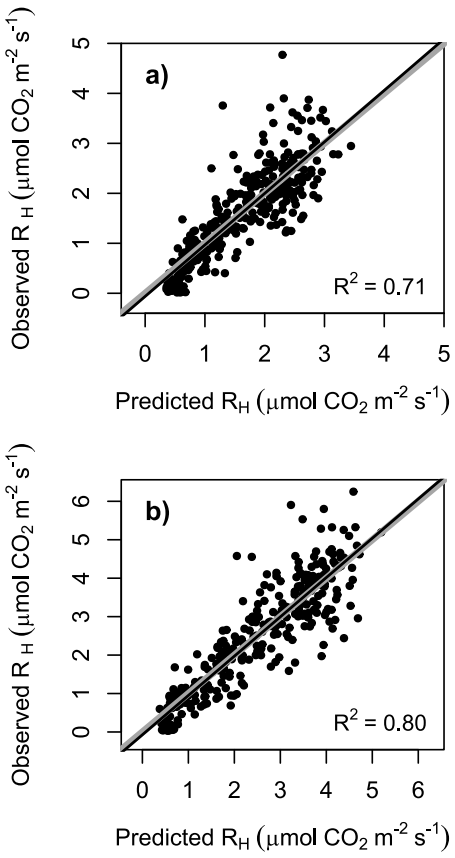

Figure 4.S.5 – Model predicted versus observed heterotrophic soil respiration in maize (a) and switchgrass (b). The gray line indicates 1:1 and the black line is the linear regression between the variables.

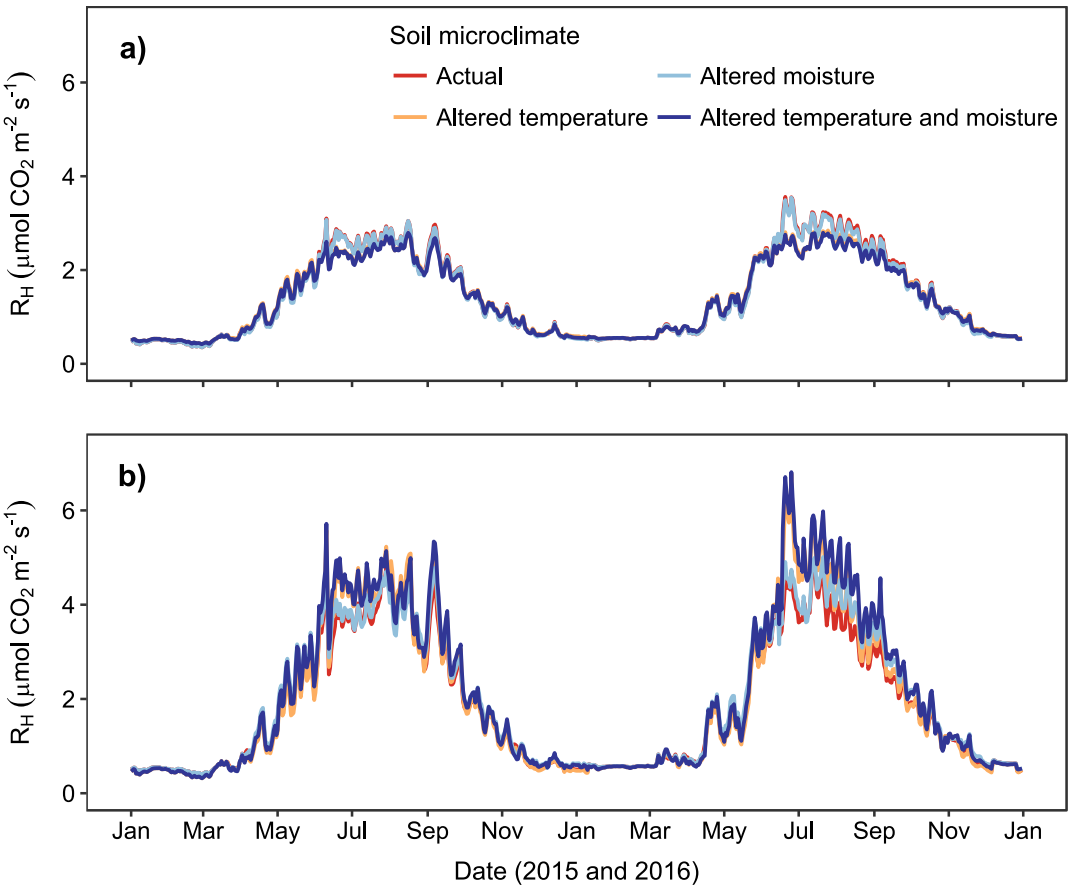

Figure 4.S.6 – Modelled heterotrophic soil respiration under four soil microclimate scenarios for maize (a) and switchgrass (b). The altered microclimate scenarios refer to the soil temperature and/or soil moisture regimes of the other cropping system.

Chapter 5

Soil texture and litter inputs control changes in soil organic carbon fractions under bioenergy cropping systems of the North Central U.S.

von Haden, A.C., Kucharik, C.J., Jackson, R.D., Marín-Spiotta, E.

Target journal: Soil Biology and Biochemistry

Abstract

Soil organic carbon (SOC) storage is a critical component of the overall sustainability of bioenergy cropping systems. Predicting the influence of cropping systems on SOC requires a mechanistic understanding of the underlying SOC formation processes. We used a density fractionation technique to isolate three SOC fractions that are thought to vary in SOC protection from decomposition. The free light fraction (FLF) is SOC that is not associated with aggregates or minerals, the occluded light fraction (OLF) is SOC released by the disruption of aggregates, and the heavy fraction (HF) is SOC recovered with minerals. We evaluated changes within each fraction in the 0 to 10 cm depth five years after biofuel cropping system establishment at two temperate sites with contrasting soil textures. The biofuel cropping systems included no-till maize, switchgrass, prairie, and hybrid poplar. The FLF C stock (g fraction C g bulk soil^{-1}) did not change significantly from baseline levels under any of the cropping systems at either site. Except for poplar, OLF C stocks were reduced in all systems from the site with coarse-textured soils and maintained at the site with fine-textured soils. In poplar systems, OLF C stocks were maintained on coarse-textured soils and increased on fine-textured soils. The HF C stocks also increased under poplar on the coarse-textured soil. A structural equation model indicated that changes in the OLF C stocks were a function of soil texture and litter C:N, whereas changes in

the HF C stocks were driven by litter quantity and litter C:N. Thus, increasing litter quantity and promoting plant species with low C:N litter may improve SOC storage in aggregate and mineral-associated soil fractions in bioenergy cropping systems.

5.1 Introduction

Bioenergy cropping systems are expected to play a significant role in meeting the future demand for sustainable energy (Robertson et al. 2017). In addition to providing a renewable energy feedstock, sustainable bioenergy cropping systems must also provide biogeochemical benefits including ecosystem carbon (C) storage (Robertson et al. 2011). Considering the large historical losses of soil organic carbon (SOC) induced by row crop agriculture (Sanderman et al. 2017), mitigating additional SOC losses and sequestering C in soils is a critical component of the biofuel sustainability equation (Robertston et al. 2008).

Compared to annual grain systems, perennial biofuel feedstocks are generally thought to enhance SOC sequestration, but the contrast between annual and perennial systems remains uncertain (Qin et al. 2016). Specific characteristics of the site, cropping system, and management practices may affect the rate or even direction of SOC change. For example, the proportion of stover harvested from maize bioenergy cropping systems affects the rate of SOC change (Anderson-Teixeira et al. 2009), with the potential for SOC losses under high stover removal or SOC gains under low stover removal (Qin et al. 2016). Differences in site-specific soil texture may influence the rate of SOC accrual through the effects of soil aggregation, with greater aggregate formation and stabilization occurring in finer-textured soils (Baer et al. 2010). Thus, broad generalizations regarding the efficacy of SOC storage of a particular bioenergy cropping system are difficult to make.

To predict the effects of a given cropping system across a wider range of management practices and soil types, a better mechanistic understanding of the underlying SOC processes is necessary. The soil density fraction scheme (Golchin et al. 1994) provides a theoretical framework of measurable SOC fractions that are related to plant and soil properties and processes (Fig. 5.1). In the model framework, plant inputs enter the SOC pool as the free-light fraction (FLF), which is primarily composed of identifiable plant material. Since the FLF is not physically protected, soil microbes may readily decompose it. Through the processes of comminution, aggregation, and microbial turnover, SOC becomes physically encapsulated within aggregates as the occluded light fraction (OLF) and thus is partially protected from decomposition (Oades 1988). Finally, the heavy fraction (HF) consists primarily of microbial-processed SOC, which is thought to be largely protected from decomposition through mineral soil-associations (Kögel-Knabner et al. 2008; Miltner et al. 2012).

Since each SOC fraction is theoretically distinct, the mechanisms controlling the dynamics of each fraction may also be unique. For example, the FLF fraction may decline when litter inputs are reduced (Lajtha et al. 2014) but does not change as a function of soil texture (Kölbl & Kögel-Knabner 2004). In contrast, the OLF fraction is dependent on texture, as fine-textured soils aggregate more readily than coarse-textured soils (Kölbl & Kögel-Knabner 2004; Baer et al. 2010). Due to the influence of soil texture on mineral surface area, HF C storage is also affected by texture (Hassink 1997; Six et al. 2002). Litter quantity and quality (e.g. C:N) may influence HF C storage through their effects on microbial biomass and carbon use efficiency (Cotrufo et al. 2013; Castellano et al. 2015). Thus, soil texture, litter quantity, and litter quality are expected to be key determinants of change for the SOC fractions, but a more comprehensive

understanding of how each fraction responds to all three factors is needed to better predict overall SOC change.

Our objective was to determine changes in SOC fractions following five years of bioenergy crop production to better understand the mechanisms controlling SOC storage. We hypothesized that soil texture (i.e. clay content), litter quantity, and litter quality (i.e. C:N) would have an overall influence on the SOC fractions. However, since the SOC fractions are proposed to be mechanistically distinct, we also expected that the changes among the fractions would not be controlled by the same factors.

5.2 Methods

5.2.1 Sites and cropping systems

We conducted this study at the Arlington Agricultural Research Station (ARL) in Wisconsin, USA (43.296° N, 89.380° W) and the Kellogg Biological Station (KBS) in Michigan, USA (42.395° N, 85.373° W). Mean annual temperature and precipitation, respectively, are 6.9 °C and 869 mm at ARL and 10.1 °C and 1005 mm at KBS (NOAA 2017). Soils at ARL are dominated by Plano silt loam, which are Fine-silty, mixed, superactive, mesic Typic Argiudolls (Soil Survey Staff 2017). KBS soils are Kalamazoo loams, classified as Fine-loamy, mixed, active, mesic Typic Hapludalfs (Soil Survey Staff 2017). Soil texture is strongly contrasted between sites, with ARL soils containing 9% sand and 25% clay and KBS soils containing 65% sand and 5% clay (Table 5.1).

The overall Biofuel Cropping Systems Experiment (BCSE) was established at each site in 2008. The BCSE is a randomized complete block design with five replicates with individual

plots measuring approximately 40 m x 30 m (Sanford et al. 2016). Prior to BCSE establishment in 2008, both sites had been in long-term agriculture. At ARL, three of the blocks had been in alfalfa for the three years prior to establishment and in maize-soy for the three years prior to that. The other two blocks at ARL had been in maize for the four years prior to the study and alfalfa for the two preceding years. All five KBS blocks had been in alfalfa for the six years prior to the study except for two blocks which had been planted to maize in 2006 only. Animal manure spreading was a typical management practice at ARL and KBS prior to the BCSE.

We focused on four bioenergy cropping systems in our study: Continuous no-till maize (*Zea mays* L.), switchgrass (*Panicum virgatum* L.), prairie, and hybrid poplar (*Populus nigra* × *P. maximowiczii* A. Henry 'NM6'). The prairie consisted of an 18 species mix of C4 grasses, C3 grasses, non-leguminous forbs, and leguminous forbs. A full agronomic description of these systems is given in Sanford et al. (2016). Maize and switchgrass systems annually received an average of 167 and 56 kg N ha^{-1}, respectively. Poplar received a single N application in 2010 at a rate of 210 and 155 kg N ha^{-1} at ARL and KBS, respectively. Prairie did not receive N fertilizer. Maize received P and K as needed, but perennials did not receive P or K. Maize grain plus about 50% of maize stover was harvested annually following the growing season (Sanford et al. 2016). Switchgrass and prairie were harvested annually except during the establishment phase, which occurred in 2008 at ARL and 2008 plus 2009 at KBS. At ARL, poplar growth was strongly impaired by *Marssonina* spp. leaf spot fungus beginning in 2010 and extending through 2013 (Sanford et al. 2016). Poplar was coppiced following the 2013 growing season at both sites, at which time standing woody biomass at KBS was more than double that of ARL (Sanford et al. 2016).

Aboveground net primary productivity (ANPP) was estimated at peak standing biomass in maize, switchgrass, and prairie using three quadrats per plot as described in Sanford et al. (2016). These systems were harvested annually at the plot level, and aboveground potential soil inputs (i.e., unharvested ANPP) were estimated as the difference between ANPP and harvest. For poplar, herbaceous understory ANPP (i.e., primarily weedy biomass) was measured identically to total ANPP in the other systems, but since the understory biomass was not harvested, all understory ANPP was considered a potential soil input. At KBS, poplar understory ANPP was not collected in 2010 and 2011, so the trend from 2009 to 2012 was linearly interpolated within each plot to estimate understory ANPP in 2010 and 2011. Leaf litterfall ANPP in poplar was measured in two 0.475 m^2 (KBS) or 0.375 m^2 (ARL) litter traps per plot. Belowground net primary productivity was estimated in the perennial cropping systems using six 5 cm diameter, 13 cm deep root ingrowth cores per plot per growing season (Sprunger et al. 2017). In maize, belowground biomass was excavated to approximately 50 cm deep following each growing season. We corrected the maize belowground biomass to a 13 cm depth based on observations at ARL that showed that approximately 60% of peak maize belowground biomass occurs within the surface 13 cm. Belowground biomass sampling (ingrowth and excavation) was largely incomplete in 2008, so the 2009 values were assumed to be representative of 2008. All biomass was oven dried and a subsample was used for combustion CN analysis. For belowground biomass (all systems), litterfall (poplar), and understory ANPP (poplar), biomass input C:N was equal to measured C:N. To account for plant N resorption during senescence, unharvested biomass C:N was equal to full plant C:N at harvest in switchgrass and prairie or C:N of harvested stover in maize (since nearly all grain was harvested). An overall C:N of biomass inputs was calculated as ratio of all carbon inputs to all nitrogen inputs.

5.2.2 Soil density fractionation

Baseline soil samples were collected in June and November 2008 at KBS and ARL, respectively. Five-year soil samples were taken in November and December 2013 at KBS and in November 2013 at ARL. The soil samples were taken from three locations in each plot which were stratified among the southern, center, and northern thirds of the plot. A 7.6 cm diameter hydraulic probe was used to take soil cores to 100 cm, and the cores were sectioned into 0-10, 10-25, 25-50, and 50-100 cm segments. Only the 0-10 cm section was used in this analysis. The soil was sieved to 4 mm at KBS and 2 mm at ARL and then dried. For consistency, all soils were re-sieved to 2 mm prior to density fractionation.

A density-based separation procedure (Fig. 5.2) was used to divide the bulk soil into three fractions (Golchin 1994; Swanston 2005; Marín-Spiotta et al. 2008). Fractionation was performed on two lab replicates per field sample. Oven-dry weight (65 °C) was determined on a subsample for each lab replicate. Approximately 20 g of soil was placed into a 250 mL centrifuge tube, and sodium polytungstate (NaPT) with a specific gravity of 1.6 g cm^{-3} was added (Cerli et al. 2012). The sample was gently rotated to ensure complete mixing and then placed in a centrifuge for 1 h at 3500 g_e (standard earth gravity). The floating FLF was aspirated and the remaining sample was stirred with a benchtop mixer at 1500 RPM for 1 min. The samples were then placed in an ice bath and sonicated using a QSonica Q500 sonicator (QSonica LLC., Newtown, CT, USA) with 475 J mL^{-1} (Schmidt et al. 1999). We verified the calibration of our sonicator following Schmidt et al. (1999) (Fig. 5.S.1). Following sonication, the samples were centrifuged for 1 h at 3500 g_e and then allowed to settle for at least 12 h prior to aspirating the floating OLF.

The FLF and OLF were rinsed over a 0.4 µm polycarbonate filter a minimum of five times with 200 mL each of ultra-high purity deionized water. The HF was rinsed five times by adding 200 mL of ultra-high purity water to the centrifuge tube, vigorously shaking the tube, centrifuging for 1 to 2 h at 3500 g_e, and aspirating the liquid from the HF pellet. All fractions were dried at 65 °C until weight was constant. The FLF and OLF were pulverized with stainless steel beads in a high-speed rocking shaker, and the HF was ground to a fine powder using a mortar and pestle. The HF was fumigated with 12 M HCl for 12 h to remove potential carbonates (Harris et al. 2001). Fractions were analyzed for CN on a Flash EA 1112 elemental analyzer (Thermo Electron Corp., Milan, Italy).

Percent mass recovery of fractions averaged 99.7% (Table 5.S.1), and there was no statistical difference in percent recovery between sites ($p = 0.92$) or among treatments ($p = 0.42$). Therefore, it was not necessary to make corrections for differences in fraction mass recovery.

We expressed the fraction C in two forms: the concentration of fraction C per unit of bulk soil (g C fraction g bulk soil^{-1}) and the relative contribution of each fraction to the total SOC among all three density fractions (g C fraction g C_{DF}^{-1}). We distinguish the SOC from the combined density fractions (C_{DF}) from total SOC because the density fractions do not contain the soluble SOC fraction (Crow 2007). For convenience, we refer to these as stocks (g C fraction g bulk soil^{-1}) and proportions (g C fraction g C_{DF}^{-1}).

5.2.3 Microbial biomass C

Soil samples for microbial biomass C (MBC) analysis were collected during the late growing season (mid-September) 2014 at ARL only. Samples from 0-10 cm were collected using

a 2 cm diameter probe from six locations per plot along a north-south transect. Samples from each plot were combined, homogenized, and stored at 4 °C until further processing could occur. Microbial biomass assays were performed on two lab replicates per sample following the direct chloroform extraction method (Gregorich et al. 1990). Extracted organic C was determined with the non-purgeable organic carbon method on a Shimadzu TOC-V CSH (Shimadzu Corp., Kyoto, Japan). The microbial extracted organic C was converted to MBC using an assumed extraction efficiency of 0.17 (Gregorich et al. 1990).

5.2.4 Statistical analyses

Soil fraction and MBC data were checked for equal variance among treatments using Levene's test. Datasets that failed Levene's test ($p < 0.05$) were natural log transformed to reduce heteroscedasticity prior to mixed-model variance analyses. Mixed models with block as a random effect and cropping system as a fixed effect were run in SAS 9.4 (SAS Institute Inc., Cary, NC, USA). Since we were interested in the changes of the soil fractions from baseline, we used contrasts to assess statistical differences from baseline for each treatment. Resulting *p*-values were adjusted for multiple comparisons using the step-down Bonferroni method. No baseline measurement was made for MBC, so treatment differences were directly assessed using least-squared mean differences with Bonferroni adjustments for multiple comparisons ($p < 0.05$).

We used a structural equation model (SEM) to test the hypothesis that changes in the SOC density fractions are related to percent clay (a proxy for mineral surface area), litter quantity (above- plus belowground), and litter C:N (a proxy for litter quality). Within the same SEM, we also tested whether changes among the fractions were interdependent. The SEM was

coded in the 'lavaan' package (Rosseel 2012) using R version 3.4.1 (R Core Team 2017), and model performance was assessed using the chi-square test ($p < 0.05$).

5.3 Results

5.3.1 Density fractions and MBC

The baseline (2008) FLF C stocks (g C fraction g bulk soil^{-1}) and OLF C stocks did not differ between sites ($p > 0.4$; Fig. 5.3a, b). However, the baseline HF C stocks were approximately twice as high at ARL compared to KBS ($p < 0.0001$). Thus, at ARL a greater proportion (g C fraction g C_{DF}^{-1}) of baseline C was stored in the HF ($p = 0.038$) and a smaller proportion of C was stored in the FLF ($p = 0.027$). On average 93% of baseline C was stored in the HF at ARL while only 86% was stored in the HF at KBS (Fig. 5.4a, b).

There were no significant changes in the FLF C or HF C stocks in any of the cropping systems at ARL (Fig. 5.3a). However, there was a two-fold increase in the OLF C stock in the ARL poplar cropping system ($p = 0.0047$). This change translated to a 117% increase in the OLF C proportion and a 5% decrease in the HF C proportion (Fig. 5.4a). The other three ARL cropping systems showed no significant change in OLF C stocks or proportions.

There were no significant changes in FLF C stocks at KBS (Fig. 5.3b). However, there were 62%-72% declines in OLF C stocks in all cropping systems ($p < 0.03$) except for poplar, and a 23% increase in HF C stocks in poplar ($p = 0.044$). Declines in the OLF C stocks resulted in 60-69% decreases in OLF C proportions ($p < 0.008$), but no significant changes in the FLF C or HF C proportions in any cropping systems (Fig. 5.4b).

Fraction C:N decreased in the order FLF > OLF > HF (Table 5.2). At ARL, the HF C:N increased significantly in all four systems ($p < 0.02$) from 2008 to 2013, with the maximum HF C:N change occurring in maize. At KBS, prairie FLF C:N increased from 18.3 to 23.0 ($p = 0.00025$) and OLF C:N increased from 15.7 to 19.7 ($p = 0.00072$). *Post hoc* t-tests revealed that when the data were pooled between sites and among cropping systems, the mean FLF C:N increased by 1.96 ($p < 0.0001$), the mean OLF C:N increased by 1.25 ($p < 0.0001$), and the mean HF C:N increased by 0.71 ($p < 0.00001$).

Soil microbial biomass carbon (MBC) at ARL ranged nearly three-fold among cropping systems (Fig. 5.5). Prairie MBC (588 mg C kg soil^{-1}) was greater than maize (214 mg C kg soil^{-1}), and switchgrass and poplar MBC were intermediate to prairie and maize.

5.3.2 Litter inputs

Unharvested aboveground biomass contributed the most to total biomass inputs in all systems except for poplar, where leaf litterfall was the most abundant input source (Table 5.3). At both sites, maize had the highest quantity of unharvested biomass, poplar had the least, and switchgrass and prairie had intermediate amounts. Belowground inputs were lowest in maize and poplar, intermediate in switchgrass, and greatest in prairie. However, at ARL poplar belowground inputs were 38% lower than maize, and poplar leaf litterfall was 70% lower at ARL than at KBS. At ARL, total cumulative biomass inputs were in the order maize > switchgrass > prairie > poplar, whereas at KBS the order was poplar > maize > prairie > switchgrass. Overall biomass input C:N varied at both sites in the order maize > switchgrass > prairie > poplar. The C:N of maize was more than double that of poplar at both sites.

5.3.3 SEM

Structural equation model fit was good, with χ^2 ($p = 0.69$). Overall, 64% of the change in OLF C stocks was explained by the model (Fig. 5.6). Clay content was positively related ($p < 0.001$) and litter C:N was negatively related to changes in the OLF C stock ($p < 0.001$). However, neither the change in FLF C stocks nor litter quantity were related to changes in the OLF C stocks. Litter quantity was positively related to HF stock changes ($p < 0.05$) and litter C:N was marginally negatively related to HF C stock changes ($p = 0.063$). Changes in the HF C stock were not related to FLF C changes, OLF C stock changes, or clay content. There was no effect of litter quantity or litter C:N on changes in FLF C stock.

5.4 Discussion

5.4.1 Soil texture and litter influence SOC fraction changes

Consistent with other studies that implicate clay as a key determinant of soil macroaggregation (Kölbl & Kögel-Knabner 2004), clay content was positively related to changes in the OLF C stocks in our study. However, soil texture was largely confounded between our two study sites, so other unaccounted factors, such as climate-driven differences in soil temperature and moisture, may be implicitly included within the clay variable in our model. In addition to the effect of clay, litter C:N was negatively correlated with the changes in OLF C stocks, indicating that litter with high N concentration enhanced the OLF C. One possible explanation is that the lower litter C:N ratio promoted greater microbial carbon use efficiency of the litter-derived FLF C, which increased microbial biomass (Manzoni et al. 2012) and subsequently increased total C

inputs into the OLF. Our microbial biomass findings provide some support for this explanation. In agreement, Jesus et al. (2016) found greater bacterial and fungal biomass in perennial systems compared to maize in soil samples collected from the same sites as our study.

The effects of litter quantity and litter C:N on HF C stocks may reflect dynamics of higher-order fractions, especially the FLF C. For example, if large quantities of low C:N litter enter the FLF C, they are likely to be efficiently converted into microbial biomass and decomposition byproducts (Cotrufo et al. 2013; Vogel et al. 2015), which then may enter the HF C stock directly (Cyle et al. 2016) or through the OLF C. Alternatively, if high C:N litter enters the FLF, then low microbial carbon use efficiency may reduce the amount of C available for other fractions. These dynamics might also be contingent upon the relative C saturation state of the HF (Castellano et al. 2015). That there was no relationship between clay content and HF C stock change does not imply that texture is not a key factor in determining HF C storage. On the contrary, the fine-textured soils in our study stored approximately twice as much C in the HF compared to the coarser textured soils. However, factors related to the litter inputs are apparently more important in determining short-term HF C stock changes in response to agricultural management.

Despite the reported sensitivity of FLF C stocks to land management practices (Wander & Yang 2000; Sequeira & Alley 2011), we did not detect any change in FLF C stocks across a two-fold range of litter inputs. In a 20-year litter manipulation study, Lajtha et al. (2014) reported no response of FLF C to doubled litter inputs, whereas decreased litter inputs caused declines in the FLF C. The authors attributed the consistency of FLF C under increased inputs to enhanced decomposition due to priming. We speculate that in systems with high litter inputs, the excessive litter entering the FLF C stock may have either been rapidly mineralized or transferred to another

SOC fraction. It is important to note that both sites in our study had been planted mainly to alfalfa, a perennial legume, for several years prior to the establishment of biofuel cropping systems. Thus, our baseline FLF C stocks were likely greater than what we would have expected if the previous land use was dominated by typical annual, tilled row crop agriculture (e.g. Jia et al. 2006), and thus the baseline FLF C stock may have been saturated.

That there were no significant relationships in C stock changes among the three SOC fractions indicates that the fractions can change independently. Thus, while the SOC fractions cannot be considered completely homogenous (Wagai et al. 2009; Schrumpf & Kaiser 2015), our results support the use of these fractions as measurable constructs for SOC modelling (Sohi et al. 2005). Our approach was simplistic in that it did not account for the spatial and temporal dynamics of litter inputs. For example, our SEM model contained only one compartment of litter inputs, but differences in the partitioning of above- and belowground litter may affect SOC fractions (Austin et al. 2017; Ghafoor et al. 2017). Ignoring this complexity was necessary to fit our model, but it should be noted that some of the unexplained variability may be attributed to differences in the spatial and temporal dynamics of litter inputs.

5.4.2 Short-term C:N trends were evident in all fractions

All fractions trended toward higher C:N, but changes in fraction-specific C:N were greatest in the FLF, intermediate in the OLF, and smallest in the HF. Considering that the fraction C turnover time tends to decrease in the order HF > OLF > FLF (Schrumpf & Kaiser 2015), our finding likely reflects the longer turnover and subsequent lower incorporation of new C inputs into lower order fractions. Given that the HF is often considered a stable SOC pool, with typical mean residence times on the order of hundreds of years (Crow et al. 2007; Schrumpf

& Kaiser 2015), it is somewhat surprising that changes in the HF C:N ratio were apparent after only five years. This could have resulted either from microbial mining of the HF N or from the replacement of older, low C:N stocks with newer, high C:N material. Irrespective of the mechanism, the rapid changes in HF C:N support the idea that a portion of the mineral-associated C turns over on yearly timescales (Torn et al. 2013) and thus is sensitive to land management practices (Grandy & Robertson 2007).

The low baseline C:N among the fractions was likely a result of the low C:N alfalfa biomass and manure inputs that had occurred for several years before the biofuel crops were established. For example, aboveground alfalfa biomass grown in 2016 at ARL had a C:N ratio of 15:1 (unpublished data). While the four biofuel cropping systems varied widely in the C:N of biomass inputs, in all systems the biomass input C:N was much greater than 15:1. Fornara et al. (2011) found a positive correlation between plant C:N and FLF C:N in temperate grasslands, suggesting a link between litter input C:N and soil fraction C:N. Thus, the trends toward higher fraction C:N in our study at least partially reflect the increased C:N of litter inputs.

5.4.3 Implications for bioenergy production

Our results provided strong evidence that soil texture and litter input dynamics differentially affected the SOC fractions, and thus specific land management decisions will influence SOC storage potential differently in contrasting settings. Soil texture is a critical part of the equation for SOC stabilization in bioenergy cropping systems (Tiemann & Grandy 2015). At least in the short-term, SOC protection in aggregates appears to be much more favorable in fine-textured soils than coarse-textured soils. However, the fact that our sites with contrasting soil texture had similar OLF C stocks prior to the study indicates that the coarse-textured soils may

continue to accrue OLF C and thus eventually reach levels similar to the fine-textured soil. Considering that bioenergy cropping systems likely will be targeted to marginally productive lands (Robertson et al. 2017), such as those with coarse-textured soils, future work will be necessary to evaluate this hypothesis.

The choice of biofuel cropping system will also affect short-term SOC protection. Maize, switchgrass, and prairie systems all had similar effects on SOC fractions, but poplar increased aggregate protected OLF C on the fine-textured soil and increased mineral associated HF C on the coarse-textured soil. Other studies at these sites have also demonstrated divergent SOC properties in poplar compared to the other systems (Sprunger & Robertson 2017; Szymanski et al. 2017). Our results indicated that the contrasting responses of poplar SOC fractions resulted from the large quantity of low C:N poplar litter inputs. Thus, increasing the quantity of litter inputs by harvesting less biomass in the non-poplar systems may increase the C in protected SOC fractions. However, litter chemistry also appears to be an important aspect of SOC protection. Planting N-rich leguminous cover crops in maize, adding legumes to the switchgrass system (e.g. Jakubowski et al. 2017), and increasing the proportion of legumes in the prairie system may increase microbial carbon use efficiency and thereby enhance C in the protected fractions. However, since legumes are generally lower-productivity, increasing the proportion of legumes in higher-productivity grass-based systems may come at the cost of lower litter inputs (e.g. Lange et al. 2015). Thus, the balance between litter inputs and litter C:N is an important consideration for SOC storage.

While we did not specifically address the effect of tillage, we found that no-till maize, switchgrass, and prairie all had similar SOC fraction responses within each site. Several studies have reported increases of FLF and OLF in no-till verses tilled annual systems (Wander & Yang

2000; Sequeira et al. 2011) and increases in the particulate organic fraction in untilled perennial systems relative to tilled annual systems (Dou et al. 2013; Kantola et al. 2017), but comparisons between no-till annual and perennial systems are scarce. Our results indicated that the no-till practice in maize was as effective as the switchgrass and prairie systems in terms of storing C in the OLF and HF at both sites. However, it is not known whether this trend would continue over longer time periods, and thus longer-term studies are necessary.

The SOC legacy of the previous cropping system is also an important consideration. Our findings may have differed if typical row crops, rather than alfalfa, were planted prior to our study. For example, if the FLF C and OLF C stocks were smaller at the beginning of the experiment, as may have been expected in a tilled annual system, then we may have observed overall increases in those fractions (e.g. Dou et al. 2013). This implies that the SOC fraction responses to cropping systems observed in our study may not be directly applicable to other locations, and reiterates that the capacity of soils to accumulate SOC is largely dependent on previous land use history (Qin et al. 2016). Experiments with varied SOC fraction baselines will be required to better understand the mechanisms of how the soil legacy affects the trajectory of SOC fractions.

5.5 Conclusions

Five years after the establishment of bioenergy cropping systems, we found the most prominent SOC changes within the aggregate-protected OLF C fraction. The response of the OLF C stocks was predominantly a function of soil type, with OLF C losses occurring on coarse-texture soils under most cropping systems. The poplar system stood out among the other cropping systems for its capacity to maintain or build OLF C stocks. The effect of cropping

system on the OLF C was driven by the apparent quality of litter inputs, with lower C:N litter promoting higher OLF C stocks. Increased HF C stocks were also detected under poplar at the site with coarse-textured soils and was attributable to high litter quantity and low litter C:N. No-till maize, switchgrass, and prairie all had similar influences on SOC fractions, with OLF C losses on coarse-textured soils and no change in OLF C stocks on fine-textured soils. All three fractions trended toward higher C:N, indicating short-term sensitivity to land-use change. Increasing the quantity and quality (e.g. lower C:N) of litter inputs may enhance the amount of SOC stored in protected fractions, but achieving these two goals concurrently in annually harvested, grass-based perennial systems will be practically challenging.

5.6 Acknowledgements

Funding was provided by the Great Lakes Bioenergy Research Center (DOE BER Office of Science DE-FC02-07ER64494 and DOE OBP Office of Energy Efficiency and Renewable Energy DE-AC05-76RL01830), the USDA National Institute of Food and Agriculture (Hatch project 0225417-WIS01586), and the National Science Foundation (grant DEB-1038759). L.G. Oates and G. Sanford provided technical support. Thanks to L. Szymanski and E. Atkinson for demonstrating the density fractionation method and to C. Cavadini, B. Dvorak, C. Rebman, and C. King for lab assistance. Additional thanks to the many individuals involved with the collection and processing of plant and soils samples, and to S. Bohm and S. VanderWulp for help with the leaf litter data.

5.7 References

Anderson-Teixeira, K. J., Davis, S. C., Masters, M. D., Delucia, E. H. 2009. Changes in soil organic carbon under biofuel crops. Global Change Biology Bioenergy 1:75–96.

Austin, E. E., Wickings, K., McDaniel, M. D., Robertson, G. P., Grandy, A. S. 2017. Cover crop root contributions to soil carbon in a no-till corn bioenergy cropping system. Global Change Biology Bioenergy 9:1252–1263.

Baer, S. G., Meyer, C. K., Bach, E. M., Klopf, R. P., Six, J. 2010. Contrasting ecosystem recovery on two soil textures: implications for carbon mitigation and grassland conservation. Ecosphere 1:art5.

Castellano, M. J., Mueller, K. E., Olk, D. C., Sawyer, J. E., Six, J. 2015. Integrating plant litter quality, soil organic matter stabilization, and the carbon saturation concept. Global Change Biology 21:3200–3209.

Cerli, C., Celi, L., Kalbitz, K., Guggenberger, G., Kaiser, K. 2012. Separation of light and heavy organic matter fractions in soil - Testing for proper density cut-off and dispersion level. Geoderma 170:403–416.

Cotrufo, M. F., Wallenstein, M. D., Boot, C. M., Denef, K., Paul, E. 2013. The Microbial Efficiency-Matrix Stabilization (MEMS) framework integrates plant litter decomposition with soil organic matter stabilization: do labile plant inputs form stable soil organic matter? Global Change Biology 19:988–995.

Crow, S. E., Swanston, C. W., Lajtha, K., Brooks, J. R., Keirstead, H. 2007. Density fractionation of forest soils: methodological questions and interpretation of incubation results and turnover time in an ecosystem context. Biogeochemistry 85:69–90.

Dou, F. G., Hons, F. M., Ocumpaugh, W. R., Read, J. C., Hussey, M. A., Muir, J. P. 2013. Soil organic carbon pools under switchgrass grown as a bioenergy crop compared to other conventional crops. Pedosphere 23:409–416.

Ghafoor, A., Poeplau, C., Kätterer, T. 2017. Fate of straw- and root-derived carbon in a Swedish agricultural soil. Biology and Fertility of Soils 53:257.

Golchin, A., Oades, J. M., Skjemstad, J. O., Clarke, P. 1994. Study of free and occluded particulate organic matter in soils by solid state 13C Cp/MAS NMR spectroscopy and scanning electron microscopy. Australian Journal of Soil Research 32:285–309.

Grandy, A. S., Robertson, G. P. 2007. Land-use intensity effects on soil organic carbon accumulation rates and mechanisms. Ecosystems 10:58–73.

Gregorich, E. G., Wen, G., Voroney, R. P., Kachanoski, R. G. 1990. Calibration of a rapid direct chloroform extraction method for measuring soil microbial biomass C. Soil Biology and Biochemistry 22:1009–1011.

Harris, D., Horwath, W. R., van Kessel, C. 2001. Acid fumigation of soils to remove carbonates prior to total organic carbon or carbon-13 isotopic analysis. Soil Science Society of America Journal 65:1853–1856.

Hassink, J. 1997. The capacity of soils to preserve organic C and N by their association with clay and silt particles. Plant and Soil 191:77–87.

Jesus, E. d. C., Liang, C., Quensen, J. F., Susilawati, E., Jackson, R. D., Balser, T. C., Tiedje, J. M. 2016. Influence of corn, switchgrass, and prairie cropping systems on soil microbial communities in the upper Midwest of the United States. Global Change Biology Bioenergy 8: 481–494.

Jia, Y., Li, F.-M., Wang, X.-L., Xu, J.-Z. 2006. Dynamics of soil organic carbon and soil fertility affected by alfalfa productivity in a semiarid agro-ecosystem. Biogeochemistry 80:233–243.

Kantola, I. B., Masters, M. D., DeLucia, E. H. 2017. Soil particulate organic matter increases under perennial bioenergy crop agriculture. Soil Biology and Biochemistry 113:184–191.

Kögel-Knabner, I., Guggenberger, G., Kleber, M., Kandeler, E., Kalbitz, K., Scheu, S., Eusterhues, K., Leinweber, P. 2008. Organo-mineral associations in temperate soils: Integrating biology, mineralogy, and organic matter chemistry. Journal of Plant Nutrition and Soil Science 171:61–82.

Kölbl, A., Kögel-Knabner, I. 2004. Content and composition of free and occluded particulate organic matter in a differently textured arable Cambisol as revealed by solid-state (13)C NMR spectroscopy. Journal of Plant Nutrition and Soil Science 167:45–53.

Lajtha, K., Bowden, R. D., Nadelhoffer, K. 2014. Litter and root manipulations provide insights into soil organic matter dynamics and stability. Soil Science Society of America Journal 78:S261-S269.

Lange, M., Eisenhauer, N., Sierra, C. A., Bessler, H., Engels, C., Griffiths, R. I., Mellado-Vázquez, P. G., Malik, A. A., Roy, J. et al. 2015. Plant diversity increases soil microbial activity and soil carbon storage. Nature Communications 6:6707.

Manzoni, S., Taylor, P., Richter, A., Porporato, A., Agren, G. I. 2012. Environmental and stoichiometric controls on microbial carbon-use efficiency in soils. New Phytologist 196:79–91.

Marín-Spiotta, E., Swanston, C. W., Torn, M. S., Silver, W. L., Burton, S. D. 2008. Chemical and mineral control of soil carbon turnover in abandoned tropical pastures. Geoderma 143:49–62.

Miltner, A., Bombach, P., Schmidt-Brücken, B., Kästner, M. 2012. SOM genesis: microbial biomass as a significant source. Biogeochemistry 111:41–55.

National Oceanic and Atmospheric Administration (NOAA). 2017. National Centers for Environmental Information: Climate Data Online. www.ncdc.noaa.gov.

Oades, J. M. 1988. The retention of organic matter in soils. Biogeochemistry 5:35–70.

Qin, Z., Dunn, J. B., Kwon, H., Mueller, S., Wander, M. M. 2016. Soil carbon sequestration and land use change associated with biofuel production: empirical evidence. Global Change Biology Bioenergy 8:66–80.

R Core Team 2017. R: A language and environment for statistical computing.

Robertson, G. P., Dale, V. H., Doering, O. C., Hamburg, S. P., Melillo, J. M., Wander, M. M., Parton, W. J., Adler, P. R., Barney, J. N. et al. 2008. Sustainable biofuels redux. Science 322:49–50.

Robertson, G. P., Hamilton, S. K., Barham, B. L., Dale, B. E., Izaurralde, R. C., Jackson, R. D., Landis, D. A., Swinton, S. M., Thelen, K. D., Tiedje, J. M. 2017. Cellulosic biofuel contributions to a sustainable energy future: Choices and outcomes. Science 356:eaal2324.

Robertson, G. P., Hamilton, S. K., Del Grosso, S. J., Parton, W. J. 2011. The biogeochemistry of bioenergy landscapes: carbon, nitrogen, and water considerations. Ecological Applications 21:1055–1067.

Rosseel, Y. 2012. lavaan: an R package for structural equation modeling. Journal of Statistical Software 48:36.

Sanderman, J., Hengl, T., Fiske, G. J. 2017. Soil carbon debt of 12,000 years of human land use. Proceedings of the National Academy of Sciences 114:9575–9580.

Sanford, G. R., Oates, L. G., Jasrotia, P., Thelen, K. D., Robertson, G. P., Jackson, R. D. 2016. Comparative productivity of alternative cellulosic bioenergy cropping systems in the North Central USA. Agriculture, Ecosystems & Environment 216:344–355.

Schmidt, M. W. I., Rumpel, C., Kogel-Knabner, I. 1999. Evaluation of an ultrasonic dispersion procedure to isolate primary organomineral complexes from soils. European Journal of Soil Science 50:87–94.

Schrumpf, M., Kaiser, K. 2015. Large differences in estimates of soil organic carbon turnover in density fractions by using single and repeated radiocarbon inventories. Geoderma 239–240:168–178.

Sequeira, C. H., Alley, M. M. 2011. Soil organic matter fractions as indices of soil quality changes. Soil Science Society of America Journal 75:1766–1773.

Sequeira, C. H., Alley, M. M., Jones, B. P. 2011. Evaluation of potentially labile soil organic carbon and nitrogen fractionation procedures. Soil Biology and Biochemistry 43:438–444.

Six, J., Conant, R. T., Paul, E. A., Paustian, K. 2002. Stabilization mechanisms of soil organic matter: Implications for C-saturation of soils. Plant and Soil 241:155–176.

Sohi, S. P., Mahieu, N., Arah, J. R. M., Powlson, D. S., Madari, B., Gaunt, J. L. 2001. A procedure for isolating soil organic matter fractions suitable for modeling. Soil Science Society of America Journal 65:1121–1128.

Soil Survey Staff. 2017. Natural Resources Conservation Service, U.S. Department of Agriculture. Official Soil Series Descriptions. www.nrcs.usda.gov.

Sprunger, C. D., Oates, L. G., Jackson, R. D., Robertson, G. P. 2017. Plant community composition influences fine root production and biomass allocation in perennial bioenergy cropping systems of the upper Midwest, USA. Biomass and Bioenergy 105:248–258.

Sprunger, C. D., Robertson, G. P. 2017. Changes in active and slow soil carbon pools under perennial bioenergy crops in contrasting soils. Submitted.

Swanston, C. W., Torn, M. S., Hanson, P. J., Southon, J. R., Garten, C. T., Hanlon, E. M., Ganio, L. 2005. Initial characterization of processes of soil carbon stabilization using forest stand-level radiocarbon enrichment. Geoderma 128:52–62.

Szymanski, L. M., Sanford, G. R., Heckman, K., Jackson, R. D., and Marín-Spiotta, E. 2017. Losses from the active carbon pool and respiration of older carbon after five years of bioenergy biomass cropping. Submitted.

Tiemann, L. K., Grandy, A. S. 2015. Mechanisms of soil carbon accrual and storage in bioenergy cropping systems. Global Change Biology Bioenergy 7:161–174.

Torn, M. S., Kleber, M., Zavaleta, E. S., Zhu, B., Field, C. B., Trumbore, S. E. 2013. A dual isotope approach to isolate soil carbon pools of different turnover times. Biogeosciences 10:8067–8081.

Vogel, C., Heister, K., Buegger, F., Tanuwidjaja, I., Haug, S., Schloter, M., Kögel-Knabner, I. 2015. Clay mineral composition modifies decomposition and sequestration of organic carbon and nitrogen in fine soil fractions. Biology and Fertility of Soils 51:427–442.

Wagai, R., Mayer, L. M., Kitayama, K. 2009. Nature of the "occluded" low-density fraction in soil organic matter studies: A critical review. Soil Science and Plant Nutrition 55:13–25.

Wander, M. M., Yang, X. 2000. Influence of tillage on the dynamics of loose- and occluded-particulate and humified organic matter fractions. Soil Biology and Biochemistry 32:1151–1160.

5.8 Tables and figures

Table 5.1 – Mean (standard error) soil particle size distribution, total carbon (TC), and total nitrogen (TN) for the 0-10 cm depth at Arlington, WI (ARL) and Kellogg Biological Station, MI (KBS).

	Sand (%)	Silt (%)	Clay (%)	TC (%)	TN (%)
ARL	9 (0.98)	66 (0.92)	25 (0.59)	2.37 (0.07)	0.23 (0.009)
KBS	65 (0.61)	30 (0.31)	5 (0.32)	1.47 (0.02)	0.14 (0.004)

Table 5.2 – Mean and standard error soil fraction C:N among cropping systems with baseline (2008) values at Arlington, WI (ARL) and Kellogg Biological Station, MI (KBS). Asterisks indicate statistically significant difference ($p < 0.05$ after adjustment for multiple comparisons) from the baseline value after five years of cropping system establishment.

Site	Treatment	FLF C:N	OLF C:N	HF C:N
ARL	Baseline	19.6 (0.79)	16.6 (0.51)	10.8 (0.19)
	Maize	21.2 (1.00)	17.3 (0.18)	12.0 (0.36) *
	Switchgrass	22.3 (1.19)	16.3 (0.34)	11.6 (0.28) *
	Prairie	21.2 (1.98)	17.3 (0.37)	11.6 (0.27) *
	Poplar	20.7 (0.86)	15.7 (0.36)	11.7 (0.30) *
KBS	Baseline	18.3 (0.48)	15.7 (0.69)	12.6 (0.20)
	Maize	19.8 (0.52)	17.6 (0.59)	13.4 (0.68)
	Switchgrass	20.1 (0.46)	17.6 (0.73)	12.9 (0.16)
	Prairie	23.0 (0.94) *	19.7 (0.50) *	12.8 (0.19)
	Poplar	19.1 (0.52)	17.5 (0.36)	12.8 (0.29)

Table 5.3 – Cumulative biomass inputs from 2008 to 2013 and C:N (mass-weighted by each group of biomass inputs) for all cropping systems at Arlington, WI (ARL) and Kellogg Biological Station, MI (KBS). For maize, switchgrass, and prairie, unharvested biomass is the difference between ANPP and yield, but in poplar it is the total herbaceous understory ANPP. Means are shown with standard errors in parentheses.

Site	Treatment	Belowground ($g\ m^{-2}$)	Unharvested ($g\ m^{-2}$)	Leaf litter ($g\ m^{-2}$)	Total ($g\ m^{-2}$)	Total C:N
ARL	Maize	607 (17)	4061 (334)		4667 (342)	61 (1.0)
	Switchgrass	776 (51)	3345 (162)		4121 (136)	57 (1.9)
	Prairie	1027 (83)	2484 (203)		3511 (233)	48 (1.8)
	Poplar	375 (27)	1264 (262)	1462 (138)	3101 (124)	23 (1.1)
KBS	Maize	736 (26)	5120 (286)		5856 (287)	66 (1.9)
	Switchgrass	1007 (138)	2066 (110)		3073 (154)	49 (1.3)
	Prairie	1488 (223)	3095 (202)		4583 (324)	48 (1.9)
	Poplar	742 (47)	1379 (107)	4610 (400)	6731 (392)	29 (0.9)

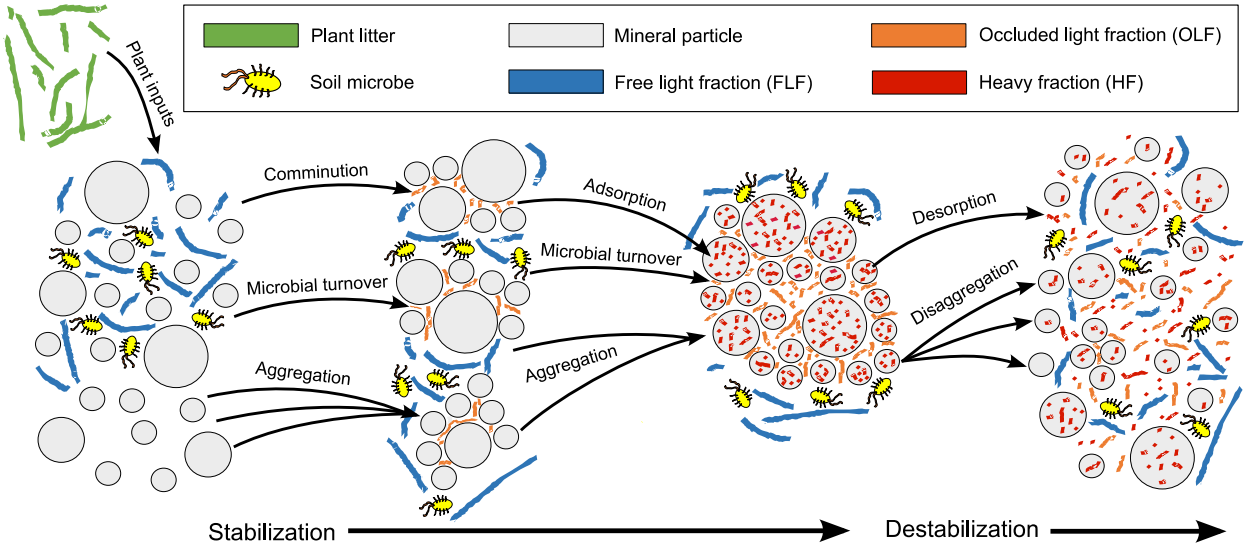

Figure 5.1 – A conceptual diagram illustrating the proposed mechanisms of soil organic carbon (SOC) protection during soil aggregate stabilization and destabilization in relation to soil fractions isolated from a density fractionation approach.

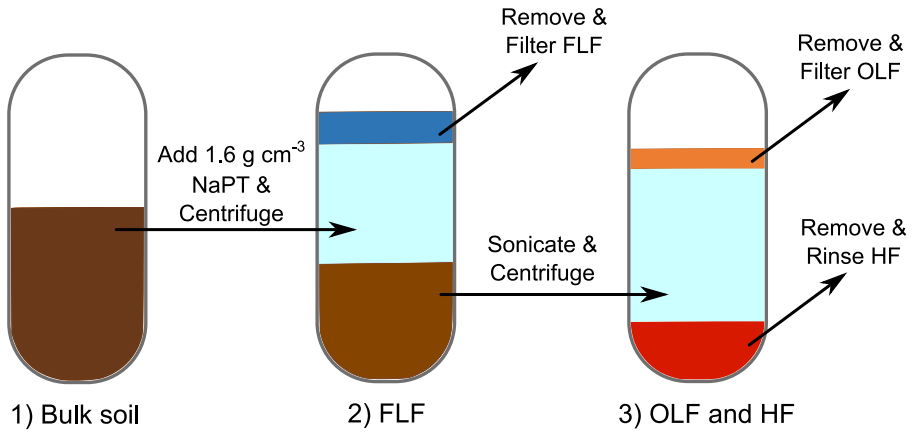

Figure 5.2 – A schematic overview of the soil density fraction method used in this study.

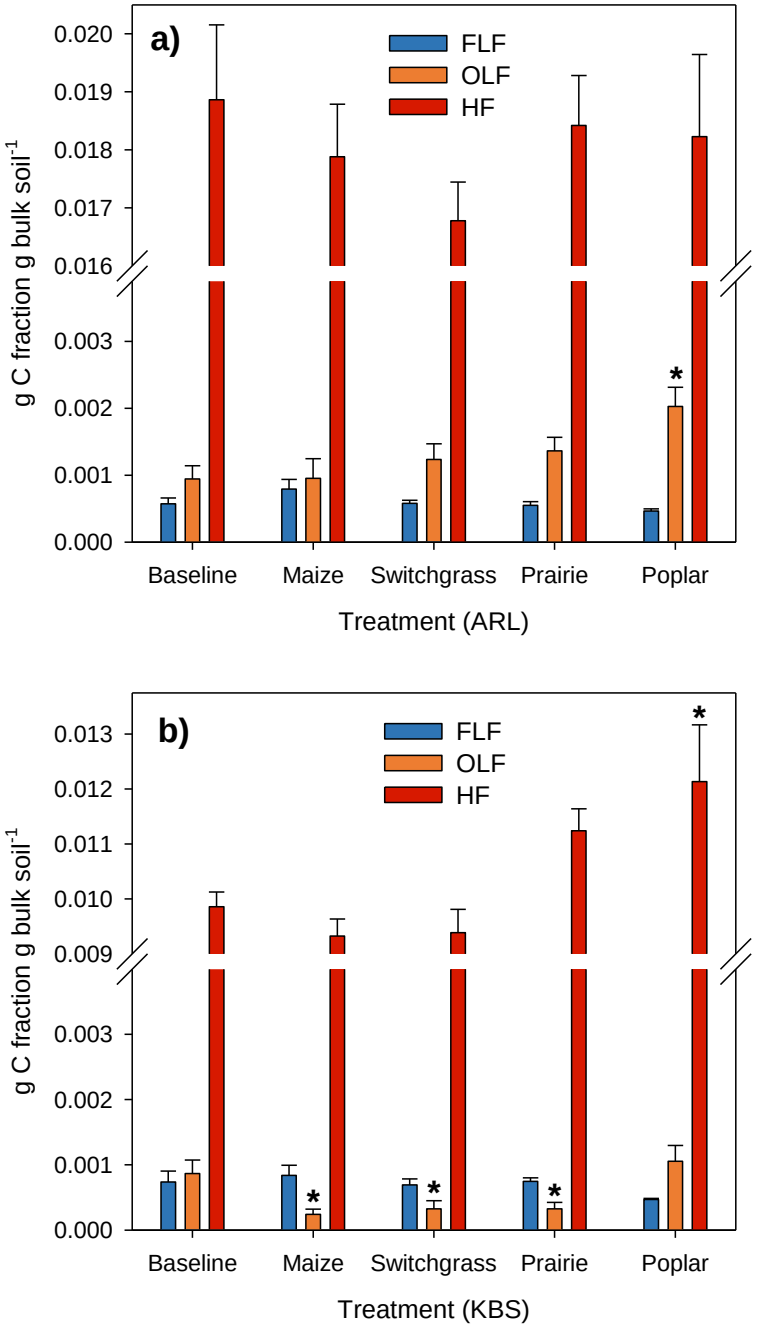

Figure 5.3 – Fraction C per unit bulk soil at (a) Arlington (ARL) and (b) Kellogg Biological Station (KBS). Asterisks indicate significant changes from baseline samples ($p < 0.05$ after multiple comparison correction), and error bars are standard errors. Note that the y-axis scales differ between panels and that both y-axes contain breaks.

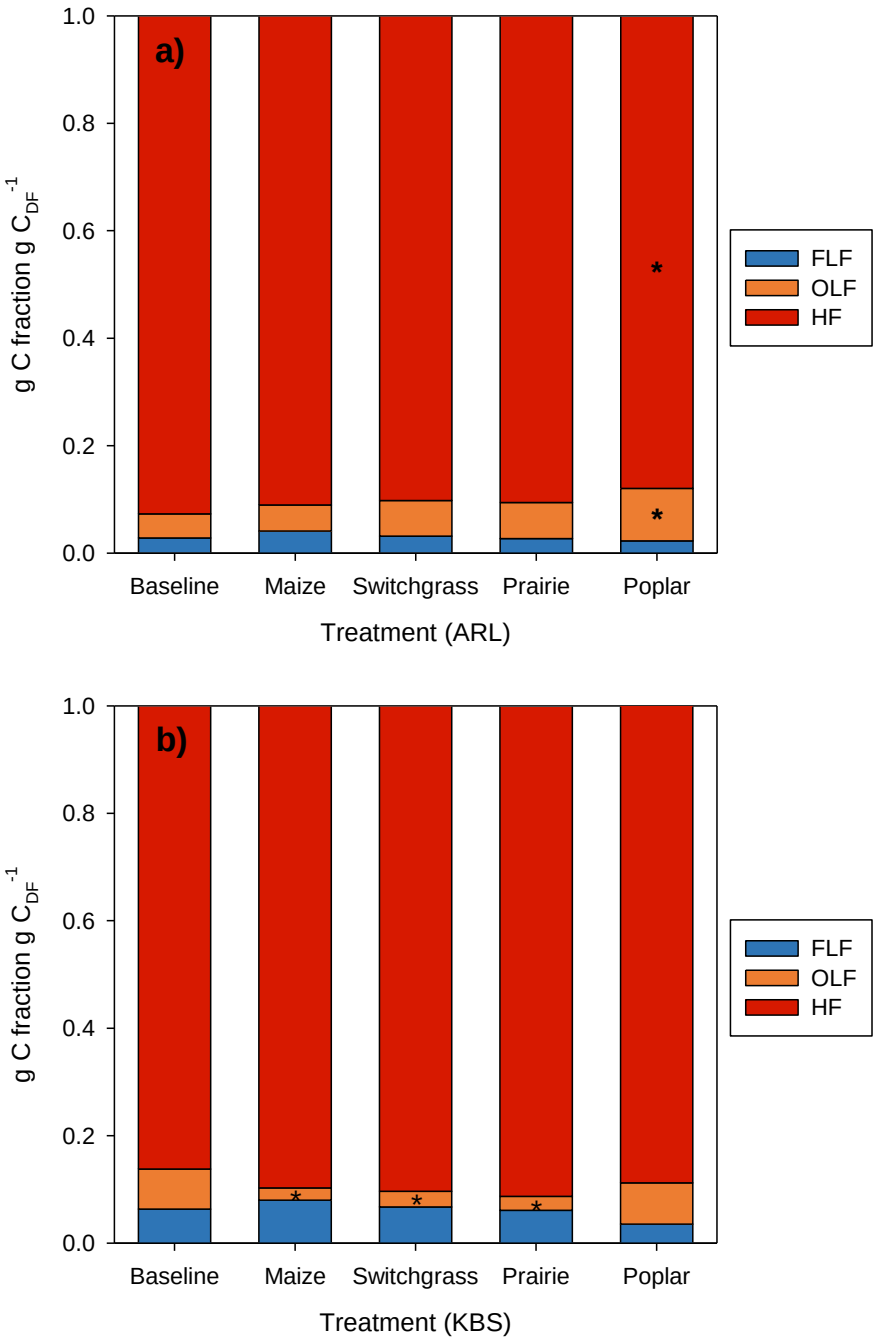

Figure 5.4 – Fraction C relative to the total C among all fractions (C_{DF}) at (a) Arlington (ARL) and (b) Kellogg Biological Station (KBS). Asterisks identify significant changes from baseline samples ($p < 0.05$ with correction for multiple comparisons).

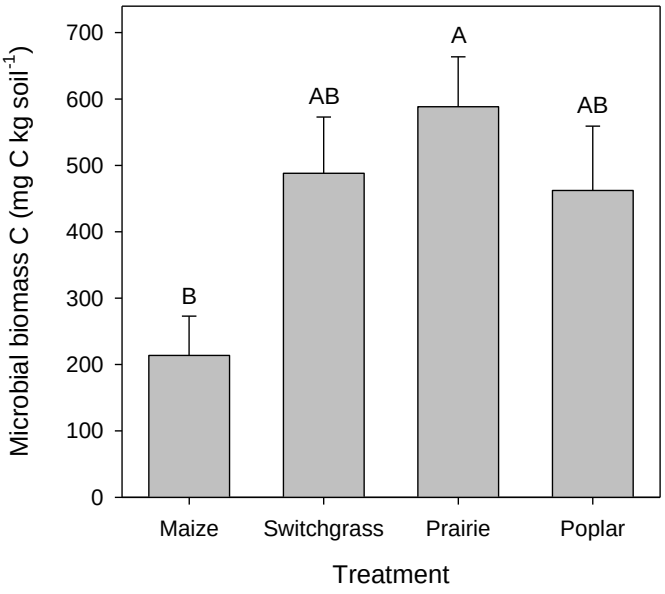

Figure 5.5 – Mean (with standard error) microbial biomass C (MBC) at Arlington, WI during late-summer 2014. Treatments with different letters are statistically different ($p < 0.05$).

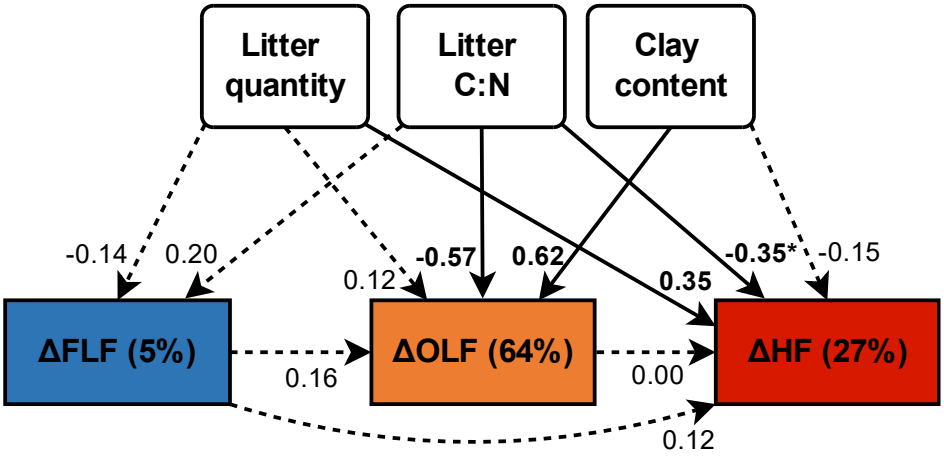

Figure 5.6 – Fitted structural equation model showing potential relationships between exogenous variables and fraction C stock changes (g C fraction g bulk soil^{-1}). Solid lines indicate statistically significant relationships ($p < 0.05$) except for the relationship denoted by the asterisk which indicates marginal significance ($p = 0.063$). Percentages indicate the R^2 values for endogenous variables, and the values along each path are the completely standardized coefficients.

5.9 Supplemental tables and figures

Table 5.S.1 – Total mass recovery of soil fractions expressed as a percent of the initial soil weight. Means are given with standard errors in parentheses. Sites are Arlington, WI, USA (ARL) and Kellogg Biological Station, MI, USA (KBS).

Site	Treatment	Recovery (%)
ARL	Baseline	99.98 (0.049)
	Maize	99.73 (0.257)
	Switchgrass	99.72 (0.178)
	Prairie	99.58 (0.099)
	Poplar	99.60 (0.109)
KBS	Baseline	99.71 (0.044)
	Maize	99.67 (0.024)
	Switchgrass	99.65 (0.019)
	Prairie	99.84 (0.119)
	Poplar	99.70 (0.079)

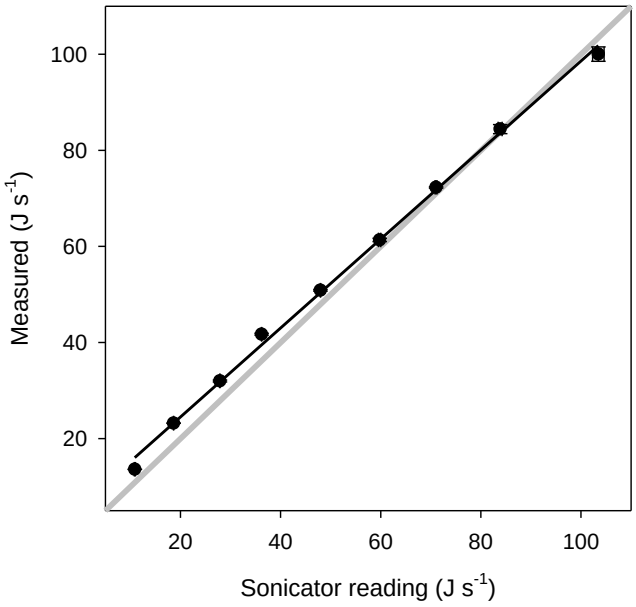

Figure 5.S.1 – Comparison of power output as indicated by the sonicator versus directly measured with a calorimetric method (Schmidt et al. 1999). The black circles are the means with standard errors for both variables (most errors are smaller than the symbols). The black line shows the linear regression between variables, and gray line is 1:1.

Chapter 6

Implementation of the root regression approach for partitioning soil respiration: theoretical and methodological considerations

von Haden, A.C., Kucharik, C.J.

Target journal: Biogeochemistry

Abstract

The root regression method, which uses the relationship between root biomass and soil respiration to separate autotropic- and heterotrophic-derived sources, has been described as a low-disturbance, *in situ* technique. However, the underlying assumptions, limitations, and methodological considerations have not been thoroughly discussed. Assumptions include consistent heterotrophic soil respiration among all measurement points, consistent autotrophic respiration per unit root biomass, and negligible lateral soil CO_2 diffusion. While these assumptions are not likely to hold under all circumstances, some limitations can be addressed with additional measurements. We used a literature survey and a field study to provide further insight. In the literature survey, we found that 71% of 256 previously published root regressions were reported as statistically significant. In the field study, we observed that the efficacy of the root regression method varied between plant types and by time of day, with stronger linear regressions corresponding to high specific root respiration rates. Increasing the number of sampling points and depth of root sampling also improved linear regression strength, but such methodological details likely will depend upon specific ecosystem type and sampling time. Thus, researchers would benefit from performing pilot studies to determine the appropriate methodological details such as the number of samples required for their study system.

6.1 Introduction

Total soil CO_2 respiration (R_S) is comprised of two primary components: autotrophic-derived respiration (R_A) from plant roots and heterotrophic-derived respiration (R_H) from the decomposition of soil organic carbon (SOC) (Kuzyakov 2006). Since the two components typically occur simultaneously, partitioning R_S is necessary to study the *in situ* dynamics of R_A and R_H independently. Thus, reliable separation of R_A and R_H is important for plant, soil, and ecosystem sciences (Baggs 2006).

The most common partitioning methods include root exclusion (i.e. trenching), tree girdling, component integration, and isotopic techniques, but each method is subject to inherent limitations (Kuzyakov 2006; Subke et al. 2006). The root regression technique is less commonly used, but it has been suggested that the method has high potential because it produces relatively little disturbance (prior to root biomass sampling) and therefore minimizes bias (Kuzyakov 2006; Koerber et al. 2010). However, the underlying assumptions, potential limitations, and practical considerations of the technique have not been thoroughly articulated and discussed. Thus, our goal was to provide theoretical framework and methodological considerations for the root regression approach.

6.1.1 Theoretical framework and underlying assumptions

The root regression method operates on the principle that R_A is proportional to live root biomass (Fig. 6.1a). A number of paired R_S and root biomass samples are used to generate a linear regression model between root biomass and R_S (Fig. 6.1b). The linear regression of R_S

against root biomass yields a slope equal to the specific R_A (i.e. R_A per unit root; SR_A). Non-linear (exponential) regressions have also been used (Bao et al. 2010), but the biological basis of such a model remains unelucidated. In both cases, the y-intercept of the regression is the estimate of R_S when root biomass is nil and therefore R_S is equal to R_H. Mean R_A ($\overline{R_A}$) is estimated as mean R_S ($\overline{R_S}$) minus R_H (Fig. 6.1a).

Implicit in the linear root regression model is that contribution of R_H is consistent across all measurements of R_S (Fig. 6.1a), yet there are several reasons that this assumption may not always hold. First, differences in SOC among sampling points may drive differences in R_H (Herbst et al. 2012). In addition, heterogeneity in plant canopy structure or microtopography may cause variability in soil microclimate among sampling points (Chapin 2003; Bennie et al. 2008), which could also affect R_H. Finally, the differences in root biomass among sampling points could drive differences in rhizodeposition, which could also alter R_H through the "priming effect" (Kuzyakov 2010). Differences in SOC content or soil microclimate can potentially be addressed by measuring these variables at each R_S sampling point and including the terms in the regression model. For example, Rodeghiero, and Cescatti (2006) added an SOC term to their root regression models. The "priming effect" of root biomass on R_H would be more difficult to address, and would likely require a separate intensive study (Kuzyakov et al. 2000).

Another primary assumption of the root regression method is that SR_A is consistent among all R_S measurements. In polyculture ecosystems, plant species may have different root respiration rates (Poorter et al. 1990) and thus S_{RA} may inherently vary spatially. Even in monocultures, realized SR_A may be in inconsistent if the root size-class distributions vary among samples. For example, studies have found that individual soil cores contain highly variable root-

class distributions (Taylor et al. 2013) and that < 0.5 mm diameter roots respire at higher rates than larger roots (Pregitzer et al. 1998). In some studies, researchers have disregarded certain root size-classes to improve the statistical fit of root regressions (Table 6.1). A more robust method would be to use a multiple linear regression with several root size-classes to estimate the SR_A for each size-class. However, this approach would likely require a much larger sample size than typical root regression studies.

A final major assumption of the root regression method is that lateral soil CO_2 diffusion is negligible. Yet, when root biomass is heterogeneous on small spatial scales, there must be lateral diffusion from high root biomass, high CO_2 spaces to low root biomass, low CO_2 spaces. Lateral CO_2 diffusion would exaggerate R_S at the low root biomass sampling points and understate R_S at the high root biomass sampling points. The slope of the regression would thus be reduced and the y-intercept elevated, thereby underestimating R_A and overestimating R_H. This may explain why comparative studies have generally found higher R_H with the root regression technique than the more common root exclusion method (Wang et al. 2008; Koerber et al. 2010; Tomotsune et al. 2013). To our knowledge, there is no practical work-around for this limitation.

6.2 Methods

6.2.1 Literature survey

We used Web of Science to conduct a literature survey of published studies that have used the linear root regression method explicitly to partition heterotrophic and autotrophic soil respiration. We report only *in situ* studies, as our discussion may be less relevant for greenhouse

studies. In total we identified 27 published studies containing 256 individual root regressions (Table 6.1).

6.2.2 Field study

We measured soil respiration and root biomass in maize (*Zea mays* L.) and switchgrass (*Panicum virgatum* L.) at the DOE-Great Lakes Bioenergy Research Center's biological cropping systems experiment in Arlington, WI, USA (Sanford et al. 2016). The dominant soil series is Plano silt loam, a fine-silty, mixed, superactive, mesic Typic Argiudoll (Soil Survey Staff 2017). We installed eighteen 10.2 cm inner diameter PVC soil respiration collars in each cropping system. The collars were 5 cm tall and were inserted 2 cm into the soil. To capture the spatial variability of root biomass, we installed collars at intra-row, inter-row, and intermediate positions in maize. Similarly, in switchgrass we installed collars on plants, inter-plant, and intermediate positions. Aboveground plant biomass was clipped within each collar one day prior to initiating soil respiration measurements. We conducted 11 total rounds of soil respiration measurements on August 13 and August 14, 2014 using a LI-COR LI-6400XT portable photosynthesis system with a 6400-09 soil chamber (LI-COR Inc., Lincoln, Nebraska, USA). Each measurement round took about 90 mins to complete. Root biomass, defined here as all belowground plant biomass, was collected on August 20, 2014 from directly beneath the soil collars. We sampled soils in 10 cm increments to a depth of 30 cm using a 10.2 cm inner diameter bucket auger. Soils were sieved to 2 mm to extract roots, and the roots were shaken for 30 mins in a 5% sodium hexametaphosphate solution. Roots were gently washed free of soil with deionized water on a 500 μm sieve (Dornbush et al. 2002), and live roots were separated based on the color, strength, and stele condition (Hayes and Seastedt 1987). Live roots were suspended

in deionized water in a 25 x 20 cm acrylic container and scanned at 600 DPI on an Epson V700 scanner (Epson America Inc., Long Beach, CA, USA). IJ_Rhizo software (Pierret et al. 2013) was used to determine live root volume, surface area, and length. Live roots were then dried at 65 °C for 48 h and weighed. Linear regressions were conducted between soil respiration and each combination of root metric (i.e. biomass, volume, surface area, and length) and sampling depth (i.e. 0-10 cm, 0-20 cm, and 0-30 cm) using the R 'stats' package (R Core Team 2017).

We used a bootstrapping method to estimate the number of field samples required to obtain a statistically significant linear regression ($p < 0.05$). We chose to run the bootstrap on early- and late-day measurement rounds from August 14, which represented times when the regression R^2 values were relatively weak and strong, respectively (Table 6.2). We also chose to bootstrap from 6 to 24 samples, as this range represents the number of samples commonly used among root regression studies (Table 6.1). For each measurement round, we randomly selected samples with replacement and ran regression analyses on 0-30 cm live root biomass and soil respiration for those samples. This procedure was repeated 10,000 times for each sample size, and we report the median *p*-value from each. Bootstrapping was conducted in R (R Core Team 2017).

We conducted statistical analyses to determine whether there were differences in linear regression R^2 values between crops, among root metrics, and among sampling depths. We used a mixed model with repeated measures for each round number to determine differences between crops. For the crop analysis, we only considered 0-30 cm live root biomass. To determine whether there were differences among root metrics, we used a mixed model with repeated measures for each root metric and treated each observation (i.e. unique combination of crop and sampling round) as a random effect. For the root metric analysis, we only considered the 0-30 cm

depth increment. To determine whether there were differences among sampling depths, we used a mixed model with repeated measures for each depth and treated each observation as a random effect. For the depth analysis, we only considered the live root biomass metric. All mixed model analyses were performed in SAS 9.4 (SAS Institute Inc., Cary, NC, USA).

6.3 Results and discussion

6.3.1 Implementation considerations and strategies

Overall, only 71% of 256 previously published root regressions were reported as statistically significant (typically $p < 0.05$), and model R^2 ranged from 0.00 to 0.98 (Table 6.1). Regression models tended to be statistically stronger in grasslands and row crops than forests and orchards or plantations. However, the number of sampling points, root sampling depths, and root size-classes all varied widely among studies, thus making overall generalizations difficult.

In our experimental study, all root regressions in maize were statistically significant ($p < 0.05$), while only 73% of root regressions were significant in switchgrass (Table 6.2). R^2 values were significantly greater in maize compared to switchgrass (Table 6.3). Linear regression model R^2 increased with regression slope (Fig. 6.2), indicating that regressions were stronger when SR_A was higher. Thus, greater R^2 in maize compared to switchgrass likely results from the fact that average SR_A was three times greater in maize. (Table 6.2). Regression model R^2 values became slightly greater with deeper sampling (Table 6.3). Surprisingly, the root biomass metric produced weaker R^2 than surface area, length, and volume metrics (Table 6.3). The number of sampling points required to produce statistically significant regressions was greater in switchgrass, but also varied by time of day (Fig. 6.3).

Even when linear regressions are statistically significant, there can be substantial uncertainty in the slope and intercept parameter estimates, which thus translate into uncertainty in the R_H and R_A values. From a logistical standpoint, while the root regression method causes little disturbance prior to R_S measurement, the sampling required to measure root biomass after R_S measurement is both destructive and labor intensive. These drawbacks may restrict temporally repeated applications of the root regression method, particularly if the study area is spatially limited.

6.4 Conclusions

The ideal implementation of the root regression method will likely vary as a function of ecosystem type and measurement timing. Ecosystems with high SR_A are most likely to yield strong linear regressions between root biomass and R_S. However, since R_A varies both seasonally and diurnally (Savage et al. 2013), the performance of the root regression method will also vary temporally. Researchers will likely benefit from pilot studies to determine the number of sampling points and root sampling depths required to produce adequate root regressions under their specific study conditions. Even when strong linear regressions are realized, the method is subject to several assumptions and potential limitations that should be explicitly considered.

6.5 Acknowledgements

This research was funded by the DOE Great Lakes Bioenergy Research Center (DOE BER Office of Science DE-FC02-07ER64494 and DOE OBP Office of Energy Efficiency and Renewable Energy DE-AC05-76RL01830) and partially supported by the USDA National

Institute of Food and Agriculture (Hatch project 0225417-WIS01586). We thank D. Williams for help with processing the root biomass samples.

6.6 References

Baggs, E. M. 2006. Partitioning the components of soil respiration: a research challenge. Plant and Soil 284:1–5.

Bao, F., Zhou, G., Wang, F., Sui, X. 2010. Partitioning soil respiration in a temperate desert steppe in Inner Mongolia using exponential regression method. Soil Biology and Biochemistry 42:2339–2341.

Behera, N., Joshi, S., Pati, D. 1990. Root contribution to total soil metabolism in a tropical forest soil from Orissa, India. Forest Ecology and Management 36:125–134.

Bennie, J., Huntley, B., Wiltshire, A., Hill, M. O., Baxter, R. 2008. Slope, aspect and climate: Spatially explicit and implicit models of topographic microclimate in chalk grassland. Ecological Modelling 216:47–59.

Buyanovsky, G. A., Kucera, C. L., Wagner, G. H. 1987. Comparative analyses of carbon dynamics in native and cultivated ecosystems. Ecology 68:2023–2031.

Ceccon, C., Panzacchi, P., Scandellari, F., Prandi, L., Ventura, M., Russo, B., Millard, P., Tagliavini, M. 2011. Spatial and temporal effects of soil temperature and moisture and the relation to fine root density on root and soil respiration in a mature apple orchard. Plant and Soil 342:195–206.

Chapin III, F. S. 2003. Effects of plant traits on ecosystem and regional processes: a conceptual framework for predicting the consequences of global change. Annals of Botany 91:455–463.

Cui, S., Zhu, X., Wang, S., Zhang, Z., Xu, B., Luo, C., Zhao, L., Zhao, X. 2014. Effects of seasonal grazing on soil respiration in alpine meadow on the Tibetan plateau. Soil Use and Management 30:435–443.

Dornbush, M. E., Isenhart, T. M., Raich, J. W. 2002. Quantifying fine-root decomposition: An alternative to buried litterbags. Ecology 83:2985–2990.

Franck, N., Morales, J. P., Arancibia-Avendaño, D., García de Cortázar, V., Perez-Quezada, J. F., Zurita-Silva, A., Pastenes, C. 2011. Seasonal fluctuations in *Vitis vinifera* root respiration in the field. New Phytologist 192:939–951.

Fu, G., Zhang, X. Z., Zhou, Y. T., Yu, C. Q., Shen, Z. X. 2014. Partitioning sources of

ecosystem and soil respiration in an alpine meadow of Tibet Plateau using regression method. Polish Journal of Ecology 62:17–24.

Gupta, S., Singh, J. 1981. Soil respiration in a tropical grassland. Soil Biology and Biochemistry 13:261–268.

Hao, Q., Jiang, C. 2014. Contribution of root respiration to soil respiration in a rape (*Brassica campestris* L.) field in Southwest China. Plant Soil and Environment 60:8–14.

Hayes, D. C., Seastedt, T. R. 1987. Root dynamics of tallgrass prairie in wet and dry years. Canadian Journal of Botany-revue Canadienne De Botanique 65:787–791.

Herbst, M., Bornemann, L., Graf, A., Welp, G., Vereecken, H., Amelung, W. 2012. A geostatistical approach to the field-scale pattern of heterotrophic soil CO_2 emission using covariates. Biogeochemistry 111:377–392.

Jakubowski, A. R., Casler, M. D., Jackson, R. D. 2017. Legume addition to perennial warm-season grass swards increases harvested biomass. Crop Science 57:3343–3351.

Koerber, G. R., Hill, P. W., Edwards-Jones, G., Jones, D. L. 2010. Estimating the component of soil respiration not dependent on living plant roots: Comparison of the indirect y-intercept regression approach and direct bare plot approach. Soil Biology and Biochemistry 42:1835–1841.

Kucera, C. L., Kirkham, D. R. 1971. Soil respiration studies in tallgrass prairie in Missouri. Ecology 52:912–915.

Kuzyakov, Y. 2006. Sources of CO_2 efflux from soil and review of partitioning methods. Soil Biology & Biochemistry 38:425–448.

Kuzyakov, Y. 2010. Priming effects: Interactions between living and dead organic matter. Soil Biology and Biochemistry 42:1363–1371.

Li, L. H., Han, X. G., Wang, Q. B., Chen, Q. S., Zhang, Y., Yang, J., Yan, Z. D., Li, X., Bai, W. M. 2002. Correlations between plant biomass and soil respiration in a *Leymus chinensis* community in the Xilin River basin of Inner Mongolia. Acta Botanica Sinica 44:593–597.

Liu, T., Xu, Z. Z., Hou, Y. H., Zhou, G. S. 2016. Effects of warming and changing precipitation rates on soil respiration over two years in a desert steppe of northern China. Plant and Soil 400:15–27.

Pierret, A., Gonkhamdee, S., Jourdan, C., Maeght, J.-L. 2013. IJ_Rhizo: an open-source software to measure scanned images of root samples. Plant and Soil 373:531–539.

Poorter, H., Remkes, C., Lambers, H. 1990. Carbon and nitrogen economy of 24 wild species differing in relative growth rate. Plant Physiology 94:621–627.

Pregitzer, K. S., Laskowski, M. J., Burton, A. J., Lessard, V. C., Zak, D. R. 1998. Variation in

sugar maple root respiration with root diameter and soil depth. Tree Physiology 18:665–670.

R Core Team 2017. R: A language and environment for statistical computing.

Rodeghiero, M., Cescatti, A. 2006. Indirect partitioning of soil respiration in a series of evergreen forest ecosystems. Plant and Soil 284:7–22.

Sanford, G. R., Oates, L. G., Jasrotia, P., Thelen, K. D., Robertson, G. P., Jackson, R. D. 2016. Comparative productivity of alternative cellulosic bioenergy cropping systems in the North Central USA. Agriculture, Ecosystems & Environment 216:344–355.

Savage, K., Davidson, E. A., Tang, J. 2013. Diel patterns of autotrophic and heterotrophic respiration among phenological stages. Global Change Biology 19:1151–1159.

Shi, J.-j., Geng, Y.-b. 2014. Study on the distinguishing of root respiration from soil microbial respiration in a *Leymus chinensis* steppe in Inner Mongolia, China. Huanjing Kexue 35:341–347.

Soil Survey Staff. 2017. Natural Resources Conservation Service, U.S. Department of Agriculture. Official Soil Series Descriptions. www.nrcs.usda.gov.

Subke, J. A., Inglima, I., Cotrufo, M. F. 2006. Trends and methodological impacts in soil CO2 efflux partitioning: A metaanalytical review. Global Change Biology 12:921–943.

Taylor, B. N., Beidler, K. V., Cooper, E. R., Strand, A. E., Pritchard, S. G. 2013. Sampling volume in root studies: the pitfalls of under-sampling exposed using accumulation curves. Ecology Letters 16:862–869.

Tomotsune, M., Yoshitake, S., Watanabe, S., Koizumi, H. 2013. Separation of root and heterotrophic respiration within soil respiration by trenching, root biomass regression, and root excising methods in a cool-temperate deciduous forest in Japan. Ecological Research 28:259–269.

Unteregelsbacher, S., Hafner, S., Guggenberger, G., Miehe, G., Xu, X. L., Liu, J. Q., Kuzyakov, Y. 2012. Response of long-, medium- and short-term processes of the carbon budget to overgrazing-induced crusts in the Tibetan Plateau. Biogeochemistry 111:187–201.

Upadhyaya, S. D., Singh, V. P. 1981. Microbial turnover of organic matter in a tropical grassland soil. Pedobiologia 21:100–109.

Wang, W., Feng, J., Oikawa, T. 2009. Contribution of root and microbial respiration to soil CO_2 efflux and their environmental controls in a humid temperate grassland of Japan. Pedosphere 19:31–39.

Wang, W., Guo, J. X. 2006. The contribution of root respiration to soil CO_2 efflux in *Puccinellia tenuiflora* dominated community in a semi-arid meadow steppe. Chinese Science Bulletin 51:697–703.

Wang, W., Guo, J. X., Oikawa, T. 2007. Contribution of root to soil respiration and carbon balance in disturbed and undisturbed grassland communities, northeast China. Journal of Biosciences 32:375–384.

Wang, W., Guo, J.-X., Feng, J., Oikawa, T. 2006. Contribution of root respiration to total soil respiration in a *Leymus chinensis* (Trin.) Tzvel. grassland of Northeast China. Journal of Integrative Plant Biology 48:409–414.

Wang, W., Ohse, K., Liu, J. J., Mo, W. H., Oikawa, T. 2005. Contribution of root respiration to soil respiration in a C-3/C-4 mixed grassland. Journal of Biosciences 30:507–514.

Wang, X., Zhu, B., Wang, Y., Zheng, X. 2008. Field measures of the contribution of root respiration to soil respiration in an alder and cypress mixed plantation by two methods: trenching method and root biomass regression method. European Journal of Forest Research 127:285–291.

Xu, M., DeBiase, T. A., Qi, Y., Goldstein, A., Liu, Z. G. 2001. Ecosystem respiration in a young ponderosa pine plantation in the Sierra Nevada Mountains, California. Tree Physiology 21:309–318.

Zhang, P., Tang, Y., Hirota, M., Yamamoto, A., Mariko, S. 2009. Use of a regression method to partition sources of ecosystem respiration in an alpine meadow. Soil Biology and Biochemistry 41:663–670.

Zhao, Z. M. 2016. Estimating 'rhizosphere priming effect': Comparison of the indirect y-intercept regression approach and direct bare plot approach. Russian Journal of Ecology 47:467–472.

6.7 Tables and figures

Table 6.1 – Literature survey of *in situ* studies using the root (linear) regression method to partition soil respiration. *P* is < 0.05 except where noted.

Ecosystem	Study	Sampling depths (cm)	Root size-classes (mm)	Sample points	Regressions	Percent significant	R^2
Forest	Behera et al. 1990	0-50	0-1, > 1, All	20	3	100	0.67-0.79
	Rodeghiero & Cescatti 2006	0-30	2-5	≥ 6	51	37[a]	NR
	Tomotsune et al. 2013	0-30	All	10-12	16	13	0.00-0.45
	Xu et al. 2001	0-50+	All (0-5)	18	1	100	0.52
Grassland	Bao et al. 2010	0-20	> 0.1	12	47	100[b]	0.25-0.97
	Buyanovsky et al. 1987	0-50	All (NR)	10	NR	NR	NR
	Cui et al. 2014	0-40	All (NR)	12	3	67	0.16-0.47
	Fu et al. 2014	0-20	All (NR)	25	11	100	0.50-0.68
	Gupta & Singh 1981	0-10	All (NR)	19	1	100	0.42
	Kucera & Kirkham 1971	0-10	All (NR)	NR	1	100[b]	0.52
	Li et al. 2002	0-30	All (NR)	7-10	12	42[b]	<0.10-0.53
	Liu et al. 2016	0-10	All (NR)	72	1	100	0.12
	Shi & Geng 2014	0-40	All (NR)	6	6	17	0.33-0.89
	Unteregelsbacher et al. 2012	0-30	All (NR)	24	1	100	0.56
	Upadhyaya & Singh 1981	0-30	All (NR)	NR	1	100[b]	0.36
	von Haden & Kucharik (this study)	0-30	All	18	11	73	0.10-0.51
	Wang & Guo 2006	NR	All (NR)	11-13	7	100	0.44-0.71
	Wang et al. 2005	0-10	All (NR)	10	13	100	0.36-0.71
	Wang et al. 2006	0-30	All (NR)	12	7	100	0.59-0.90
	Wang et al. 2007	0-30	All (0-2)	12	14	100	0.44-0.94
	Wang et al. 2009	0-50	All (NR)	12	6	100	0.35-0.62
	Zhang et al. 2009	0-20	All (NR)	20	3	33	0.01-0.57
Row crop	Hao & Jiang 2014	0-30	All (NR)	6	6	100	0.69-0.94
	Koerber et al. 2010	NR	All (NR)	4-48	14	71	0.00-0.80
	von Haden & Kucharik (this study)	0-30	All	18	11	100	0.48-0.69
	Zhao 2016	NR	All (NR)	45	4	100	0.43-0.68
Orchard or plantation	Ceccon et al. 2011	0-40	0-2	20-40	4	25[a]	0.05-0.35
	Franck et al. 2011	0-60	0-2, > 2	6	12	42	0.19-0.98
	Wang et al. 2008	0-30	0-2	10-17	12	100	0.34-0.73

[a] $p < 0.10$
[b] *p* not given
NR = not reported

Table 6.2 – Results of linear regressions between 0 to 30 cm live root biomass (g DM m^{-2}) and soil respiration (µmol CO_2 m^{-2} s^{-1}).

		Maize				**Switchgrass**			
Date	*Time*	*Intercept*	*Slope*	*R^2*	*P*	*Intercept*	*Slope*	*R^2*	*P*
8/13/2014	6:30	3.2	3.5E-03	0.48	< 0.01	3.9	3.2E-03	0.51	< 0.001
8/13/2014	8:30	3.0	4.0E-03	0.53	< 0.001	4.2	1.8E-03	0.23	< 0.05
8/13/2014	10:30	3.2	4.4E-03	0.57	< 0.001	4.4	1.4E-03	0.25	< 0.05
8/13/2014	12:30	3.2	4.5E-03	0.55	< 0.001	4.6	1.0E-03	0.10	> 0.15
8/14/2014	6:30	2.4	4.5E-03	0.58	< 0.001	3.4	1.6E-03	0.20	> 0.05
8/14/2014	10:00	2.7	4.7E-03	0.59	< 0.001	3.8	1.8E-03	0.46	< 0.01
8/14/2014	12:00	2.7	5.0E-03	0.59	< 0.001	3.8	1.3E-03	0.25	< 0.05
8/14/2014	14:00	2.9	5.7E-03	0.58	< 0.001	4.0	1.8E-03	0.42	< 0.01
8/14/2014	17:00	2.9	6.3E-03	0.63	< 0.0001	4.3	2.0E-03	0.38	< 0.01
8/14/2014	18:30	2.8	6.8E-03	0.67	< 0.0001	3.9	1.9E-03	0.38	< 0.01
8/14/2014	20:30	3.1	6.9E-03	0.69	< 0.0001	4.7	1.2E-03	0.20	> 0.05

Table 6.3 – Comparison of linear root regression R^2 values between crops and among depths and root metrics. Except for the root metric category, all other categories use root biomass as the independent variable. Mean and standard error are from mixed-model least squared means.

Variable	Categories	Summary and comparative statistics			
		Mean R^2	Std. Err.	*F*	*p*
Crop	Maize	0.59	0.03	42.65	<0.0001
	Switchgrass	0.31	0.03		
Depth	0-10 cm	0.39	0.04	139.39	<0.0001
	0-20 cm	0.43	0.04		
	0-30 cm	0.45	0.04		
Root metric	Biomass	0.45	0.04	7.93	0.0001
	Volume	0.49	0.04		
	Length	0.48	0.04		
	Surface area	0.50	0.04		

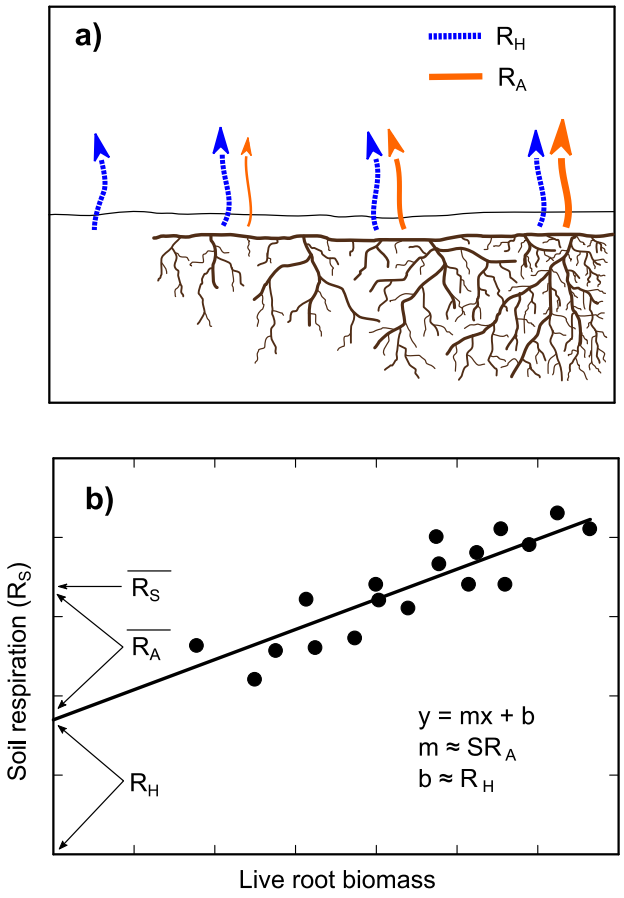

Figure 6.1 – (a) Conceptual depiction of autotrophic (R_A) and heterotrophic (R_H) soil CO_2 respiration under varying live root biomass quantities; arrow widths are proportional to the CO_2 flux. (b) Idealized linear regression between live root biomass and soil CO_2 respiration (R_S); SR_A is the specific root respiration rate.

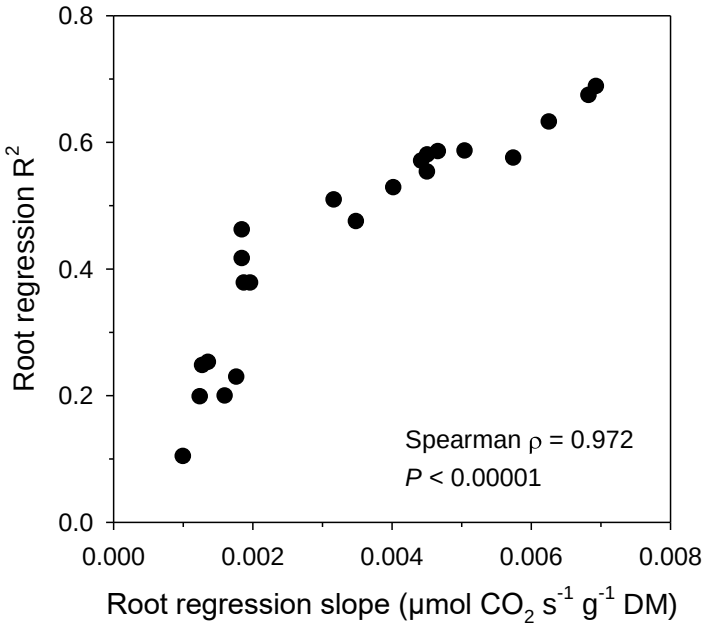

Figure 6.2 – Relationship between root regression slope and root regression R^2. Spearman's nonparametric rank correlation coefficient (ρ) shows the monotonic relationship.

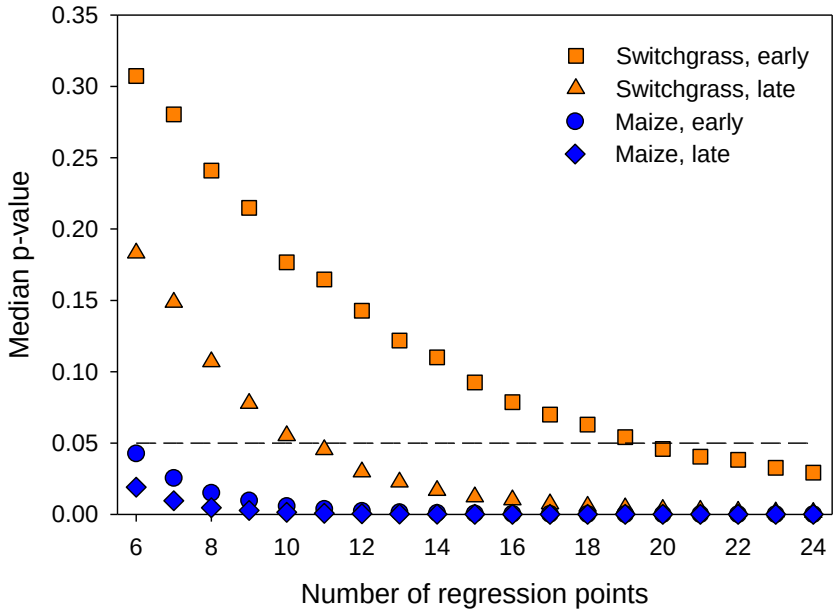

Figure 6.3 – Median *p*-values from bootstrapped linear regressions with varying number of data points the regression. Each point represents the median of 10,000 bootstrapped samples.

Chapter 7

Conclusions

7.1 Summary

I attempted to gain a better understanding of the mechanisms contributing to ecosystem carbon (C) storage by measuring ecosystem processes in bioenergy cropping systems. During the two years when the net ecosystem C balance (NECB) was studied, maize generally had a more favorable NECB than switchgrass, although there was high variability in the overall NECB estimates. While there were slight differences in net photosynthesis and belowground net primary productivity between maize and switchgrass systems, most of the NECB difference was attributable to higher residue retention, lower heterotrophic soil respiration (R_H), and lower autotrophic soil respiration (R_A) in maize compared to switchgrass. Although the lower residue removal in maize was a simple function of aboveground net primary production and harvest efficiency, the potential mechanisms causing the differences and heterotrophic and autotrophic soil respiration were not immediately apparent and thus were further investigated. This work suggests that contrary to our expectations, mature switchgrass stands may not have higher short-term C storage potential than long-term no-till maize under certain conditions.

Differences in R_A between maize and switchgrass were assessed using the maintenance respiration-growth respiration framework. Both root growth and specific root growth respiration were greater in switchgrass than maize, and thus annual root growth respiration was higher in switchgrass. Although specific root maintenance respiration was greater in maize, average root biomass was much greater in switchgrass, and therefore annual root maintenance respiration was also higher in switchgrass than maize. I hypothesize that the greater specific root growth respiration rate in switchgrass was primarily due to the lower relative growth rate of switchgrass,

and that the lower specific root maintenance respiration rate in switchgrass resulted from a lower proportion of non-structural root tissues. Overall, this work demonstrates that the maintenance respiration-growth respiration framework is useful at the ecosystem level, and that physiological differences in R_A may be more generalizable based on other well-known species traits.

Soil microclimates among maize, switchgrass, and poplar bioenergy systems were identified from 2011-2016. In general, the poplar and switchgrass soil microclimates were better buffered from extreme air temperatures than maize, likely due to the higher summer leaf area index and greater winter soil insulation in the latter systems. Using a simple model that accounted for the direct effects of soil temperature and moisture, I found that altering the soil microclimates between maize and switchgrass could cause moderate changes in the annual C losses from R_H. However, since switchgrass R_H was found to be greater under the maize microclimate, the direct microclimate effect does not explain the greater R_H measured in the NECB study. Nonetheless, the modeling exercise indicates that it may be possible to reduce C losses via R_H by managing the soil microclimate, although indirect effects must also be considered.

Soil organic carbon (SOC) fractions were isolated from samples collected at the time of biofuel cropping establishment and again after five years. The occluded light fraction (OLF), which represents SOC released from aggregates, showed the most change among all fractions, with poplar systems typically maintaining or accruing SOC in the OLF. Increases in the OLF were associated with higher litter quality (i.e. lower C:N) and soil clay content, whereas increases in the mineral-associated heavy fraction (HF) were related to litter input quantity and quality (i.e. C:N). Overall, these results indicate that clay-dominated soils may more quickly

accrue aggregate-protected SOC, and that adding more or higher quality litter may also increase SOC in protected fractions.

The root regression method for partitioning soil respiration was evaluated using a literature survey and *in situ* measurements. An overview of the basic theory and assumptions of the method was also given. The literature survey revealed that the method produced statistically significant regressions about three-quarters of the time, indicating that the performance of the method is not always acceptable. Field results indicated that sampling roots deeper into the soil profile may marginally enhance the method, but the method performance was nearly always better in maize than switchgrass. Thus, the root regression method may be inherently better suited for some ecosystems than others.

7.2 Synthesis and future work

Perennial cropping systems are generally expected to have more favorable NECB primarily due to increased belowground C allocation (Crews & Rumsey 2017). However, at our site we found that the slightly greater belowground root C production in the perennial switchgrass system were outweighed by the greater soil respiration C outputs in that system. The large standing root stock in perennial systems must be continually maintained via respiration, even during the non-growing season, and thus a substantial proportion of plant fixed C must be expended and released as CO_2. In contrast, the annual crop root system is relatively small and only needs to be maintained for about half of the year. Thus, greater belowground C allocation will not necessarily lead to more favorable NECB in perennial systems because a large proportion of belowground C must be used to maintain the expansive perennial root system.

Future work is still necessary to constrain the temperature response of autotrophic soil respiration and to further validate these results at other sites.

Residue management in annual cropping systems has been a subject of interest for many years, with many authors concluding that residue removal must be limited to maintain SOC stocks (Liska et al. 2014). In this study, residue return was greater in maize than switchgrass, and maize had a more favorable NECB than switchgrass, reaffirming that residue return rates are an important consideration for both annual and perennial cropping system (Lal & Pimentel 2009). To some extent, this dynamic was also reflected in the SOC fraction study: At the site where poplar litter inputs were much greater than the other systems, the poplar system consistently maintained aggregate-protected SOC when other cropping systems did not. Considering that the NECB in many herbaceous perennial systems is near neutral or slightly negative even when aboveground biomass is not harvested (e.g. Oates & Jackson 2014; von Haden & Dornbush 2017), it is perhaps not surprising that harvesting the majority of aboveground biomass would result in negative NECB. Perennial herbaceous systems with higher aboveground productivity, such as miscanthus (*Miscanthus* × *giganteus*), could provide similar or greater biomass yield while maintaining greater residue inputs (e.g. Sanford et al. 2016). Future residue removal experiments would be helpful to quantify the amount of residue needed to maintain or build SOC in perennial systems. Altering the soil microclimate may also provide the potential to decrease C losses from litter and SOC through reduced R_H. Direct manipulative experiments would be necessary to determine the extent to which management practices within a given cropping system can be used create soil microclimates that are less conducive to R_H.

7.3 Concluding remarks

While NECB is just one of many environmental, economic, and social considerations of biofuels, it plays a key role in determining the overall ecological footprint – and hence the sustainability – of biofuel cropping systems (Rist et al. 2009; Tilman et al. 2009). Although it is generally thought that perennial, cellulosic biofuel cropping systems will sequester atmospheric C, achieving neutral NECB may be a more realistic goal depending on the environmental envelope. Practices that reduce soil disturbances and increase litter input quality (i.e. lower C:N) and quantity are likely to enhance the NECB in both annual and perennial biofuel cropping systems. Landscape-level scenario modelling will be necessary to comprehensively determine the most effective C storage and sequestration strategies. Continuing research to better understand the mechanisms of ecosystem C processes will therefore increase the overall potential to store C across the landscape.

7.4 References

Crews, T. E., Rumsey, B. E. 2017. What agriculture can learn from native ecosystems in building soil organic matter: a review. Sustainability 9:578.

Lal, R., Pimentel, D. 2009. Biofuels: beware crop residues. Science 326:1345–1346.

Liska, A. J., Yang, H., Milner, M., Goddard, S., Blanco-Canqui, H., Pelton, M. P., Fang, X. X., Zhu, H., Suyker, A. E. 2014. Biofuels from crop residue can reduce soil carbon and increase CO_2 emissions. Nature Climate Change 4:398–401.

Oates, L. G., Jackson, R. D. 2014. Livestock management strategy affects net ecosystem carbon balance of subhumid pasture. Rangeland Ecology & Management 67:19–29.

Rist, L., Lee, J. S. H., Koh, L. P. 2009. Biofuels: social benefits. Science 326:1344–1344.

Sanford, G. R., Oates, L. G., Jasrotia, P., Thelen, K. D., Robertson, G. P., Jackson, R. D. 2016. Comparative productivity of alternative cellulosic bioenergy cropping systems in the North Central USA. Agriculture, Ecosystems & Environment 216:344–355.

Tilman, D., Socolow, R., Foley, J. A., Hill, J., Larson, E., Lynd, L., Pacala, S., Reilly, J., Searchinger, T. et al. 2009. Beneficial biofuels-The food, energy, and environment trilemma. Science 325:270–271.

von Haden, A. C., Dornbush, M. E. 2017. Ecosystem carbon pools, fluxes, and balances within mature tallgrass prairie restorations. Restoration Ecology 25:549–558.